НАУКОВІ ВІСТІ КПІ

Міжнародний науково-технічний журнал

№ 2 (143) 2026

Започаткований у вересні 1997 року

Головний редактор
М.О. Безуглий, д-р. техн. наук, проф.

Заступник головного редактора
М.Ю. Ільченко, акад. НАН України

Відповідальний секретар –
випусковий редактор
П.П. Маслянко, канд. техн. наук, доц.

У номері:

Системний аналіз
та наука про дані

Електроніка,
електронні комунікації,
приладобудування
та радіотехніка

Автоматизація,
комп'ютерно-інтегровані
технології та робототехніка

Адреса редакції:
КПІ ім. Ігоря Сікорського
просп. Берестейський, 37,
Київ, 03056, Україна

Тел. (+38 044) 204-94-53
E-mail: n.visti@kpi.ua
https://scinews.kpi.ua

© Національний технічний університет України «Київський політехнічний інститут імені Ігоря Сікорського», 2026

Засновник – Національний технічний університет України
«Київський політехнічний інститут імені Ігоря Сікорського»

Внесений до реєстру суб'єктів у сфері медіа з присвоєнням ідентифікатора медіа R30-02405
(рішення Національної ради з питань телебачення і радіомовлення № 1794 від 21.12.2023)

Згідно з наказом МОН України № 928 від 11.06.2026,
журнал включено до категорії «Б» Переліку наукових фахових видань України з технічних наук
за спеціальностями кластера «Інформаційні технології та електроніка»:

- *F2 Інженерія програмного забезпечення;*
- *F3 Комп'ютерні науки;*
- *F4 Системний аналіз та наука про дані;*
- *F5 Кібербезпека та захист інформації;*
- *F6 Інформаційні системи та технології;*
- *F7 Комп'ютерна інженерія;*
- *G5 Електроніка, електронні комунікації, приладобудування та радіотехніка;*
- *G6 Інформаційно-вимірювальні технології;*
- *G7 Автоматизація, комп'ютерно-інтегровані технології та робототехніка*

Рекомендовано Вченою радою Національного технічного університету України
«Київський політехнічний інститут імені Ігоря Сікорського», протокол № 6 від 08.06.2026 р.

Члени редакційної колегії

М.О. Безуглий,	д-р техн. наук, проф., Україна
М.Ю. Ільченко,	д-р техн. наук, проф., Україна
І.А. Дичка,	д-р техн. наук, проф., Україна
Г.С. Тимчик,	д-р техн. наук, проф., Україна
І.І. Синявський,	д-р техн. наук, ст. дослідник, Україна
Antoine Manzanera,	д-р наук, проф., Франція
Jozef Korbicz,	д-р наук, проф., Польща
María T. Orvañanos-Guerrero,	д-р філософії, доц., Мексика
Oleksandr Vasilevskyi,	д-р наук, проф., США
Pawel Komada,	д-р наук, проф., Польща
Sergii Babichev,	д-р техн. наук, проф., Чехія

Секретар редакції Т.Г. Кулікова

Редактор Н.В. Мурашова

Комп'ютерна верстка Л.М. Котовська

Національний технічний університет України
«Київський політехнічний інститут імені Ігоря Сікорського»
Свідоцтво про державну реєстрацію: серія ДК № 5354 від 25.05.2017 р., просп. Берестейський, 37, Київ, 03056

Підп. до друку 09.06.2026. Формат 60×84 1/8. Папір офс. Гарнітура UkrainianTimesET.
Спосіб друку – електрографічний. Ум. друк. арк. 7. Обл.-вид. арк. 5,69.
Наклад 30 пр. Зам. № 26-039.

Видавництво «Політехніка» КПІ ім. Ігоря Сікорського
вул. Політехнічна, 14, корп. 15, Київ, 03056
Тел. (044) 204-81-78

KPI SCIENCE NEWS

International research journal

№ 2 (143) 2026

Founded in September, 1997

Editor-in-chief
M.O. Bezuglyi, Prof.

Deputy editor-in-chief
M.Yu. Ilchenko, Academician of NASU

Executive editor — release editor
P.P. Maslianko, Assoc. Prof., PhD

In the issue:

System Analysis
and Data Science

Electronics, Electronic
Communications, Instrument
Making and Radio Engineering

Automation,
Computer-Integrated
Technologies and Robotics

Editorial office:
Igor Sikorsky Kyiv Polytechnic Institute,
ave. Beresteiskyi, 37,
Kyiv, 03056, Ukraine

E-mail: n.visti@kpi.ua
https://scinews.kpi.ua

© National Technical University of Ukraine “Igor Sikorsky Kyiv Polytechnic Institute”, 2026

Founder: National Technical University of Ukraine "Igor Sikorsky Kyiv Polytechnic Institute"

Entered into the Register of Media Entities with the assigned media identifier R30-02405 (pursuant to Decision No. 1794 of the National Council of Television and Radio Broadcasting of Ukraine, dated December 21, 2023)

According to the Order of the Ministry of Education and Science of Ukraine No. 928, dated June 11, 2026, the journal is included in Category "B" of the List of Scientific Professional Publications of Ukraine in Technical Sciences for the specialties of the "Information Technologies and Electronics" cluster:

- *F2 Software Engineering;*
- *F3 Computer Science;*
- *F4 System Analysis and Data Science;*
- *F5 Cyber Security and Data Protection;*
- *F6 Information Systems and Technologies;*
- *F7 Computer Engineering;*
- *G5 Electronics, Electronic Communications, Instrument Making and Radio Engineering;*
- *G6 Information-Measuring Technology;*
- *G7 Automation, Computer-Integrated Technologies and Robotics*

Approved by the Academic Council of the National Technical University of Ukraine "Igor Sikorsky Kyiv Polytechnic Institute" (Minutes No. 6, dated June 8, 2026)

Editorial Board

Mykhailo Bezuglyi,	Dr. Sc., Prof., Ukraine
Mykhailo Ilchenko,	Dr. Sc., Prof., Ukraine
Ivan Dychka,	Dr. Sc., Prof., Ukraine
Hryhorii Tymchyk,	Dr. Sc., Prof., Ukraine
Ivan Syniavskyi,	Dr. Sc., Sr. Researcher, Ukraine
Antoine Manzanera,	Dr. Sc., Prof., France
Jozef Korbicz,	Dr. Sc., Prof., Poland
María T. Orvañanos-Guerrero,	PhD, Associate Professor, Mexico
Oleksandr Vasilevskyi,	Dr. Sc., Prof., USA
Pawel Komada,	Dr. Sc., Prof., Poland
Sergii Babichev,	Dr. Sc., Prof., Czech Republic

Editorial Secretary T.G. Kulikova

Editor N.V. Murashova

Layout & Typography L.M. Kotovska

National Technical University of Ukraine "Igor Sikorsky Kyiv Polytechnic Institute"
Registration Certificate – ДК № 5354 dated May 25, 2017, 37 Beresteiskyi Ave., Kyiv, 03056, Ukraine

Approved for printing: June 9, 2026. Format 60×84 1/8. Offset paper. Font UkrainianTimesET.
Print. meth.: Electrographic. Conditional printed sheets: 7. Publisher's signatures: 5,69.
Print run: 30 copies. Order No. 26-039.

"Polytechnica" Publishing House of Igor Sikorsky Kyiv Polytechnic Institute
14 Politekhnichna Str., Building 15, Kyiv, 03056, Ukraine
Tel. (044) 204-81-78

ЗМІСТ

Системний аналіз та наука про дані

Грішин К.Д., Недашківська Н.І. Модель машинного навчання для розпізнавання конфігурацій рук української жестової мови 7

Голубінка В.П. Автономна система рекомендації індексів для реляційних баз даних на основі Cost-Model та Plan Covering 20

Електроніка, електронні комунікації, приладобудування та радіотехніка

Гліненко Л.К., Кость П.І. Методика вибору структури передавального тракту для термоядерних установок..... 27

Автоматизація, комп'ютерно-інтегровані технології та робототехніка

Петренко Д.В., Протасов А.Г. Алгоритм безкартографічної навігації робота Husky на основі моделей глибокого навчання з підкріпленням та адаптивного навчального плану 36

Бровко К.Ю., Буданов П.Ф., Великогорський О.В., Олійник Ю.С., Винокурова Н.Д., Войтенко С.М. Імітаційна модель цифрового двійника технологічного процесу енергоблоку АЕС..... 44

Панкратов Є.В., Тимчик Г.С. Мікросервісна архітектура та алгоритми модульної системи автоматизації технологічних процесів малого бізнесу..... 52

Автори номера..... 59

CONTENTS

System Analysis and Data Science

Grishyn K.D., Nedashkovskaya N.I. Machine learning model for recognition of ukrainian sign language hand configurations 7

Holubinka V.P. Autonomous index recommendation system for relational databases based on cost-model and plan covering 20

Electronics, Electronic Communications, Instrument Making and Radio Engineering

Hlinenko L.K., Kost P.I. Methodology for selecting the transmission path structure in fusion power plants.. 27

Automation, Computer-Integrated Technologies and Robotics

Petrenko D.V., Protasov A.G. Deep reinforcement learning-based mapless navigation algorithm for Husky robot with adaptive curriculum learning 36

Brovko K.Yu., Budanov P.F., Velykohorskyi O.V., Oliinyk Yu.S., Vynokurova N.D., Voitenko S.M. Simulation model of a digital twin for an NPP power unit technological process 44

Pankratov Ye.V., Tymchik G.S. Microservice architecture and algorithms of a modular automation system for small business technological processes 52

Contributors to the issue 59

СИСТЕМНИЙ АНАЛІЗ ТА НАУКА ПРО ДАНІ

DOI: https://doi.org/10.20535/kpisn.2026.2.352330
UDC 004.85:811.161.2'221.24

K.D. Grishyn[1]*, https://orcid.org/0009-0006-5950-3739
N.I. Nedashkovskaya[1], https://orcid.org/0000-0002-8277-3095

[1]National Technical University of Ukraine "Igor Sikorsky Kyiv Polytechnic Institute",
Educational and Research Institute for Applied System Analysis,
Kyiv, Ukraine, https://ror.org/00syn5v21

*Corresponding author: constantine1223h@gmail.com

MACHINE LEARNING MODEL FOR RECOGNITION OF UKRAINIAN SIGN LANGUAGE HAND CONFIGURATIONS

Background. Sign language recognition using Artificial Intelligence (AI) is a relevant and still unsolved problem. For Ukrainian Sign Language (USL), the task is complicated by a lack of publicly available datasets. Consequently, researchers operating under data-constrained conditions should apply additional features to improve model accuracy. Hand configuration is a fundamental characteristic of lexical units in any sign language. There are 40 configurations in USL. The ability to accurately identify configuration would provide relevant features for AI-based sign language recognition systems.

Objective. The paper aims to develop a machine learning model capable of frame-by-frame recognition of USL hand configurations on a video stream with an accuracy of at least 95 % on the test set and an average inference time not exceeding 70 ms.

Methods. As input data for the USL hand configurations recognition models, a system of mathematical indicators, calculated from the keypoints coordinates, extracted via the MediaPipe pose estimation system, was proposed. The training dataset was created from camera images of USL hand configurations performed by middle-aged subjects. Following keypoint extraction through MediaPipe, the corresponding vectors of mathematical indicators were computed. Various architectures of random forest and perceptron were evaluated.

Results. The highest performance was achieved by the perceptron with two hidden layers of 300 neurons each, which takes the vector of proposed mathematical indicators as input. The model reached an accuracy of 98.18 % on the test set. During testing on a video stream, it identified without error 32 out of 40 USL configurations, and with only sporadic deviations. The average inference latency was 46 ms. Notably, a perceptron of identical architecture trained on raw MediaPipe keypoint coordinates exhibited lower accuracy on a video stream. Furthermore, the proposed indicators improved the random forest model performance, confirming their universality.

Conclusions. The optimal model among the considered architectures was a perceptron with two hidden layers of 300 neurons each, which takes the vector of proposed mathematical indicators as input. It identifies in real-time USL hand configurations, achieving an accuracy of 98.18 % on the test set. In experiments based on the proposed expert assessment criterion on the video stream, it correctly identified 35 % more configurations (80 % vs. 45 %), compared to the model based on raw keypoint coordinates. Therefore, implementing additional verification based on expert assessment in addition to the standard accuracy metric on the test data is effective. The presented architecture is the first artificial intelligence-based model for the USL hand configuration recognition. Future research will focus on integrating this network into a system for isolated recognition of USL.

Keywords: Ukrainian Sign Language; machine learning; neural networks; computer vision; gesture recognition; model quality assessment; feature engineering; system analysis.

Пропозиція для цитування цієї статті: К.Д. Грішин, Н.І. Недашківська, «Модель машинного навчання для розпізнавання конфігурацій рук української жестової мови», *Наукові вісті КПІ*, № 2, с. 7–19, 2026. doi: https://doi.org/10.20535/kpisn.2026.2.352330

How to cite this article: K.D. Grishyn, N.I. Nedashkovskaya, "Machine learning model for recognition of ukrainian sign language hand configurations", *KPI Science News*, No. 2, pp. 7–19, 2026. doi: https://doi.org/10.20535/kpisn.2026.2.352330

© The Autor(s).
The article is distributed under the terms of the license CC BY 4.0

Introduction

There are more than 300 sign languages worldwide, used by over 72 million deaf people [1]. Sign language was the native language for approximately 230,000 Ukrainians in 2025 [2]. Moreover, during the full-scale war, the number of hearing-impaired individuals has increased as a result of sustained injuries, some of whom will begin to use sign language. These people face daily difficulties in communicating with the hearing population. Given the lack of professional interpreters in Ukraine, the development of an AI system for USL recognition seems a promising solution.

The ultimate goal of the sign language recognition is to develop an AI-based system that enables a person to record a message in sign language on video and get as output a translation into a spoken language. Such projects have already been implemented in other countries:

• SignGPT – the large language model development for British Sign Language. It is expected to translate sign language into spoken language and vice versa (via video generation) [3];

• SignGemma – a Google model for translating American Sign Language (ASL) into text [4];

• SLAIT – developed a lightweight model that classifies 343 ASL signs with 92% accuracy [5];

• KinTrans – a system that converts sign language into text/voice messages and vice versa, presented at Expo 2020 Dubai for Arabic and English. Other sign language support is planned [6];

• Google organised two competitions on the Kaggle platform focused on recognising fingerspelling and isolated ASL signs in video, with a total prize pool of 300,000 USD. The presented models achieved an accuracy that exceeded 80 % [7].

The field of AI-based USL recognition remains underdeveloped. Consequently, the researchers should apply additional features to improve the model's accuracy. Every sign is defined by hand configuration, hand motion, and spatial positioning. Different signs can be expressed with the same configuration by varying motion and spatial position. For example, a fist can represent the words "victory" or "grandmother" depending on hand movement. USL comprises 40 distinct hand configurations [8]. Determining configuration, spatial position, and motion trajectory makes a complete set of features necessary to identify sign from a linguistic point of view.

Thus, hand configurations are promising features for improving sign language recognition models' accuracy. *The objective of this study is USL hand configurations recognition on video frames captured by a camera using machine learning models.*

Problem statement

The problem of frame-by-frame recognition of 40 USL hand configurations on video stream is considered. The aim is to develop a machine learning model which recognises configurations on static images with high accuracy and computational efficiency using keypoints obtained by a pose estimation system.

A system approach

A system approach to solving the problem of frame-by-frame recognition of 40 USL hand configurations is proposed. It is grounded on mathematical formalization and advances in data science.

Given. N hand configuration classes. The training dataset is

$$(X_i, y_i), i = \overline{1, N_s}, \quad (1)$$

where $X_i \in \mathbb{R}^{k\times 3}$ – sample, on which hand configuration is demonstrated, represented as a vector of three-dimensional coordinates of k hand keypoints obtained via pose estimation technology (in this study, MediaPipe is employed, which outputs $k = 21$ keypoints based on hand image); $y_i \in \{1,...,N\}$ – the configuration label, in this study, from 1 to 40 [8]; N_s – training dataset size. In general case X_i (1) can be not only a keypoint vector but also an image of the hand.

Objective. To develop a machine learning model

$$f : \mathbb{R}^{k\times 3} \to \{1,\ldots,N\}, \quad (2)$$

that maps elements from the multidimensional feature space to the set of configurations. Accuracy must be at least 95 % on the test set, and the average inference time must not exceed 70 ms. It should be noted that model (2) is trained on static samples X_i (1), however, its task is to recognise hand shape $X_i \in \mathbb{R}^{k\times 3}$ on video stream, which will produce a sequence $\{(X_{i1}, y_i), (X_{i2}, y_i), ..., (X_{iT}, y_i)\}$. The samples X_{ij} will differ due to variations in hand position, tilt, and distance from the camera for a fixed y_i. Therefore, the model's (2) generalisation ability should be validated not only on test set of static samples but also on real-time video. For this reason, an additional evaluation criterion was proposed.

Evaluation criteria. The generalisation ability of the model will be assessed using two criteria. The first criterion is the standard evaluation of the machine

learning model's accuracy on the test set, calculated using the formula

$$y = \frac{N_{true}}{N}, \quad (3)$$

where N_{true} – number of correctly classified samples in test set; N – total number of samples in test set.

As a second criterion, an expert assessment of the model's ability to classify configurations on a video stream is proposed. The procedure is as follows:

1. For each configuration, the corresponding hand shape is demonstrated on camera in real time, while varying the hand position, tilt, distance from the camera, and hand shape versions (if exist).

2. The researcher records the model's output during the demonstration, comparing instances of correct and incorrect classification, and assigns each configuration to one of the following cases:

• "+" – correct configuration classification for any hand position;

• "+–" – generally correct classification with errors in certain cases;

• "–" – incorrect classification, indicating an unsatisfactory result.

3. A vector is calculated

$$\overrightarrow{r_{res}} = [n_+, n_{+-}, n_-], \quad (4)$$

where n_+, n_{+-}, n_- – number of configurations assigned to the cases "+", "+–", "–" respectively.

4. Vector $\overrightarrow{r_{res}}$ measures the model's generalisation ability.

In further studies, the hand shapes recognised from the video stream will serve as input data for more general isolated sign language recognition model.

Related work

The use of configurations as additional features in AI-based sign language recognition models is an active area of research. The operating principle of such approach is illustrated in Fig. 1. Model 1 performs hand shape recognition on each frame of the video, and the resulting configuration sequence is provided as a feature synchronously with the video to Model 2 for sign language recognition. Depending on the task formulation, Model 2 may perform recognition of a single sign in a video, sign sequence, or translation into spoken-language text.

This approach was first applied in 2017 to the RWTH-PHOENIX-Weather-2014 dataset (German): a neural network, trained to recognise hand shapes, generated sequences of embeddings from video, which were input to the sign language recognition model. The configuration recognition model was trained on Danish, New Zealand, and German sign language datasets, which included a total of over 1 million labelled images covering 60 hand shapes [9]. Results were further improved by adding a lip-shape recognition model, achieving a Word Error Rate (WER) of 26 % [10]. Subsequent models reached a WER of 21.8 % [11]. A similar example has been reported for ASL [12]. There is another known case of a configuration recognition model: graph neural network achieved 46 % accuracy in classifying 37 ASL hand shapes [13]. A random forest model has successfully identified Turkish Sign Language configurations [14].

Researchers categorise the sign language recognition task into several subproblems:

• Isolated Sign Language Recognition, ISLR;

• Continuous Sign Language Recognition, CSLR;

• Sign Language Translation, SLT.

ISLR – the task of classification of videos containing a single sign. Solving this problem is insufficient for developing a translator, as in real-world scenarios, a model takes as input sequence of signs.

In CSLR, the input is a video with a sequence of signs $\{y_1,..., y_m\}$ that must be recognised. Tem-

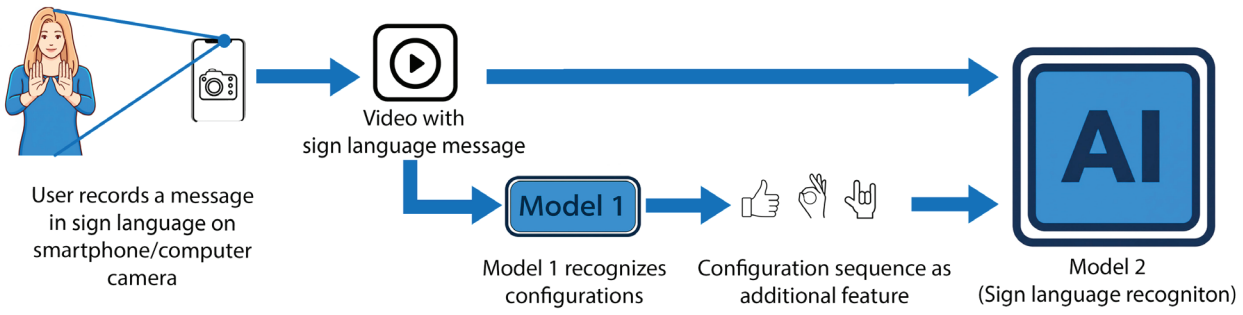


Fig. 1. Operating principle of the sign language recognition system using configurations as features. Made by authors

poral boundaries corresponding to each y_i are unknown. The components y_i are referred to as glosses. Neural networks solving this task have Connectionist Temporal Classification (CTC) loss function, which compares ground-truth and predicted sequences. Pretraining a CSLR model on ISLR task can improve its performance [15, 16]. It is possible to transit directly from ISLR to CSLR by combining segmentation and isolated recognition: segmentation divides the video into individual signs, which are then fed into the recognition model [17, 18]. The output of CSLR is a gloss sequence, which is not equal to translation: it lacks grammatical inflections, sign language grammar is different from that of spoken language. To achieve translation, large language models, linguistic rules, etc., need to be applied [19].

SLT is a translation of a video with signs sequence into spoken-language text. While the preceding tasks fall primarily within the computer vision domain, SLT involves machine translation. The data requirements are more stringent, as words must occur across diverse contexts. Model performance is evaluated via standard machine translation metrics such as BLEU, ROUGE, and METEOR. The neural network architectures for SLT are not fundamentally different from networks for CSLR.

So far there exist only a limited number of datasets available for CSLR and SLT due to the complexity of annotation. The most well-known of them are RWTH-PHOENIX-Weather-2014T and CSL-Daily (Chinese), which became benchmarks for comparing the models [20, 21]. No datasets for isolated recognition, continuous recognition, or translation of USL are publicly available.

The input data for the models can include RGB-video, depth camera video, optical flow, body keypoints coordinates (hands, torso, face) obtained by a motion capture system that utilizes sensors or AI models. RGB-videos have the highest dimensionality, requiring complex architectures and large datasets [22].

USL recognition has been studied by Yu.V. Krak. Fingerspelling recognition using statistical methods and AI has been implemented [23]. There are cases of USL alphabet recognition on isolated videos via long short-term memory network (LSTM) [24]. A neural network achieving isolated recognition of 38 static USL signs with 85 % accuracy was developed [25]. A generalised methodology for USL analysis on video using neural networks was proposed in [26]

Hand configuration recognition models

The developed model has to satisfy high computational efficiency requirements to enable real-time operation. For USL configurations recognition on video frames, random forest and multilayer perceptron models were chosen.

1. Random forest. An ensemble machine learning model consisting of decision trees, trained using bagging or, more rarely, pasting methods. Each tree produces an independent prediction, the result is obtained through aggregation. In this study, a classification task is considered; therefore, the prediction will be the class that received the majority vote from the trees. The advantages of the model are robustness to overfitting, the ability to handle discrete and continuous features, and the absence of priori assumptions about the data [27].

Decision trees are machine learning models that constitute the base learners of a random forest. They are constructed by recursively splitting the dataset into two subsets according to a threshold value of a selected feature. The process continues until further reduction of a homogeneity criterion is impossible, maximum tree depth is reached, or due to other stopping criteria. As a result, samples of a single class are isolated. In this study, random forest from scikit-learn library, which utilizes bagging, is chosen [27].

2. Multilayer perceptron. Feedforward neural network capable of modelling complex nonlinear relationships. Its architecture consists of a sequence of fully connected layers, each performing a linear transformation followed by an activation function to introduce nonlinearity. The first and last layers are referred to as the input and output layers, respectively, the intermediate layers are called hidden. The mathematical transformations between layers are described by equation (5), and illustrated in Fig. 2,

$$x_i^{k+1} = f^k\left(\sum_{j=1}^{N_k} \omega_{ij}^k x_j^k + b_i^k\right), i = \overline{1, N_{k+1}}, \qquad (5)$$

where ω_{ij}^k, b_i^k – weights of k-th layer linear transformation; f^k – k-th layer activation function; x_j^k –

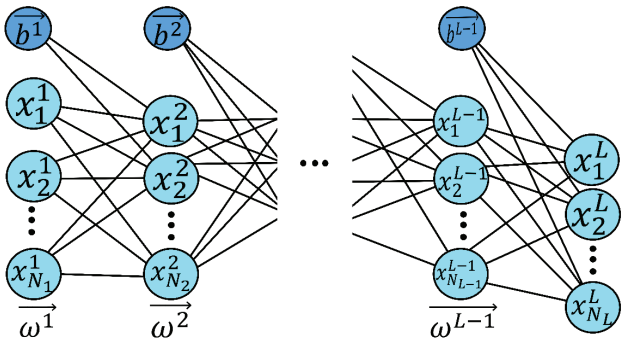


Fig. 2. Multilayer perceptron architecture. Made by authors

j-th coordinate of the data transformation vector at k-th layer (for $k = 1$ it is a coordinate of input data vector); N_k, N_{k+1} – number of neurons in k-th and $k+1$-th layer, respectively.

The number of neurons N_k and activation functions f^k can be different across layers. Training is performed by alternation between forward propagation and backpropagation. During the forward propagation, the model's prediction and intermediate variables are computed, from which the error is calculated. In backpropagation, the gradient of neural network parameters is determined based on this error. In TensorFlow it is implemented via a computation graph. After finding the gradient, the weights are updated using optimisation algorithms such as Adam, AdaDelta, or AdaGrad [28].

Input data formation

The keypoints, obtained by MediaPipe pose estimation system, were chosen as the input data for the configuration recognition system, considered in this study. MediaPipe identifies 543 keypoints in three-dimensional space corresponding to the body contour, limbs, and face (Fig. 3). This data representation allows for high accuracy while maintaining low input dimensionality [29]. A drawback is missing data in the stream, as MediaPipe does not always successfully detect the human pose. In this study, only the hand keypoints will be used (21 points per hand).

Even when hand shapes are represented as three-dimensional keypoints, their recognition remains a challenging task due to the large number of classes, the existence of multiple variations for a single configuration, and the diversity of possible hand positions. Therefore, it is advisable to introduce features that simplify the classification for the model without losing essential information. *In this study, a set of such features was proposed, and their effectiveness was evaluated.*

Bent indicator. The sum of the absolute values of the angles between two pairs of finger phalanges: proximal and middle, middle and distal. It is computed according to the formula

$$Bent(\vec{a},\vec{b},\vec{c}) = \left|\angle(\vec{a},\vec{b})\right| + \left|\angle(\vec{b},\vec{c})\right|, \qquad (6)$$

where $\vec{a},\vec{b},\vec{c}$ – vectors connecting the start and end points of the proximal, middle, and distal phalanges, respectively.

Metrics (6) measures the degree of finger flexion. For a straight finger, the angles between $\vec{a},\vec{b}$ and $\vec{b},\vec{c}$ are close to zero, and the *Bent* value is small. *Bent* reaches its maximum when the angles between the phalanges approach right angle (Fig. 4, left). The vectors of the index finger phalanges $\vec{a},\vec{b},\vec{c}$ and angles between them are shown in red, while vectors of the extended middle finger are shown in blue. Here, the index finger exhibits a higher *Bent* value than the middle.

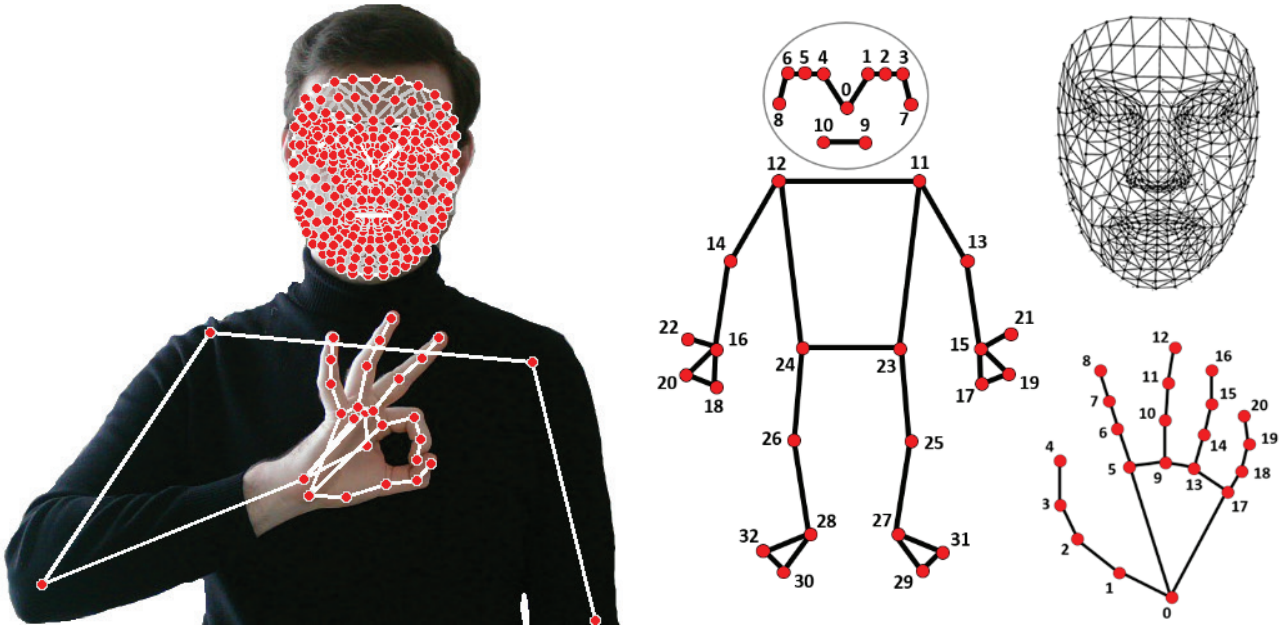


Fig. 3. Key points obtained using the MediaPipe pose estimation system. Made by authors

Joined indicator. Measures the distance between the tip of the thumb and the tip of another finger. It is calculated with formula

$$Joined(\vec{x},\vec{y}) = \|\vec{x} - \vec{y}\|, \quad (7)$$

where $\vec{x},\vec{y}$ – coordinates of the tip of the thumb and the tip of the other specified finger, respectively.

The illustration of is shown in Fig. 4 (right). The *Joined* will be close to zero in the following cases:

• thumb and index finger – in configurations 3, 4, 6, 7, 8, 34, 38, 40;

• thumb and middle finger – in configurations 14, 16, 17, 31, 37, 38, 40;

• thumb and ring finger – in configurations 16, 17, 18, 26, 27, 29, 31;

• thumb and little finger – in configurations 23 [8].

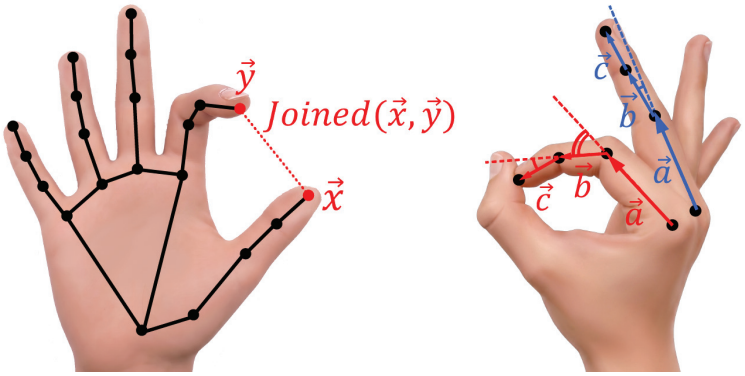


Fig. 4. *Bent* indicator for a folded finger and extended middle finger (left). Example of *Joined* indicator as the distance between the tips of the thumb and the index finger (right). Made by authors

Angle indicator. Estimates the angle between two fingers, enabling discrimination between cases when the fingers are pressed together (angle close to zero, planes nearly parallel) and when they are separated. The indicator is computed via the following algorithm:

• build a linear regression plane through four points of the first finger;

• build another linear regression plane through four points of the second finger;

• determine $\overrightarrow{n_a},\overrightarrow{n_b}$ – the normal vectors to the planes obtained in the two previous steps;

• compute the angle α between $\overrightarrow{n_a},\overrightarrow{n_b}$, which constitutes the *Angle* value.

If four points of a finger lie on a single line, there are infinitely many possible planes; therefore, *Angle* becomes undefined. However, experiments have shown that due to noise in MediaPipe pose estimation process, such cases are rare and do not affect the model's accuracy. The computation of *Angle* for the thumb and index fingers is illustrated in Fig. 5 (left).

$\overrightarrow{Dir}$ indicator. A vector defined by subtracting the fingertip point from the finger base point. It preserves the information about the finger's direction. This is the only indicator among the proposed that is not invariant to hand rotations. An illustration is shown in Fig. 5 (right).

Straight indicator. Evaluates how close the hand is to a flat palm. It is computed using the following algorithm:

• construct a linear regression plane through the 21 hand keypoints estimated by MediaPipe;

• compute the coefficient of determination R^2 for the regression.

For flat palm, all points lie near the plane, resulting in R^2 close to 1 (as in configuration No. 9 and certain version of No. 12), and lower R^2 values (Fig. 6).

The indicators are designed to provide the machine learning model with relevant features that describe the fingers' arrangement while maintaining low data dimensionality.

Experiments and results

To evaluate the proposed indicators' effectiveness, experiments on hand configuration recognition were conducted. We compared models with two types of input data:

• *raw data* – vector of MediaPipe hand keypoints coordinates (a 63-dimensional vector, which

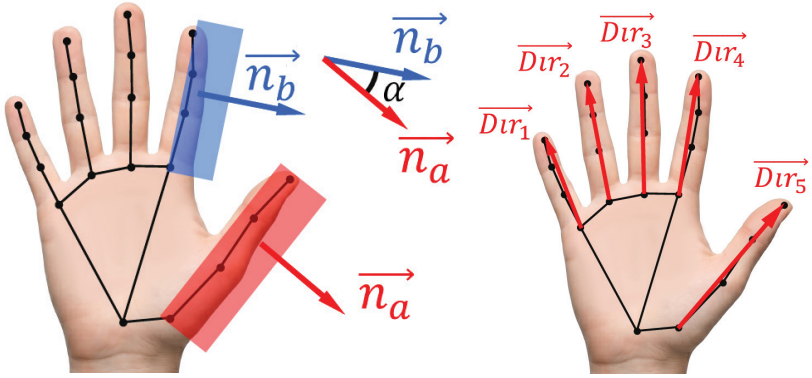


Fig. 5. Computation of *Angle* indicator for the thumb and index finger (left) $\overrightarrow{Dir}$ indicator for each finger (right). Made by authors

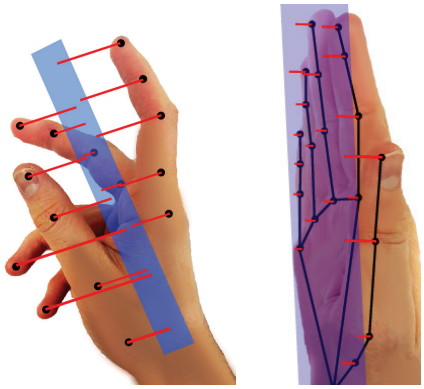


Fig. 6. *StraightHand* measure computation for semi-bent hand (left) and extended hand (right). Made by authors

contains 21 points with three spatial coordinates each);

• *processed data* – vector of the proposed indicators

$$[Bent_i,...,Joined_j,...,Angle_k,...,StraightHand,$$

$$Dir_{mx},Dir_{my},Dir_{mz},...]\in\mathbb{R}^{29}, \quad (8)$$

where $Bent_i, i=\overline{1,5}$ – finger flexion indicators for 5 fingers; $Joined_j, j=\overline{1,4}$ – indicatorsof the distance betweenthetipofthethumbandthetipsofotherfingers; $Angle_k, k=\overline{1,4}$ – angles between fingers: thumb and index finger, index and middle, middle and ring, ring and little fingers; *StraightHand* – indicators of closeness of the hand to the flat palm; $Dir_{mx}, Dir_{my}, Dir_{mz}, m=\overline{1,5}$ – coordinates of finger m direction.

Using Python script, images of USL configurations from No. 1 to No. 40 were recorded on a camera [8]. Hand orientation, hand shape versions, and distance to the camera were varied to ensure dataset diversity. The configurations were demonstrated by both left and right hands. Hand keypoints were detected in the images via MediaPipe pose estimation system, then used for computing the corresponding vectors of the proposed measures through software (8). Data collection was carried out according to the following algorithm:

• for each of the 40 classes, 1,000 images were initially collected;

• the trained models (random forest with 300 trees and multilayer perceptron with two hidden layers of 300 neurons each) with (8) as input were tested on a video stream; if a model misclassified a configuration on some images, additional images similar to those were added;

• the procedure was repeated several times, resulting in an uneven distribution of data across classes.

Distribution of the number of samples per class in the dataset is shown in Fig. 7.

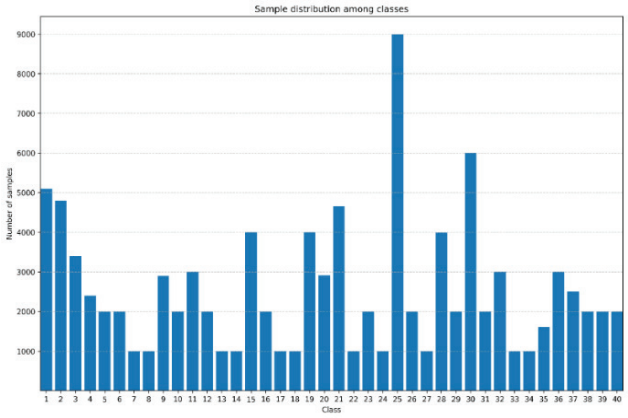


Fig. 7. Number of images per class distribution for 40 configurations in the dataset. Made by authors

The dataset (1) was split into training and test sets in a 7:3 ratio, the proportion of samples per class in each subset corresponded to the original dataset. The performance of random forest and multilayer perceptron models were compared. The random forest was built using the scikit-learn library, while the perceptron was implemented with the TensorFlow Keras.

For the perceptron, the input data were normalised to the range from 0 to 1 (including 0 and 1). A batch size of 128, a learning rate of 0.0001 (with exponential decay of 0.96 every 20,000 steps, the Adam optimiser, and cross-entropy as the loss function were chosen. ReLU was selected as the activation function for hidden layers, and softmax for the output layer. Training was conducted over 2,000 epochs using a GPU. To prevent overfitting, early stopping with a patience of 50 epochs if the validation accuracy did not increase by at least 0.01 % was implemented.

The accuracy metrics of the evaluated models, computed by formula (3), is presented in Table 1. Models that achieved top performance are highlighted in green.

On test set of static hand configuration samples, the highest accuracy was achieved by the perceptron with two hidden layers of 300 neurons each, both for raw (99.11 %) and processed data (98.18 %). The random forest with 150 trees trained on processed data achieved a test accuracy of 98.44 %, where-

Table 1. Accuracy of the models on the training and test sets

Model	Architecture	Raw input data		Processed input data	
		Accuracy on the training set	Accuracy on the test set	Accuracy on the training set	Accuracy on the test set
Random forest	100 trees	100 %	98.08 %	100 %	98.40 %
	150 trees	100 %	98.17 %	**100 %**	**98.44 %**
	200 trees	100 %	98.18 %	100 %	98.41 %
	250 trees	100 %	98.17 %	100 %	98.38 %
	300 trees	**100 %**	**98.20 %**	100 %	98.42 %
Perceptron (the architecture specifies the number of hidden layers and the number of neurons in each layer)	1 layer, 100 neurons	93.17 %	92.03 %	92.48 %	91.98 %
	1 layer, 200 neurons	95.78 %	95.44 %	96.25 %	95.67 %
	1 layer, 300 neurons	97.38 %	96.94 %	97.1 %	96.08 %
	2 layers, 200 neurons	98.91 %	97.95 %	99.10 %	98.09 %
	2 layers, 300 neurons	**99.77 %**	**99.11 %**	**99.53 %**	**98.18 %**

as the model with 300 trees trained on raw data achieved 98.20 %.

The accuracy values are consistent with previously reported results on the application of machine learning methods for recognising the dactyl alphabet of USL on static images [30]. The confusion matrix for the test set indicates a uniform distribution of errors among classes and the absence of problematic classes (Fig. 8).

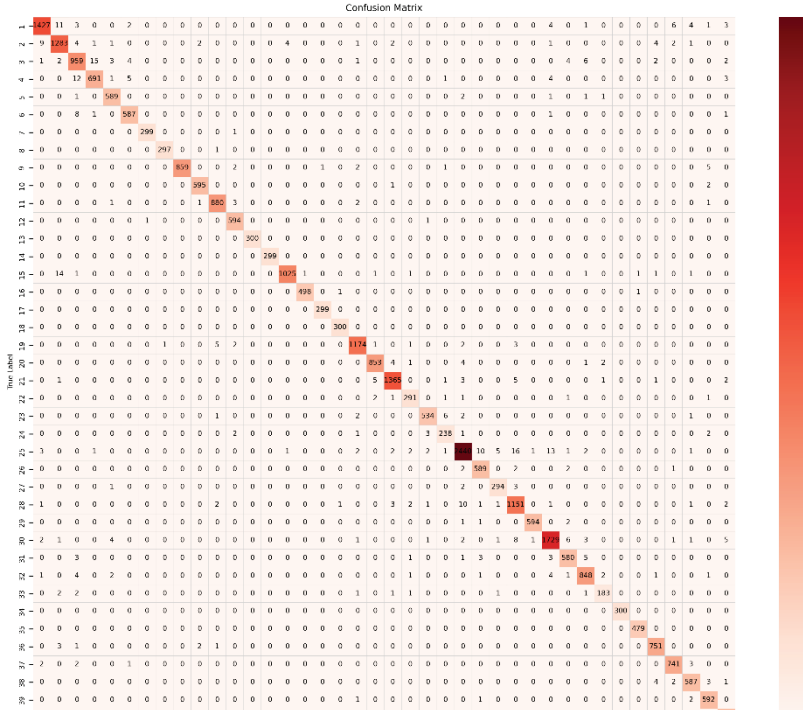


Fig. 8. Confusion matrix of the perceptron with two hidden layers of 300 neurons each, which takes processed data as input, evaluated on the test set. Made by authors

The random forest and perceptron models trained on processed and unprocessed data with the highest accuracy on the test set were selected for further evaluation via expert assessment, as described in the "Evaluation Criteria" section. This was conducted in order to test the models' ability to perform configuration classification on frames of the video stream and identify the most accurate model.

Python program was developed that detects hand keypoints on video stream via MediaPipe. Keypoints coordinates are either applied directly as input or used for computing the proposed indicators, then fed into the model. Afterwards, the program displays predicted hand configuration on the screen in real time.

The results of configuration classification by the top-performing random forest models on video stream are presented in Table 2, the results for the perceptron models are shown in Table 3. The enumeration of USL configurations follows the paper [8]. The sum of correct (+), generally correct (+−), and incorrect (−) classifications, computed by formula (4), are reported in Table 4.

Models trained on raw data made significantly more errors compared to their counterparts trained on processed data. The perceptron with two hidden layers of 300 neurons each trained on processed data correctly classified 80 % of configurations and generally correctly classified 20 %, making it the most accurate model. An example when the chosen perceptron trained on raw data misclassified configuration No. 35, while the corresponding model trained on processed data gave the correct answer, is shown in Fig. 9. *This suggests that the proposed indicators provide the model with high generalisation capability.* Average inference time was 46 ms, so the model could be applied in real-time.

The experiments showed that models can achieve a higher value of the accuracy metric (3) on test set of static samples of USL hand configurations, while making more errors evaluating the same configurations on a video stream. For example, the selected perceptron model that used raw data achieved test accuracy (3) of 99.11 %, however, it made more errors on a video stream compared to the perceptron of the same architecture that used processed data and had 98.18 % of test accuracy (3). This confirms the necessity of an additional model evaluation criterion based on expert assessment on video stream.

Thus, the perceptron with two hidden layers of 300 neurons each, which used the mathematical indicators proposed in this study as input, successfully recognised USL hand configurations. Its accuracy

Table 2. Results of configuration classification by the top-performing random forest models

Configuration No.	Input features		Configuration No.	Input features		Configuration No.	Input features	
	Raw data	Processed data		Raw data	Processed data		Raw data	Processed data
1	−	+	15	+	+	29	+	+
2	+	+	16	+−	+	30	+	+
3	−	+	17	+−	+	31	+−	+−
4	−	+−	18	+	+	32	−	+−
5	−	+	19	+−	+−	33	−	+−
6	−	−	20	+	+	34	−	+−
7	−	+	21	+	+	35	+−	+
8	−	+	22	−	+	36	+−	+−
9	+−	+	23	−	+−	37	+	+
10	−	+	24	−	+−	38	+	+
11	+−	+	25	−	+	39	+	+
12	+−	+	26	−	+−	40	+−	+
13	−	+	27	−	+−			
14	+	+−	28	+−	+			

Table 3. Results of configuration classification by the top-performing perceptron models

Configuration No.	Input features		Configuration No.	Input features		Configuration No.	Input features	
	Raw data	Processed data		Raw data	Processed data		Raw data	Processed data
1	−	+	15	+−	+	29	+	+−
2	+−	+	16	−	+−	30	+	+
3	+	+	17	+	+	31	+	+
4	+	+	18	+−	+−	32	−	+
5	+−	+	19	+	+	33	+−	+
6	−	+	20	+	+	34	+−	+
7	+−	+−	21	+	+	35	−	+
8	−	+	22	+−	+	36	+	+
9	+−	+	23	+−	+	37	+	+
10	+	+	24	−	+−	38	+−	+
11	+	+	25	+	+	39	+−	+
12	+	+	26	−	+−	40	+	+
13	+	+	27	−	+−			
14	+−	+−	28	+	+			

was validated on a video stream. The limitation of the model is that, during the video stream evaluation, it could make brief misclassifications due to noise and high complexity of data. However, such errors can be corrected as outliers – for example, by replacing them with values corresponding to the majority class within a sliding window. It is reasonable to investigate the model's generalisation capability across different people in future works.

It was found that, after hand movements exceed certain speed, the classification accuracy reduces due to motion blur. This issue can be mitigated by using a camera with a higher frame rate. For instance, iPhone starting from version 16 can capture video at 240 frames per second.

The model is expected to recognise configurations on video and provide relevant feature for other models. In the future work, this model will be used as a component of a sign language recognition system.

Conclusions

Hand configuration is a fundamental characteristic of lexical units in any sign language. The ability to recognise USL configurations provides relevant features for AI-based sign language recognition systems. In this study, a multilayer perceptron model was trained to recognise 40 USL hand configurations on static camera images with high accuracy. A system of five indicators was proposed as the model's input: *Bent*, *Joined*, *Angle*, $\overrightarrow{Dir}$, *StraightHand*. These indicators were computed based on 21 hand keypoints coordinates obtained using the MediaPipe pose estimation system. The proposed five features

Table 4. Recognition of configurations from No. 1 to No. 40 by top-performing models on video stream

Top model	Input features	Recognition results for configurations from No. 1 to No. 40		
		+	+–	–
Random forest	Raw data	12 (30 %)	10 (25 %)	18 (45 %)
	Processed data	27 (67.5 %)	12 (30 %)	1 (2.5 %)
Perceptron	Raw data	18 (45 %)	13 (32.5 %)	9 (22.5 %)
	Processed data	**32 (80 %)**	**8 (20 %)**	**0 (0 %)**

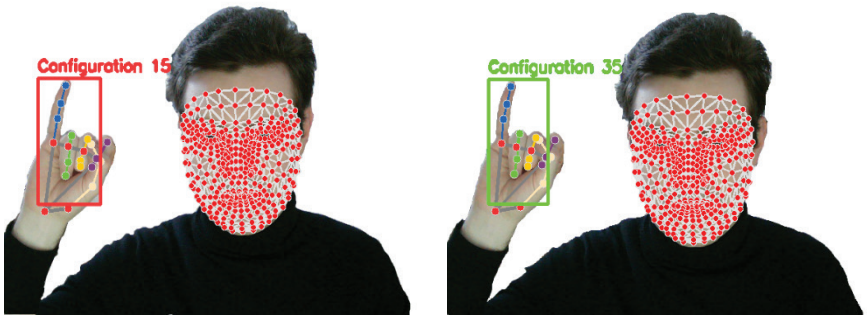


Fig. 9. Classification of configuration No. 35 by the top-performing perceptron model with raw input data (left) and processed data (right). Made by authors

provide information about finger arrangement while ensuring interpretability and low dimensionality of the training data. To develop the model, a dataset of images of 40 USL hand configurations was collected, with variations in hand shape versions, hand orientation, and distance from the camera to maximise diversity.

Different versions of random forest models (with varying numbers of trees) and multilayer perceptrons (with varying numbers of layers and neurons) were compared. Models either took raw input data – 21 hand keypoints coordinates, or processed data – the proposed 5 mathematical indicators. The perceptron with two hidden layers of 300 neurons each, trained on processed data, achieved the 98.18 % accuracy on test set of images and an average inference time 46 ms. *Hence, the proposed features significantly improved the model's generalisation capability, which was demonstrated in experiments on hand configuration recognition on a video stream.*

The experiment showed that higher accuracy on test set of static hand configuration samples is not the sole indicator of a model's performance on practice. The necessity of introducing an additional evaluation criterion based on expert assessment was substantiated. The developed multilayer perceptron model can effectively recognise USL hand configurations on a video stream, meeting the requirements for high accuracy and real-time performance. In future works, it is planned to use this model as a component of an isolated sign language recognition system.

References

[1] "'Sign Languages are for Everyone!' UN International Day of Sign Languages". [Online]. Retrieved from: https://www.european-agency.org/news/sign-languages-are-everyone-un-international-day-sign-languages. Accessed: Apr. 13, 2026.

[2] "UNICEF Ukraine Facebook post February 20, 2025". [Online]. Retrieved from: https://www.facebook.com/1789994851793391. Accessed: Apr. 13, 2026.

[3] "SignGPT Building Generative Predictive Transformers for Sign Language. An EPSRC Programme Grant 1/5/2025-30/4/2031". [Online]. Retrieved from: https://sites.google.com/view/signgpt/team. Accessed: Apr. 13, 2026.

[4] "Google DeepMind SignGemma announcement". [Online]. Retrieved from: https://x.com/GoogleDeepMind/status/1927375853551235160. Accessed: Apr. 13, 2026.

[5] "SLAIT at DeafIT Conference about "Breaking communication barriers between Deaf & hearing people". [Online]. Retrieved from: https://www.youtube.com/watch?v=UZ1FJP7uO9Y. Accessed: Apr. 13, 2026.

[6] "A software that can translate any sign language // Expo Live – KinTrans Inc. – USA". [Online]. Available: https://www.youtube.com/watch?v=29n1YhOVHHA. Accessed: Apr. 13, 2026.

[7] "1st place solution – 1DCNN combined with Transformer". [Online]. Retrieved from: https://www.kaggle.com/competitions/asl-signs/writeups/hoyeol-sohn-1st-place-solution-1dcnn-combined-with. Accessed: Apr. 13, 2026.

[8] S.V. Kulbida, "Konfihuratsiia yak komponent zhestu [Configuration as a sign component]", Osoblyva dytyna : navchannia i vykhovannia. [Special child: teaching and raising], 2018, Vol. 4, pp. 15–30. Retrieved from: https://doi.org/10.33189/ectu.v4i89.6

[9] N. Camgoz *et al.*, "SubUNets: End-to-End Hand Shape and Continuous Sign Language Recognition", in *IEEE International Conference on Computer Vision* (ICCV), Venice, Italy, 2017. Retrieved from: https://doi.org/10.1109/ICCV.2017.332

[10] O. Koller *et al.*, "Weakly Supervised Learning with Multi-Stream CNN-LSTM-HMMs to Discover Sequential Parallelism in

Sign Language Videos", in *IEEE Transactions on Pattern Analysis and Machine Intelligence*, 2020, Vol. 42, No. 9, pp. 2306–2320. Retrieved from: https://doi.org/10.1109/TPAMI.2019.2911077

[11] X. Zhang and K. Duh, "Handshape-Aware Sign Language Recognition: Extended Datasets and Exploration of Handshape-Inclusive Methods", in *Findings of the Association for Computational Linguistics*: *EMNLP*, Singapore, 2023, pp. 2993–3002. Retrieved from: https://doi.org/10.18653/v1/2023.findings-emnlp.198

[12] A.A. Hosain *et al.*, "FineHand: Learning Hand Shapes for American Sign Language Recognition", in *15th IEEE International Conference on Automatic Face and Gesture Recognition* (FG 2020), 2020, pp. 700–707. Retrieved from: https://doi.org/10.1109/FG47880.2020.00062

[13] A. Carbo and E. Nalisnick, "Improving Handshape Representations for Sign Language Processing: A Graph Neural Network Approach", in *Proceedings of the 2025 Conference on Empirical Methods in Natural Language Processing*, Suzhou, China, pp. 29122–29135. Retrieved from: https://doi.org/10.18653/v1/2025.emnlp-main.1483

[14] B. Demircioğlu, G. Bülbül and H. Köse, "Turkish Sign Language recognition with Leap Motion", in *24th Signal Processing and Communication Application Conference* (SIU), pp. 589–592. Retrieved from: https://doi.org/10.1109/SIU.2016.7495809

[15] S. Sharma *et al.*, "Continuous sign language recognition using isolated signs data and deep transfer learning", *Journal of Ambient Intelligence and Humanized Computing*, 2023, Vol. 14, No. 3, pp. 1531–1542. Retrieved from: https://doi.org/10.1007/s12652-021-03418-z

[16] S. Alyami *et al.*, "Reviewing 25 years of continuous sign language recognition research: Advances, challenges, and prospects", *Information Processing & Management*, 2024, Vol. 61, No. 5. Retrieved from: https://doi.org/10.1016/j.ipm.2024.103774

[17] K. Myagila *et al.*, "Framework for detecting and recognizing sign language using absolute pose estimation difference and deep learning", *Machine Learning with Applications*, 2025, Vol. 21. Retrieved from: https://doi.org/10.1016/j.mlwa.2025.100723

[18] R. Rastgoo *et al.*, "Word separation in continuous sign language using isolated signs and post-processing", *Expert Systems with Applications*, 2024, Vol. 249. Retrieved from: https://doi.org/10.1016/j.eswa.2024.123695

[19] O.V. Lozynska, "Systema kompiuternoho perekladu ukrainskoi zhestovoi movy z vykorystanniam hramatychno dopovnenoi ontolohii" [System of computer translation for Ukrainian Sign Language using grammatically augmented ontology] Ph.D. dissertation, Lviv Polytechnic National University, Lviv, 2016. [Online]. Retrieved from: https://lpnu.ua/sites/default/files/2020/dissertation/1452/dyserlozynska1.pdf. Accessed: Apr. 13, 2026.

[20] N.C. Camgɯz *et al.*, "Neural Sign Language Translation", *IEEE Conference on Computer Vision and Pattern Recognition*, Salt Lake City, UT, 2018. [Online]. Retrieved from: https://www-i6.informatik.rwth-aachen.de/~koller/RWTH-PHOENIX-2014-T/. Accessed: Apr. 13, 2026.

[21] H. Zhou *et al.*, "CSL-Daily Dataset", 2021. Retrieved from: https://ustc-slr.github.io/datasets/2021_csl_daily/. Accessed: Apr. 13, 2026.

[22] J. Yu *et al.*, "Dynamic gesture recognition based on 2D convolutional neural network and feature fusion", *Scientific Reports*, 2022, Vol. 12. Retrieved from: https://doi.org/10.1038/s41598-022-08133-z

[23] Yu.V. Krak *et al.*, "Matematychni metody ta prykladni informatsiini tekhnolohii modeliuvannia, perekladu ta navchannia dlia ukrainskoi zhestovoi movy [Mathematical methods and applied informational technologies of modeling, translation and learning for Ukrainian Sign Language]", *Bulletin of Lviv Polytechnic National University: information technologies and networks*, 2016, No. 854, pp. 210–227. [Online]. Retrieved from: http://nbuv.gov.ua/UJRN/VNULPICM_2016_854_22

[24] A. Hlybovets and M. Bikchentayev, "Recognizing gestures of the ukrainian dactylic alphabet", *International Scientific Technical Journal* "*Problems of Control and Informatics*", 2023, Vol. 68, No. 3, pp. 86–100. Retrieved from: https://doi.org/10.34229/1028-0979-2023-3-9

[25] I.O. Burkhan and O.V. Barabanov, "Rozpiznavannia ukrainskoi zhestovoi movy na osnovi kliuchovykh tochok z vykorystanniam rekurentnykh neironnykh merezh [Keypoint-based Ukrainian Sign Language translation using Recurrent Neural Networks]", *Science and Technology Today*, 2023, Vol. 4, No. 18. Retrieved from: https://doi.org/10.52058/2786-6025-2023-4(18)-280-292

[26] N.V. Kuznietsova and S.S. Smirnov, "Uzahalnena metodolohiia rozpiznavannia movy zhestiv na videopotokakh na osnovi neironnykh merezh i transformeriv [A generalized methodology of sign language recognition on video streams based on neural networks and transformers]", Data Recording, Storage & Processing, 2023, Vol. 25, No. 2. pp. 66–76. Retrieved from: https://doi.org/10.35681/1560-9189.2023.25.2.300527

[27] A. Géron, Hands-on Machine Learning with Scikit-Learn, Keras, and TensorFlow (2nd ed.), O'Reilly Media Inc., Sebastopol, CA, 2019. [Online]. Retrieved from: https://shashwatwork.github.io/assets/files/ml_ebook.pdf. Accessed: Apr. 13, 2026.

[28] A. Zhang *et al.*, "Dive into Deep Learning. 5. Multilayer Perceptrons". [Online]. Retrieved from: https://www.d2l.ai/chapter_multilayer-perceptrons/index.html. Accessed: Apr. 13, 2026.

[29] W.F. Maia *et al.*, "Automatic sign language to text translation using MediaPipe and transformer architectures", *Neurocomputing*, 2025, Vol. 642. Retrieved from: https://doi.org/10.1016/j.neucom.2025.130421

[30] "1 Urok Daktylna abetka, kanal "Ukrainska Zhestova mova" [1 Lesson Dactyl alphabet, channel "Ukrainian Sign Language"]. [Online]. Retrieved from: https://www.youtube.com/watch?v=DHo96OMHRyE. Accessed: Apr. 13, 2026.

[31] S.S. Kondratiuk, "Ukrainian dactyl alphabet gesture recognition using cross platform software and convolutional neural networks", *Artificial Intelligence*, 2019, Vol. 24, pp. 107–113. Retrieved from: https://doi.org/10.15407/jai2019.03-04.107

[32] B. Alsharif *et al.*, "Deep Learning Technology to Recognize American Sign Language Alphabet", *Sensors*, 2023, Vol. 23, No. 18, P. 7970. Retrieved from: https://doi.org/10.3390/s23187970

К.Д. Грішин, Н.І. Недашківська

МОДЕЛЬ МАШИННОГО НАВЧАННЯ ДЛЯ РОЗПІЗНАВАННЯ КОНФІГУРАЦІЙ РУК УКРАЇНСЬКОЇ ЖЕСТОВОЇ МОВИ

Проблематика. Розпізнавання жестової мови на основі штучного інтелекту є актуальною, не розв'язаною досі проблемою. Для української жестової мови (УЖМ) завдання ускладнене нестачею публічно доступних датасетів. Тому дослідникам, які працюватимуть в умовах обмежених даних, доцільно використовувати додаткові ознаки для підвищення точності моделей. *Конфігурація рук – основна характеристика лексичних одиниць у будь-якій жестовій мові; в УЖМ їх 40*. Можливість точно визначати конфігурацію надасть інформативні ознаки для систем розпізнавання жестової мови на основі штучного інтелекту.

Мета дослідження. Побудувати модель машинного навчання, здатну розпізнавати покадрово конфігурації УЖМ на відеопотоці з точністю не менше 95 % на перевірочній вибірці та середнім часом виведення результату не більше 70 мс.

Методика реалізації. Як вхідні дані для моделей розпізнавання конфігурацій УЖМ запропоновано систему математичних показників, які обчислюються на основі координат ключових точок, отриманих системою захоплення пози MediaPipe. Навчальну вибірку створено із зображень конфігурацій рук УЖМ з камери, продемонстрованих різними особами середнього віку. Далі через MediaPipe на зображеннях визначено ключові точки руки, розраховано відповідні вектори математичних показників. Було випробовано різні архітектури персептрона та випадкового лісу.

Результати дослідження. Найвищу ефективність показала модель персептрона з двома прихованими шарами по 300 нейронів, яка використовує як вхідні дані вектор запропонованих математичних показників. Модель досягла точності 98,18 % на перевірочній вибірці. Під час апробації у відеопотоці мережа із 40 конфігурацій УЖМ ідентифікувала 32 безпомилково, а 8 – з поодинокими відхиленнями. Середній час виведення результату – 46 мс. Персептрон ідентичної архітектури, що приймав координати ключових точок, показав нижчу точність у режимі відеопотоку. Також запропоновані ознаки підвищили ефективність моделі випадкового лісу, що підтверджує їх універсальність.

Висновки. Серед розглянутих архітектур оптимальною є модель персептрона з двома прихованими шарами по 300 нейронів, яка використовує як вхідні дані вектор запропонованих математичних показників. Вона ідентифікує конфігурації УЖМ у реальному часі, досягаючи точності 98,18 % на перевірочній вибірці. У випробуваннях на основі запропонованого критерію експертного оцінювання на відеопотоці вона безпомилково ідентифікувала на 35 % більше конфігурації (80 % проти 45 %), порівняно з моделлю, що ґрунтується на необроблених координатах ключових точок. Впровадження додаткової верифікації на основі експертних висновків є доцільним, окрім стандартної оцінки точності на перевірочних даних. Зазначена архітектура є першою моделлю для розпізнавання конфігурацій УЖМ на основі штучного інтелекту. Надалі планується інтеграція розробленої мережі в систему розпізнавання ізольованих жестів УЖМ.

Ключові слова: українська жестова мова; машинне навчання; нейронні мережі; комп'ютерний зір; розпізнавання жестів; оцінка якості моделі; інженерія ознак; системний аналіз.

Recommended by the Council
of the Educational and Research Institute
for Applied System Analysis
of Igor Sikorsky KPI

Received: 16 February 2026

Accepted: 08 June 2026

Published: 29 June 2026

DOI: https://doi.org/10.20535/kpisn.2026.2.352454
UDC 004.65

V.P. Holubinka, https://orcid.org/0009-0001-3676-3566
Lviv Polytechnic National University, Lviv, Ukraine, https://ror.org/0542q3127
*Corresponding author: vitalii.p.holubinka@lpnu.ua

AUTONOMOUS INDEX RECOMMENDATION SYSTEM FOR RELATIONAL DATABASES BASED ON COST-MODEL AND PLAN COVERING

Background. Indexing is a key tool for improving the performance of relational databases, but manual index selection remains complex and subjective. As data volumes grow, the demands on the adaptability of optimisation systems increase. Machine and deep learning-based approaches provide high accuracy, but require significant resources and have a "cold start" problem, which necessitates autonomous solutions with balanced accuracy and complexity characteristics.

Objective. Development and experimental evaluation of an autonomous index recommendation system that combines a Query Cost-Model with a Plan Covering algorithm to improve query performance in relational databases while simultaneously taking into account the cost of index storage.

Methods. The system has a pipeline architecture and includes a workload analyser, a cost model, and a Plan Covering algorithm. The analyser generates a query profile, the cost model evaluates their performance with hypothetical indexes, and the algorithm performs a greedy index selection based on the benefit-to-cost ratio. Experimental testing was performed on a synthetic e-commerce system dataset in the PostgreSQL environment.

Results. The system generated 7 index recommendations, of which 6 were successfully created. The average query execution time improvement was 22.54 %, with the largest improvement (26.06 %) being obtained for the most frequently executed query with the JOIN operation. The total execution time of all queries decreased from 0.2751 s to 0.2131 s.

Conclusions. The proposed combination of Cost-Model and Plan Covering provides effective automation of the indexing process without the use of resource-intensive neural network approaches, demonstrating a significant improvement in performance and rational use of storage resources.

Keywords: database indexing; query optimisation; autonomous recommendation systems; cost mode; Plan Covering.

Introduction

Database performance optimisation is a fundamental prerequisite for the efficient operation of modern information systems. Among the most effective means of accelerating query execution, indexing holds a prominent place. However, manually selecting an optimal set of indexes remains a complex, laborious, and largely subjective process. Consequently, the automation of index design has gained renewed momentum in recent scientific research. Analysis of the current body of literature reveals a dominance of English-language publications, reflecting global trends in IT science development. Notably, researchers from leading Asian universities and research centers have made significant contributions to shaping modern approaches to optimisation [1–4].

The current spectrum of solutions in this field [1] encompasses both classical heuristic and deterministic algorithms, as well as adaptive systems built on machine learning [2] and deep reinforcement

Пропозиція для цитування цієї статті: В.П. Голубінка, «Автономна система рекомендації індексів для реляційних баз даних на основі Cost-Model та Plan Covering», *Наукові вісті КПІ*, № 2, с. 20–26, 2026. doi: https://doi.org/10.20535/kpisn.2026.2.352454

How to cite this article: V.P. Holubinka, "Autonomous index recommendation system for relational databases based on Cost-Model and Plan Covering", *KPI Science News*, No. 2, pp. 20–26, 2026. doi: https://doi.org/10.20535/kpisn.2026.2.352454

© The Autor(s).
The article is distributed under the terms of the license CC BY 4.0

learning methods [3, 4]. Despite their high autonomy and self-learning capabilities, these approaches are characterised by high computational costs, implementation complexity, and the "cold start" problem. Under resource constraints, the use of resource-intensive neural network models is often economically and technologically impractical. Therefore, the scientific challenge of finding a compromise between the accuracy of recommendations, system stability, and computational complexity remains relevant. Classical deterministic algorithms, such as Plan Covering, retain their competitiveness due to their transparency, reproducibility of results, and predictable behaviour.

Methods

This research employed a combination of theoretical and experimental methods to ensure the validity of the findings.

During the theoretical stage, methods of structural analysis, systematisation, and comparison of scientific sources were used to investigate contemporary approaches to automated index recommendation in relational databases. Existing methods were classified based on their construction principles, and a comparative analysis of deterministic algorithms and machine learning methods regarding their effectiveness in optimising SQL queries was conducted.

To formalise the task of index selection, mathematical modelling was applied, including the construction of a Query Cost-Model that considers costs associated with table scanning, index usage, and query frequency. The problem of selecting an optimal set of indexes was formalised as a combinatorial optimisation problem with storage budget constraints.

The Plan Covering algorithm was implemented for index selection using an optimisation method that sequentially maximises the ratio of benefit to storage cost.

The autonomous index recommendation system's effectiveness experimental validation, which combines the Cost-Model and Plan Covering algorithm, was performed through computational experiments based on a synthetic dataset simulating typical workloads of an e-commerce system. Performance evaluation involved measuring the execution time of SQL queries before and after applying recommended indexes, followed by statistical averaging of the results.

Descriptive statistics methods were employed to process experimental results, including calculating mean values, percentage improvements, and an integrated performance indicator considering query frequencies.

Problem Statement

The paper aims to develop and experimentally evaluate an autonomous index recommendation system that combines a Query Cost-Model with the Plan Covering algorithm. The goal is to improve query performance while considering the storage cost of indexes. This approach seeks to balance recommendation effectiveness with computational simplicity, avoiding resource-intensive neural network techniques.

Autonomous Index Recommendation System Architecture and Plan Covering Algorithm

The proposed system consists of three main components:

– Workload Analyser: collects and analyses incoming queries;

– Cost-Model: evaluates the cost of executing queries with different index configurations;

– Plan Covering algorithm: selects an optimal set of indexes based on performance improvement within a given storage budget.

These components interact in a sequential data processing pipeline. The process initiates with the Analyser gathering actual query statistics to establish a contemporary system workload profile. The data is subsequently transmitted to the Cost-Model, which functions as a virtual optimiser: it emulates the existence of theoretical indexes (utilising a "what-if" mechanism) and computes the anticipated decrease in query execution costs without the need to physically establish any data structures. Ultimately, the Plan Covering algorithm employs these cost estimates as input parameters to address a combinatorial optimisation challenge, pinpointing a selection of indexes that enhances performance improvement within the designated memory budget. The Cost-Model assesses the execution of query Q with index set I as (1) [1, 2]:

$$Cost(Q,I) = \sum_{op \in Operation(Q)} cost(op,I), \qquad (1)$$

where cost(op, I) is the cost of op operation given I indexes.

For table scan operation (2):

$$cost_{scan}(T,I) = \begin{cases} |T| \cdot c_{page}, & \text{if } I = \varnothing \\ |T| \cdot c_{index} + |R| \cdot c_{page}, & \text{if } \exists idx \in I, \end{cases} \qquad (2)$$

where $|T|$ is the table size; $|R|$ is the result size; c_{page} and c_{index} are cost constants.

Let's describe the Plan Covering algorithm.

Input Data:

– a set of queries $Q = \{q1, q2, ..., qn\}$;

– a set of index candidates $C = \{c1, c2, ..., cm\}$.

Output Data:

– optimal set of indexes I^*.

Algorithm:

Step 1: Initialisation.

1.1. Initialise the optimal set of indexes I^* as an empty set:

– $I^* = Ø$ (empty set).

1.2. Initialise the benefit dictionary, benefit, as empty:

– benefit = Ø (empty dictionary).

Step 2: Calculate benefit for each candidate.

For each candidate *ci* from the set *C* do:

2.1. Set initial benefit:

– benefit[*ci*] = 0.

2.2. For each query *qj* from the set *Q* do:

2.2.1. Calculate the cost of executing query *qj* with the current set of indexes I^*:

– cost_old = *Cost*(*qj*, I^*).

2.2.2. Calculate the cost of executing query *qj* by adding candidate *ci*:

– cost_new = *Cost*(*qj*, $I^* \cup \{ci\}$);

– (where symbol ∪ denotes set union).

2.2.3. Update the benefit for candidate *ci*:

– benefit[*ci*] = benefit[*ci*] + (cost_old − cost_new);

– (Benefit equals the decrease in query execution cost).

Step 3: Select optimal set of indexes.

While the candidate set *C* is not empty, do:

3.1. Find the best candidate with the maximum benefit-to-storage cost ratio:

– *c*_best = argmax_{$c \in C$} (benefit[*c*] / storage(*c*)),

where:

– benefit[*c*] is the total benefit from index *c*;

– storage(*c*) is the storage cost of index *c*;

– argmax means finding the argument (candidate) for which the function reaches its maximum.

3.2. Add the best candidate to the optimal set:

– $I^* = I^* \cup \{c_best\}$;

– (add *c*_best to the set I^*).

3.3. Remove the best candidate from the candidate set:

– $C = C \setminus \{c_best\}$;

– (remove *c*_best from the set *C*).

3.4. Update benefit for remaining candidates considering the new index *c*_best;

– (Since adding a new index may change the benefit of other candidates).

Step 4: Result return.

Return the optimal set of indexes I^*.

The Plan Covering algorithm is a greedy algorithm that sequentially selects indexes with the maximum benefit-to-storage cost ratio. The benefit of an index is defined as the sum of reductions in execution cost for all queries that can use this index. The algorithm considers query execution frequencies through the Cost function, which may multiply the execution cost by the query frequency.

The subsequent points outline the essential characteristics of the algorithm:

1. It considers both the benefit of improved performance and the storage cost of indexes, thereby preventing the creation of an excessive number of indexes.

2. Index selection is determined by the benefit-to-cost ratio, rather than solely by the benefit itself, thereby guaranteeing the optimal utilisation of storage resources.

3. Following the addition of each index, the benefit for the other candidates is reassessed, since the introduction of a new index can alter the efficacy of the existing indexes.

4. The algorithm continues to operate until every candidate has been evaluated or the storage budget limit is reached.

Experimental Evaluation of the Autonomous Index Recommendation System Efficiency

To verify the effectiveness of the proposed autonomous indexing recommendation system based on Cost-Model + Plan Covering, a series of experiments was conducted on a synthetic dataset. The goal of the experimental evaluation was to determine how effectively the system can automatically generate index recommendations and improve query execution performance compared to a baseline configuration without indexes. Experiments included measuring query execution time before and after applying recommended indexes, analysing the number of generated recommendations, and evaluating the overall improvement in system performance.

Experiments were conducted on PostgreSQL 15 in a Docker container with the following parameters:

– database: PostgreSQL 15 (Alpine Linux);

– environment: Docker container;

– database size: 61 000 records (10 000 customers + 1000 products + 50 000 orders);

– measurement method: each query was executed 3 times to average the results.

Experiments were conducted on a synthetic dataset modelling a typical e-commerce system:

– customers table – 10 000 records (customers with the following fields: name, email, city, registration_date);

– products table – 1000 records (products with the following fields: name, category, price, stock_quantity);

– orders table – 50 000 records (orders with the following fields: customer_id, product_id, order_date, quantity, total_amount).

Five test queries of differing complexity were developed:

1. Simple SELECT with WHERE and ORDER BY (frequency: 10).

2. JOIN with WHERE condition (frequency: 15).

3. GROUP BY with aggregation (frequency: 8).

4. Complex JOIN with GROUP BY and HAVING (frequency: 5).

5. Subquery with ORDER BY (frequency: 12).

The following metrics were used to evaluate the system's effectiveness:

1. Execution time improvement (3):

$$\frac{T_{before} \cdot T_{after}}{T_{before}} \times 100\%, \quad (3)$$

where T_{before} and T_{after} are the execution times before and after optimisation.

2. Average improvement – arithmetic mean improvement across all queries.

3. Total improvement – improvement in total execution time taking into account query frequency.

4. Number of recommended indexes – the number of indexes generated by the Plan Covering algorithm.

5. Number of successfully created indexes – the number of indexes that were successfully created in the database.

Each query was performed three times to average the results and reduce the influence of random factors.

All experimental results were recorded and organised for analysis, and are accessible for reproduction.

Research findings indicated that the proposed system yields the subsequent outcomes. The system evaluated 5 test queries and produced 7 index recommendations, out of which 6 were successfully established. The results obtained are as follows:

– average execution time improvement: 22.54 %;

– total performance improvement: 22.54 %;

– execution time before optimisation: 0.0550 s (average), 0.2751 s (total);

– execution time after optimisation: 0.0426 s (average), 0.2131 s (total);

– number of recommended indexes: 7;

– number of successfully created indexes: 6.

Table 1 presents the precise numerical values of query execution durations prior to and following optimisation.

Table 1. Results of query performance improvement

Request	Frequency	Time before, s	Time after, s	Improvement, %
1	10	0.0065	0.0057	11.78
2	15	0.2186	0.1617	26.06
3	8	0.0035	0.0035	–0.12
4	5	0.0165	0.0143	13.17
5	12	0.0300	0.0279	7.00

The most significant enhancement (26.06 %) was realised for query 2, which exhibits the highest execution frequency (15) and involves a JOIN operation. This validates the system's capability in pinpointing critical indexes for the most frequently used queries. Figures 1 and 2 depict the overall patterns in performance variations and facilitate a visual assessment of the efficiency of the suggested indexes.

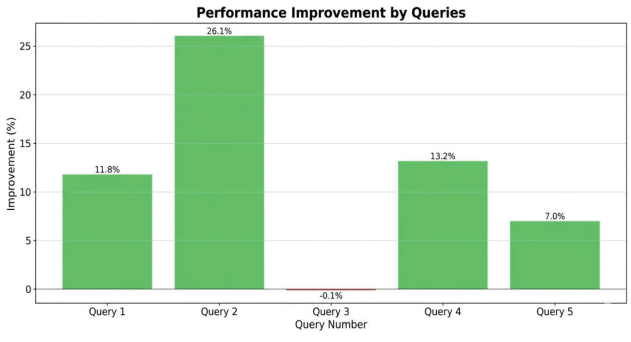


Fig. 1. Comparison of query performance before and after optimisation

The system generated the following index recommendations:

– customers (city) – for filtering by city;

– orders (customer_id) – for JOIN operations;

– products (stock_quantity) – for filtering by availability;

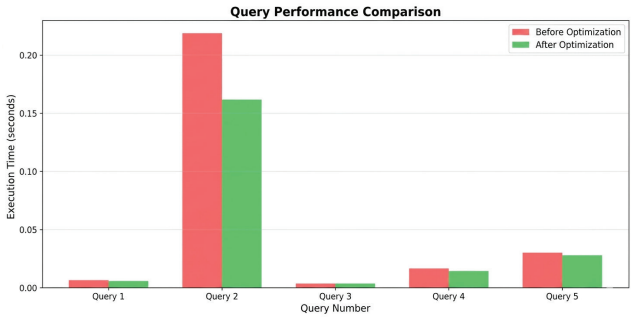


Fig. 2. Query performance improvement, %

– customers (customer_id) – for JOIN operations;

– orders (order_date) – for filtering by date;

– customers (registration_date) – for sorting;

– orders (category) – not created (column does not exist).

An examination of the execution duration for each stage of the experiment facilitates an assessment of the impact of every system component on the overall performance. As illustrated in Fig. 3, the majority of the time is allocated to the Cost-Model operation and candidate evaluation, whereas workload analysis and the final index selection occupy a minimal fraction of the total time. This observation underscores the computational efficiency of the proposed methodology and its appropriateness for implementation in systems characterised by dynamic workloads.

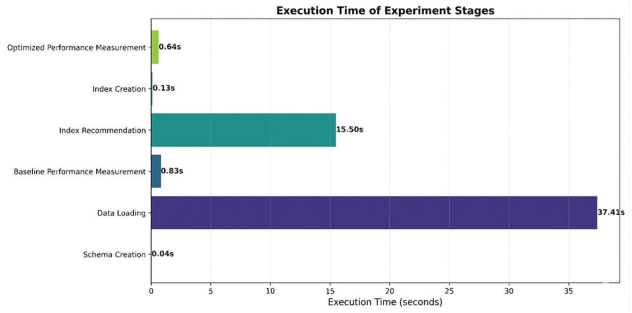


Fig. 3. Duration of the execution phases of the experiment

To comprehensively assess the effectiveness of the proposed system, summary metrics from the experiment were computed, which included performance improvement, query execution duration prior to and following optimisation, along with the count of indexes that were generated and created. The findings are displayed in Table 2.

All experimental data, encompassing detailed metrics for each query, were preserved in structured CSV and JSON formats to facilitate analysis, further processing, and result reproduction.

Table 2. Results of query performance improvement

Metric	Value
Performance gain (average)	22.54 %
Performance gain (overall)	22.54 %
Time before optimisation (average)	0.0550 s
Time after optimisation (average)	0.0426 s
Time before optimisation (overall)	0.2751 s
Time after optimisation (overall)	0.2131 s
Number of recommended indexes	7
Number of successfully created indexes	6

To exemplify the effectiveness of the results obtained, consider an instance of applying the system to a real e-commerce dataset. The system evaluated five test queries of varying complexity and automatically produced seven index recommendations. The most significant query (query 2 with a frequency of 15) realised a performance enhancement of 26.06 %, showcasing the system's capability to accurately identify and optimise the most frequently utilised queries. The generated indexes contributed to a reduction in the total execution time of all queries from 0.2751 seconds to 0.2131 seconds, representing a substantial improvement for high-load systems.

Future research avenues include broadening the functionality and enhancing the accuracy of the proposed system. A promising direction involves the integration of machine learning techniques to refine the accuracy of the query Cost-Model, enabling more precise predictions of index efficiency based on historical query execution data and fluctuations in workload.

A crucial area for further investigation is the development of mechanisms for the dynamic adaptation of indexes in response to workload changes, which would enable the system to automatically refresh the index configuration when the nature of queries or data structure evolves, eliminating the need to rerun the recommendation process.

Another promising path is the expansion of the system to accommodate complex types of indexes, such as Generalized Inverted Index and Generalized Search Tree, which are utilised for specialized data types and search operations, thereby broadening the system's applicability to a wider array of database optimisation tasks.

Conclusions

The study introduces an autonomous index recommendation system tailored for relational databases, which integrates a Query Cost-Model with the Plan Covering algorithm. This innovative system employs a pipeline approach that encompasses workload analysis, assessment of SQL query execution costs, and a greedy selection process for indexes based on the criterion of benefit-to-storage cost ratio.

Experimental investigations carried out on a synthetic dataset simulating an e-commerce system demonstrated that the system is capable of autonomously generating effective index recommendations without resorting to resource-intensive machine learning techniques. Throughout the experiment, seven index recommendations were produced, six of which were successfully implemented within the database.

The results obtained validated the efficacy of the proposed method: the average reduction in SQL query execution time was 22.54 %, and the total execution time for all queries diminished from 0.2751 seconds to 0.2131 seconds. The most significant optimisation effect (26.06 %) was noted for the most frequently executed JOIN query, thereby affirming the accuracy of the mechanism that accounts for query execution frequency.

Consequently, the findings of this research substantiate the effectiveness of the autonomous index recommendation system based on Cost-Model and Plan Covering as a viable tool for automating the indexing process in relational databases. The suggested approach strikes a balance between query performance and storage costs, rendering it appropriate for application in real information systems characterised by dynamic workloads.

References

[1] S. Huang *et al.*, "Survey on performance optimization for database systems", *Science China Information Sciences*, 2023, Vol. 66, No. 12, pp. 1–22. Retrieved from: https://doi.org/10.1007/s11432-021-3578-6

[2] J. Shi *et al.*, "Learned index benefits: Machine learning based index performance estimation", P*roceedings of the VLDB Endowment*, 2022, Vol. 15, No. 13, pp. 3950–3962. Retrieved from: https://doi.org/10.14778/3565838.3565848

[3] H. Lan *et al.*, "An index advisor using deep reinforcement learning", in *Proceedings of the 29th ACM International Conference on Information and Knowledge Management (CIKM)*, 2020, pp. 2105–2108. Retrieved from: https://doi.org/10.1145/3340531.3412106

[4] X. Huang *et al.*, "Ditune: A reinforcement learning based framework for automated database index selection", in *Proceedings of the 18th International Conference on Ubiquitous Information Management and Communication (IMCOM)*, 2024, pp. 1–8. Retrieved from: https://doi.org/10.1109/IMCOM60618.2024.10418292

Голубінка В.П.

АВТОНОМНА СИСТЕМА РЕКОМЕНДАЦІЇ ІНДЕКСІВ ДЛЯ РЕЛЯЦІЙНИХ БАЗ ДАНИХ НА ОСНОВІ COST-MODEL ТА PLAN COVERING

Проблематика. Індексація є ключовим засобом підвищення продуктивності реляційних баз даних, однак ручний вибір індексів залишається складним і суб'єктивним. Зі зростанням обсягів даних підвищуються вимоги до адаптивності систем оптимізації. Підходи на основі машинного і глибокого навчання забезпечують високу точність, але потребують значних ресурсів і мають проблему «холодного старту», що зумовлює необхідність автономних рішень із збалансованими характеристиками точності та складності.

Мета дослідження. Розроблення та експериментальне оцінювання автономної системи рекомендації індексів, що поєднує модель вартості виконання запитів (Cost-Model) з алгоритмом Plan Covering для підвищення продуктивності виконання запитів у реляційних базах даних з одночасним врахуванням вартості зберігання індексів.

Методика реалізації. Система має конвеєрну архітектуру і включає аналізатор робочого навантаження, модель вартості й алгоритм Plan Covering. Аналізатор формує профіль запитів, модель вартості оцінює їх виконання з гіпотетичними індексами, а алгоритм здійснює жадібний вибір індексів за співвідношенням вигоди до вартості зберігання. Експериментальну перевірку виконано на синтетичному наборі даних e-commerce системи в середовищі PostgreSQL.

Результати дослідження. Системою згенеровано 7 рекомендацій індексів, з яких 6 було успішно створено. Середнє покращення часу виконання запитів склало 22,54 %, а найбільше покращення (26,06 %) отримано для найбільш часто виконуваного запиту з операцією JOIN. Загальний час виконання всіх запитів зменшився з 0,2751 с до 0,2131 с.

Висновки. Запропоноване поєднання Cost-Model і Plan Covering забезпечує ефективну автоматизацію процесу індексації без використання ресурсоємних нейромережевих підходів, демонструючи суттєве покращення продуктивності й раціональне використання ресурсів зберігання.

Ключові слова: індексація баз даних; оптимізація запитів; автономні системи рекомендацій; модель вартості; Plan Covering.

Recommended by the Council
of the Faculty of Software Systems
and Applied Mathematics
of Igor Sikorsky KPI

Received: 19 February 2026

Accepted: 08 June 2026

Published: 29 June 2026

ЕЛЕКТРОНІКА, ЕЛЕКТРОННІ КОМУНІКАЦІЇ, ПРИЛАДОБУДУВАННЯ ТА РАДІОТЕХНІКА

DOI: https://doi.org/10.20535/kpisn.2026.2.356692
UDC 621.39:681.586:621.039:539.1.04

L.K. Hlinenko[1], https://orcid.org/0000-0002-3105-4568
P.I. Kost[1*], https://orcid.org/0009-0002-9863-6172
Lviv Polytechnic National University, Lviv, Ukraine, https://ror.org/0542q3127
*Corresponding author: pavlo.kost.asp.2025@lpnu.ua

METHODOLOGY FOR SELECTING THE TRANSMISSION PATH STRUCTURE IN FUSION POWER PLANTS

Background. In fusion facilities, the transmission of measurement signals from sensors takes place under conditions of intense ionising radiation, high temperatures and significant electromagnetic interference, leading to the degradation of sensors and transmission lines, increased signal loss and a reduction in the signal-to-noise ratio. The transmission of weak signals over long distances is particularly critical, requiring a well-founded choice of transmission path structure based on a systematic consideration of the characteristics of the sensors and transmission lines, taking into account a range of influencing factors, including radiation exposure, temperature conditions, electromagnetic interference, signal loss and changes in the signal-to-noise ratio.

Objective. The paper aims to justify an approach to selecting the transmission path structure for long data transmission lines in thermonuclear facilities based on a systematic and multi-criteria analysis of sensor and transmission channel characteristics.

Methods. A systematic analysis of modern sensor solutions and transmission line types was employed, alongside a multi-criteria approach taking into account radiation immunity, temperature stability, noise immunity, signal-to-noise ratio and long-term parameter stability. The transmission path is considered as a set of interrelated elements: the sensor, local converter, transmission line and data acquisition module, which determine the efficiency of signal transmission. To compare alternatives, the characteristics were normalised and visualised using polar diagrams.

Results. It has been established that inductive sensors are characterised by high radiation resistance but are limited in measuring static fields, whereas Hall sensors provide direct measurement of static and alternating magnetic fields, yet are subject to radiation-induced drift. It has been shown that bismuth and ceramic Hall sensors exhibit enhanced long-term stability. It has been determined that coaxial cables are susceptible to radiation ageing and signal loss, whereas fibre-optic and mineral-insulated lines provide better noise immunity and parameter stability. The feasibility of local signal digitisation and the use of optical transmission channels is justified. Based on the analysis carried out, the structure of the transmission path has been established, whilst the merits of local signal digitisation and the use of fibre-optic transmission channels to improve reliability and noise immunity have been demonstrated.

Conclusions. An approach to selecting the structure of the transmission path is proposed, based on a comprehensive consideration of the characteristics of sensors and transmission lines. It is shown that the most effective solutions for constructing the transmission path are those involving a combination of radiation-resistant sensors, local signal processing and digitisation directly at the sensor, and the use of fibre-optic transmission channels. This approach ensures improved measurement accuracy and data transmission reliability in the long transmission lines of thermonuclear facilities under conditions of ionising radiation, high temperatures and electromagnetic interference.

Keywords: transmission path; long-distance data transmission lines; information transmission channels; noise immunity; signal-to-noise ratio; electromagnetic interference; fibre-optic communication channels; digital signal processing; telecommunications systems; radiation immunity.

Пропозиція для цитування цієї статті: Л.К. Гліненко, П.І. Кость, «Методика вибору структури передавального тракту для термоядерних установок», *Наукові вісті КПІ*, № 2, с. 27–35, 2026. doi: https://doi.org/10.20535/kpisn.2026.2.356692

How to cite this article: : L.K. Hlinenko, P.I. Kost, “Methodology for selecting the transmission path structure in fusion power plants”, *KPI Science News*, No. 2, pp. 27–35, 2026. doi: https://doi.org/10.20535/kpisn.2026.2.356692

© The Autor(s).
The article is distributed under the terms of the license CC BY 4.0

Introduction

Modern tokamak installations are characterised by a complex interplay of ionising radiation, high temperatures, and Electromagnetic Interference (EMI), significantly complicating the transmission of weak signals over long communication lines. In scenarios with considerable transmission path lengths (tens to hundreds of meters), signal losses, distortions, and degradation of the Signal-to-Noise Ratio (SNR) occur, limiting measurement accuracy and reliability. Under these conditions, the justified selection of a transmission tract structure becomes crucial, considering the combined influence of factors such as radiation degradation of components, temperature instability of parameters, EMI impact, signal losses in transmission lines, and SNR variations.

Analysis of current research reveals that signal transmission efficiency is determined by sensor and transmission channel characteristics, as well as their interaction under radiation and electromagnetic influences. Inductive and Hall-effect sensors are widely used in magnetic diagnostics but experience parametric drift and sensitivity limitations due to irradiation. Long cable transmission lines are highly susceptible to degradation caused by radiation-induced material ageing, temperature variations, and EMI, leading to increased signal losses. Optical fibre channels offer high noise immunity but also have limitations associated with radiation attenuation.

Despite the availability of individual technical solutions, a comprehensive approach to selecting a transmission tract structure based on systematic consideration of radiation resistance, temperature stability, noise immunity, and signal characteristics is lacking. The formal comparison of alternative solutions and ensuring stable transmission of weak signals over long lines under complex destabilising factors remain underexplored.

Therefore, this work addresses the challenge of justifying an approach to selecting a transmission tract structure based on multi-criteria analysis of sensor and channel characteristics to enhance measurement reliability in tokamak installations.

Problem Statement

Given the complex operating conditions of tokamak installations characterised by intense ionising radiation, high temperatures, and significant EMI, there is a need to ensure reliable transmission of weak measurement signals over long distances.

Analysis of current research indicates that existing technical solutions are typically focused on individual elements of the transmission tract (sensors or transmission lines) and do not provide for their comprehensive coordinated consideration in terms of radiation resistance, temperature stability, noise immunity, and impact on the SNR.

Therefore, the objective of this work is to develop a methodology for selecting the structure of a transmission tract for long data transmission lines in tokamak installations based on a systematic and multi-criteria analysis of sensor and channel characteristics.

Analysis of Modern Approaches to Long Data Transmission Lines

The effectiveness of signal transmission over long lines under intense neutron and γ-radiation, high temperatures, and strong EMI depends on a combination of various physical, design, and technological factors. A key feature of such systems is the use of long signal transmission lines connecting primary sensors located near the plasma chamber to remote data acquisition and processing systems located outside the radiation zone [1, 2, 3].

Effective transmission of weak signals requires ensuring a high SNR and minimising distortions [4, 5, 6]. The transmission tract includes: sensor → local transducer → transmission line → Data Acquisition Module (DAM) [7, 8, 9, 10, 11, 12]. A generalised structure of the transmission tract used in tokamak installations is shown in Fig. 1. The sensor node provides direct measurement of plasma physical parameters; the integrated transducer performs local processing and digitisation of the signal (noise filtering, calibration, preparation for further transmission); the long line and final DAM transmit data to central data acquisition and processing systems. Critical factors include the small amplitude of signals and their high sensitivity to noise and radiation [9, 10, 13, 14, 15]. This has necessitated the deve-

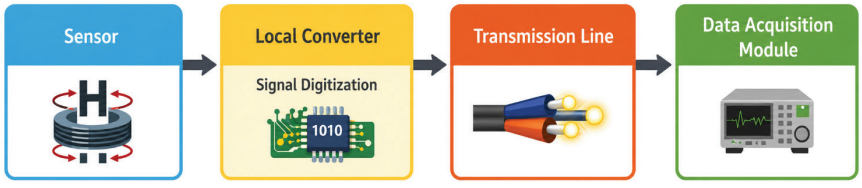


Fig. 1. Structure of a Transmission Tract for Tokamak Installations

lopment of specialised approaches that ensure not only the stability of electrical parameters of lines but also their radiation resistance, mechanical strength, and electromagnetic compatibility [9, 10, 16, 17].

The primary challenges facing sensors operating under intense ionising radiation, high temperatures, and EMI include radiation-induced parameter drift, reduced sensitivity, and the need for error compensation [7, 8, 9, 10, 11, 12, 18, 19]. Requirements for magnetic diagnostic systems in tokamak installations necessitate radiation resistance, high measurement accuracy, and stable operation during long plasma pulses [3, 20, 21]. Improved efficiency of transmission tracts is achieved by integrating a portion of the signal conversion directly within the sensor zone, which minimises the impact of induced voltages and parametric drifts in long transmission lines [7, 22].

The choice of sensor type is a defining factor in transmission tract design as it dictates the requirements for the transmission channel structure and signal processing methods [7, 8]. Table 1 presents relevant types of magnetic sensors and their key characteristics.

To generalise the results and justify the selection of sensors and transmission channels, a multi-criteria approach is appropriate. Based on an analysis of sensor characteristics (Table 1), a system of evaluation criteria has been developed, including radiation resistance, temperature stability, noise immunity, and suitability for use in long transmission lines [3, 12, 18].

Analysis shows that inductive coils exhibit high radiation resistance but are limited in measuring DC magnetic fields and prone to distortion during long-distance signal transmission [4, 18]. Hall sensors allow direct measurement of both DC and AC magnetic fields created by DC and AC currents, but experience parametric drift under radiation exposure [12]. Meanwhile, bismuth Hall sensors demonstrate enhanced long-term stability and are more suitable for stationary operating modes [23, 24, 25].

Thus, the analysis results confirm the advisability of using combined sensor solutions considering operating conditions and requirements for the transmission tract [3, 18, 22, 26].

Experimental studies of neutron effects have demonstrated that:

- Inductive coils do not structurally degrade but accumulate *integration drift* [3, 9].
- Hall sensors remain functional but experience *radiation-induced parameter drift* [8, 11, 12].

Table 1. Types of Magnetic Sensors and Their Key Characteristics

Sensor type	Stability	Range	Key issues	Benefits for long lines	Source
Inductive coils	–	variable fields	integration drift	simplicity, radiation resistance	[3, 9, 20, 21]
Hall sensors (InSb/GaAs)	medium to high (~10^{17}–10^{18} n/cm^2)	~150–220 °C	drift, variable sensitivity	direct measurement of direct current	[11, 12, 8]
Hall sensors (Bi)	very high (~10^{18}–10^{19} n/cm^2)	direct and alternating current up to 200 °C	radiation defects, control of temperature dependencies	direct measurement of direct current	[8, 11,18, 19]
Ceramic Hall sensors	very high, stable up to ~550 °C	~up to 550 °C	manufacture and calibration	direct measurement of direct current	[4, 8]
Fluxgate sensors	average	depends on the design	limited linearity	–	[3, 9]
Optical sensors	high (up to radiation-induced attenuation)	depends on the glass	radiation-induced attenuation	–	[23, 24]
High-frequency sensors	–	high frequencies	noise, interference	local processing	[22]
Integrated FIMDs	–	direct current (DC) – alternating current (AC)	complexity	minimisation of linear distortion	[7]

• Bismuth Hall sensors demonstrate better long-term stability, making them promising for International Thermonuclear Experimental Reactor (ITER) [8, 18].

Radiation hardness and temperature stability of sensors determine their suitability for use in long transmission lines [9, 12]. Hall sensors enable measurements of both DC and AC magnetic fields over a wide range of conditions but suffer from parametric drift under irradiation [11, 12]. Ceramic and bismuth Hall sensors exhibit enhanced stability, expanding their applicability in environments with intense radiation exposure [23, 24, 25].

Fluxgate sensors are used as auxiliary tools for refining local magnetic profiles [9], while optical sensors and fibre optic lines provide high noise immunity and minimal signal loss over long distances [23, 27].

Generalising the results of experiments shows the effectiveness of combined sensor systems for ensuring stability and accuracy in long-distance data transmission [7, 8, 17, 22].

Long transmission lines are the most vulnerable part of the transmission tract as they experience a complex interplay of radiation, temperature, and electromagnetic factors [1, 2, 23, 27]. Research shows that coaxial cables degrade due to dielectric damage, while fibre optic lines are susceptible to radiation-induced attenuation [6, 28, 29, 30].

Signal transmission over tens of meters from sensors to Data Acquisition Systems (DAS) is accompanied by increased losses, induced noise, and changes in line electrical parameters, which complicates ensuring stability and accuracy of measurements [2, 23].

Therefore, the main limiting factors for long transmission lines are radiation degradation of materials, EMI, and parametric changes in cables. This necessitates the application of specialised technical solutions to improve noise immunity and data transmission reliability.

Long cable transmission lines exhibit increased sensitivity to interference, leading to signal quality degradation during long-distance transmission. This is particularly evident in high-frequency channels where cable parameters and shielding effectiveness significantly influence transmission accuracy [22]. Additionally, temperature and mechanical influences cause changes in line electrical characteristics, which, combined with radiation effects, complicate signal stability assurance.

Radiation-induced ageing of cable materials leads to increased signal loss, changes in characteristic impedance, and degraded insulation properties [4, 23, 24, 26, 27]. Consequently, traditional electrical transmission lines are inferior to fibre optic systems, which offer higher noise immunity, lower losses, and provide galvanic isolation between transmission channels [27, 28].

A review of current solutions indicates that tokamak facilities for data transmission employ coaxial, mineral-insulated, fibre optic, and hybrid metal-optic transmission lines [6, 31, 32, 33] (Table 2).

Table 2. Types of transmission lines and their main characteristics

Line type	Radiation resistance	Temperature range	Advantages	Restrictions	Scope of application
Copper coaxial cables (standard polymer insulation) [6]	≈10^4 Gr	up to ~250 °C	affordable, easy to connect, stable impedance	low radiation resistance, signal loss, radiation ageing of insulation, noise induction	secondary control circuits
Mineral-insulated cables (MgO, Al_2O_3) [31]	≈10^7 Gr	up to ~900 °C	high resistance to radiation and heat	high rigidity, difficult to install	current sensors, magnetic diagnostics
Fibre-optic lines (SiO_2) [32]	≈10^5 Gr	up to ~300 °C	high SNR, immunity to EMI	radiation opacification of glass at doses >10^6 Gr	transfer of ITER diagnostic data
Hybrid metal-fibre lines (fibre + copper) [33]	≈10^6–10^7 Gr	~300–500 °C	the ideal balance, combining reliability and speed, with the option of redundancy	greater system complexity, high cost, complex temperature compensation	recording of transient processes in plasma

Methodology for Selecting the Structure of a Transmission Tract

Considering the analysis of sensor and transmission line characteristics (Table 1), it is advisable to develop a methodology for selecting the structure of a transmission tract based on multi-criteria evaluation. This approach allows us to move from a descriptive analysis to a formalised comparison of alternative solutions, taking into account the operating conditions in tokamak installations.

To tackle this task and execute the suggested methodology, the subsequent essential steps are advised:

– define a system of criteria for evaluating sensor and transmission line characteristics that influence signal transmission efficiency;

– formulate the structure of the transmission tract as a set of interconnected elements: sensor, local converter, transmission line, DAM;

– identify the main factors influencing signal parameters under operating conditions: ionising radiation, temperature, EMI;

– analyse the mutual influence of transmission tract elements and environmental factors on signal characteristics;

– conduct multi-criteria evaluation of alternative options for building a transmission tract;

– develop comprehensive visualisation of evaluation results (including the use of polar diagrams) to compare alternatives;

– select a rational structure for the transmission tract, considering operating conditions and requirements for signal transmission reliability.

The following criteria should be used as the main evaluation criteria:

– radiation resistance of tract elements;

– temperature stability;

– SNR;

– sensitivity to EMI;

– stability of parameters during long-term operation;

– suitability for use in long transmission lines.

Based on these criteria, a generalised evaluation system is formed, which allows comparing different types of sensors (inductive, Hall, Bismuth Hall, optical) and transmission lines (coaxial, mineral-insulated, fibre optic, hybrid).

To visually represent the results of multi-criteria analysis, it is advisable to use polar diagrams [34], which allow simultaneously visualising and comparing several parameters. This approach provides the possibility of visual comparison of alternatives and determining the most effective configurations of the transmission tract depending on the level of radiation load, temperature conditions, and accuracy measurement requirements.

The application of the proposed methodology shows that for conditions of intense radiation exposure and significant transmission line lengths, the most appropriate solution is to use combined solutions, which involve:

– local conversion and digitisation of the signal directly near the sensor;

– using fibre optic channels for transmitting digital data;

– applying radiation-resistant sensors (in particular, Bismuth Hall sensors or integrated modules);

– redundancy of transmission channels to improve reliability.

Thus, the proposed methodology allows us to rationally form the structure of a transmission tract that ensures minimisation of information loss and increased measurement accuracy in the complex operating conditions of tokamak installations.

This section proposes a multi-criteria approach to sensor selection using polar diagrams for comparison. To facilitate comparison, parameters were normalised on an ordinal scale of 1–4 based on the comparison of real values (Table 1). The results are visualised in Fig. 2.

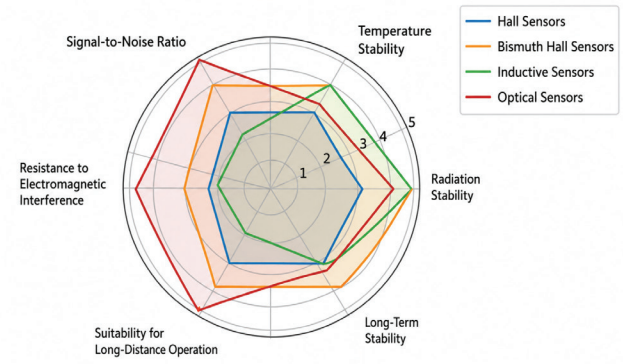


Fig. 2. Polar diagram comparing sensor types based on key criteria

The constructed polar diagram allows us to move from a qualitative description of sensor characteristics to their formalised comparison based on a set of criteria that define their effectiveness in long data transmission lines.

Optical sensors excel in interference immunity, SNR, and long-distance transmission efficiency. Bismuth Hall sensors demonstrate superior radiation hardness and long-term stability. In contrast, inductive and classic Hall sensors form a limited application area due to their lower values of integrated characteristics for long transmission tracts.

Thus, the results of the system analysis confirm that the optimal structure of a transmission tract should be based on a combination of different sensor types, considering dominant influencing factors. This approach minimises information loss and enhances measurement accuracy.

Research in [6, 31, 32, 33] examines the behaviour of various transmission lines under tokamak conditions. Tracts using coaxial cables for transmitting analog signals from sensors (inductive coils, Hall sensors) typically employ copper or shielded lines with subsequent digitisation in the DAS zone. While these cables are easily shielded, their parameters deteriorate significantly under radiation and temperature exposure, leading to signal loss, noise, and phase distortions, especially over long distances [1, 14, 22].

To reduce interference effects, signal digitisation directly at the sensor with subsequent data transmission via fibre optic cable is implemented [23, 27]. This approach ensures high interference immunity and minimises the impact of radiation effects on the analog part of the tract. Studies show that fibre optic lines exhibit significantly lower sensitivity to EMI and radiation-induced losses, ensuring reliable data transmission over long distances even at high speeds [23].

Mineral-insulated cables are also used in areas with high fluences due to their enhanced thermal and radiation resistance compared to polymeric counterparts, which is critical for long transmission lines [31].

As seen in Table 2, fibre optic and mineral-insulated cables are the most promising for operation in environments with intense ionising radiation. They provide parameter stability under prolonged irradiation and require less frequent maintenance [16].

Table 3 presents a comparison of the main techniques used to improve the reliability of signal transmission channels in environments with radiation activity [1, 4, 10, 23, 24, 27].

One approach to improving the reliability of communication channels is using redundant transmission lines (Table 3), which ensure system continuity in case of degradation of the primary channel [30, 35].

The ITER project has implemented a radiation-resistant optical diagnostics concept utilising Bragg gratings (FBG sensors) for temperature and strain measurements without signal degradation at doses exceeding 1 MGy [36, 37]. Additionally, active thermostabilisation systems are employed to compensate for temperature changes in cable tracts, reducing measurement error to 0.1% over lengths exceeding 100 m [6].

Therefore, combining radiation-resistant materials, optical technologies, digital compensation, and channel redundancy ensures reliable data transmission in fusion installations even under intense ionising and neutron radiation.

Conclusions

The analysis of current research highlights that ensuring the reliable operation of long data transmission lines in fusion reactors is a complex multi-factor challenge influenced by simultaneous radiation, thermal, and electromagnetic factors. Existing approaches to building transmission tracts rely on different sensor types (inductive, Hall, optical) and transmission lines (coaxial, mineral-insulated, fibre optic), each with its limitations. Traditional coaxial cables suffer significant degradation due to radiation ageing of materials and temperature influences, leading to increased signal loss and worsened SNR. Conversely, fibre optic and mineral-insulated lines exhibit significantly higher re-

Table 3. Methods for enhancing signal transmission reliability in radiation environments [30, 35]

Approach	The essence of the method	The result of using
Radiation-resistant materials	use MgO, Al_2O_3, SiO_2	improving the stability of parameters up to the doses 10^7 Gr
Optical data transmission	the use of low-attenuation optical fibre	no EMI, high transmission speed
Active dubbing	parallel backup lines with automatic switching	reducing the risk of data loss
Digital distortion compensation	algorithmic equalisation of amplitude-frequency and phase-frequency characteristics	real-time signal reconstruction
Temperature stabilisation	monitoring of thermal changes in the cable	improved measurement accuracy

silience to extreme conditions and provide more stable signal transmission parameters over long distances.

The paper proposes a methodology for selecting the structure of a transmission tract based on multi-criteria evaluation, considering radiation resistance, temperature stability, interference immunity, SNR, and long-term stability of characteristics. A key feature of the proposed methodology is the combination of system analysis of sensors and transmission channels with their formalised comparison, allowing for a reasoned determination of the feasibility of using different transmission tract configurations depending on operating conditions. The results demonstrate that combined solutions are most effective, involving the use of radiation-resistant sensors (specifically Hall and Bismuth Hall sensors), local signal conversion and digitisation near the sensor, and data transmission via fibre optic channels. The advantages of this approach include reduced interference effects, minimised parametric drifts, increased measurement accuracy, and enhanced reliability in the demanding conditions of fusion reactors.

The obtained results expand the possibilities for designing transmission tracts under intense radiation exposure and long transmission line lengths while creating a foundation for improving weak signal transmission accuracy. However, further research is needed on the long-term stability of material characteristics, the impact of radiation-induced ageing on transmission line parameters, and refinement of noise and signal drift compensation methods.

Future research should focus on developing new types of radiation-resistant sensors and materials, optimising hybrid data transmission systems combining electrical and optical channels, and implementing methods for local signal processing directly at the measurement zone. Experimental investigation of the long-term reliability of such systems under conditions closely resembling those in fusion reactors is also promising, paving the way for their practical application in projects like ITER and DEMOnstration Power Plant (DEMO).

References

[1] A.J.H. Donné and A.E. Costley, "Key issues in diagnostics for burning plasma experiments", *IEEE Trans. Plasma Sci.*, 2004, Vol. 32, No. 1, pp. 177–186. Retrieved from: https://doi.org/10.1109/TPS.2004.823895

[2] G. Vayakis *et al.*, "Generic diagnostic issues for a burning plasma experiment", *Fusion Sci. Technol.*, 2008, Vol. 53, No. 2, pp. 699–750, 2008. Retrieved from: https://w3.pppl.gov/~neumeyer/ITER_IVC/References/2008_Vayakis_ITER.pdf, https://doi.org/10.13182/FST08-A1684

[3] R. Chavan *et al.*, "The magnetics diagnostic set for ITER", *Fusion Eng. Des.*, 2009, Vol. 84, No. 2–6, pp. 295–299. Retrieved from:: https://doi.org/10.1016/j.fusengdes.2008.12.103

[4] M. Decréton *et al.*, "Performance of functional materials and components in a fusion reactor: The issue of radiation effects in ceramics and glass materials for diagnostics", *J. Nucl. Mater.*, 2004, Vol. 329, No. 1, pp. 125–132. Retrieved from: https://doi.org/10.1016/j.jnucmat.2004.04.012

[5] N. Casal *et al.*, "Functional materials for ITER diagnostic systems – Radiation aspects", *Fusion Eng. Des.*, 2017, Vol. 125, pp. 277–282. Retrieved from: https://doi.org/10.1016/j.fusengdes.2017.08.017

[6] S. Girard *et al.*, "Radiation effects on silica-based optical fibers: Recent advances and future challenges", *IEEE Trans. Nucl. Sci.*, 2013, Vol. 60, No. 3, pp. 2015–2036. Retrieved from: https://doi.org/10.1109/TNS.2012.2235464

[7] I. Bolshakova *et al.*, "Structure and calibration of functionally integrated devices of magnetic diagnostics of thermonuclear reactors", *Infocommun. Technol. Electron. Eng.*, 2022, Vol. 2, No. 1, pp. 61–73. Retrieved from: https://doi.org/10.23939/ictee2022.01.061

[8] S. Entler *et al.*, "Ceramic-chromium Hall sensors for environments with high temperatures and neutron radiation", *Sensors*, 2021, Vol. 21, No. 3, p. 721. Retrieved from: https://doi.org/10.3390/s21030721

[9] P.E. Stott *et al.*, *Diagnostics for Experimental Thermonuclear Fusion Reactors 2. Dordrecht: Springer*, 1998. Retrieved from: https://doi.org/10.1007/978-1-4615-5353-3

[10] J. Kim *et al.*, "Sensor fusion and magnetic drift estimation in magnetic measurements using Kalman filter for long-duration plasma operations", *Nucl. Fusion*, 2025. Retrieved from: https://doi.org/10.1088/1741-4326/adb599

[11] I. Ďuran *et al.*, "Irradiation tests of ITER candidate Hall sensors using two types of neutron spectra", *Rev. Sci. Instrum.*, 2010, Vol. 81, No. 10, doi: 10(Rev. Sci. Instrum. vol. 81, no. 10E122, 2010)). Retrieved from: https://doi.org/10.1063/1.3479115

[12] I. Ďuran *et al.*, "Stability of the Hall sensors performance under neutron irradiation", *Hal open science*, 2004. Retrieved from: https://hal.science/hal-00001781v1

[13] A.E. Costley *et al.,* "Overview of the ITER Diagnostic System", in *Diagnostics for Experimental Thermonuclear Fusion Reactors 2*, Eds. Boston, MA: Springer, 1998, pp. 41–56. Retrieved from: https://doi.org/10.1007/978-1-4615-5353-3_3

[14] A.E. Costley *et al.*, "ITER Diagnostics: Design Choices and Solutions", IAEA-2002-CT-5, 2002, pp. 1–8. Retrieved from: https://www-pub.iaea.org/mtcd/publications/pdf/csp_019c/pdf/ct_5.pdf

[15] K.M. Young and A.E. Costley, "An overview of ITER diagnostics", *Rev. Sci. Instrum.*, 1997, Vol. 68, No. 1, pp. 862–867. Retrieved from: https://doi.org/10.1063/1.1147710

[16] K.Y. Vukolov *et al.*, "Effect of Radiation Exposure on Optics in ITER", *Phys. At. Nucl.*, 2024, Vol. 87, No. 7, pp. 829–847. Retrieved from: https://doi.org/10.1134/S1063778824070160

[17] I. Bolshakova *et al.*, "Radiation-Resistant Hall Magnetic Field Sensors and Instrumentations". Lviv: Lviv Polytechnic National University; Dallas, USA: Primedia eLaunch LLC, 2022. Retrieved from: https://doi.org/10.36074/rrhmfsai-monograph.2022

[18] I. Ďuran *et al.*, "Development of bismuth Hall sensors for ITER steady state magnetic diagnostics", *Fusion Eng. Des.*, 2017, Vol. 123, pp. 690–694. Retrieved from: https://doi.org/10.1016/j.fusengdes.2017.05.142

[19] Ph. Moreau, "IIS magnetic diagnostics: overview", presented at the 13th ITER International School, 2024. Retrieved from: https://www.iter.org/sites/default/files/media/2024-12/l2_iis-magnetic-diagnostics-ph-moreau-v2-reduced.pdf

[20] N. Marconato, "The magnetic diagnostic set for ITER", *IEEE Trans. Plasma sci.*, 2010, Vol. 38, No. 3, pp. 284–294. Retrieved from: https://doi.org/10.1109/tps.2009.2037226

[21] D. Testa *et al.*, "The magnetic diagnostic set for ITER", in *Proc. 23rd IEEE/NPSS Symp. Fusion Engineering*, San Diego, CA, USA, 2009, pp. 1–4. Retrieved from: https://doi.org/10.1109/FUSION.2009.5226525

[22] Y. Ma *et al.*, "Design and development of ITER high-frequency magnetic sensor", *Fusion Eng. Des.*, 2016, Vol. 112, pp. 594–612. Retrieved from: https://doi.org/10.1016/j.fusengdes.2016.05.002

[23] K.Yu. Vukolov, "Fiber optics for plasma diagnostics in ITER", *Fusion Eng. Des.*, 2017, Vol. 123, pp. 919–922. Retrieved from: https://doi.org/10.1016/j.fusengdes.2017.03.075

[24] J. Li *et al.*, "Radiation damage mechanisms and research status of radiation-resistant optical fibers: A review", *Sensors*, 2024, Vol. 24, No. 10, pp. 3235. Retrieved from: https://doi.org/10.3390/s24103235

[25] F. Esposito *et al.*, "Editorial to the special issue optical fiber sensors in radiation environments", *Sensors*, 2023, Vol. 23, No. 22, pp. 9117. Retrieved from: https://doi.org/10.3390/s23229117

[26] L. Anghelescu *et al.*, "Degradation pathways of electrical cable insulation: A review of aging mechanisms and fire hazards", *Fire*, 2025, Vol. 8, No. 10, pp. 397. Retrieved from: https://doi.org/10.3390/fire8100397

[27] M. Van Uffelen *et al.*, "Radiation tolerance qualification for maintenance tasks in the future fusion reactors: From fibre-optic components to robust data links", *Fusion Eng. Des.*, 2003, Vvol. 69, No. 1–4, pp. 191–195. Retrieved from: https://doi.org/10.1016/S0920-3796(03)00335-1

[28] K. Vukolov *et al.*, "Irradiation tests of fiber optics for H-alpha diagnostics in ITER", *Fusion Eng. Des.*, 2019, Vol. 146A, pp. 796–799. Retrieved from: https://doi.org/10.1016/j.fusengdes.2019.01.082

[29] R. Zhang *et al.*, "Research on self-diagnosis and self-healing redundant optical fiber sensor network", *Sensors*, 2025, Vol. 25, No. 6, pp. 1641. Retrieved from: https://doi.org/10.3390/s25061641

[30] V. Plaček *et al.*, "Dose rate effects in radiation degradation of polymer-based cable materials", *Nucl. Instrum. Methods Phys. Res. B*, 2003, Vol. 208, pp. 448–453. Retrieved from: https://doi.org/10.1016/S0168-583X(03)00626-8

[31] M. Decréton *et al.*, "Performance of functional materials and components in a fusion reactor: The issue of radiation effects in ceramics and glass materials for diagnostics", *J. Nucl. Mater.*, 2004, Vol. 329–333, part. A, pp. 125–132. Retrieved from: https://doi.org/10.1016/j.jnucmat.2004.04.012

[32] M. Van Uffelen *et al.*, "Gamma radiation effects in Er-doped silica fibers", *IEEE Trans. Nucl. Sci.*, Oct. 2004, Vol. 51, No. 5, pp. 2763–2769. Retrieved from: https://doi.org/10.1109/TNS.2004.835059

[33] N. Casal *et al.*, "Functional materials for ITER diagnostic systems – Radiation aspects", *Fusion Eng.*, 2017, Vol. 125, pp. 277–282. Retrieved from: https://doi.org/10.1016/j.fusengdes.2017.08.017

[34] L.K. Glinenko and V.M. Fast, "System choice of the optimal 3D MID technological solution", [Systemnyi vybir optymalnoho tekhnolohichnoho rishennia 3D MID], *Visn. NTUU KPI. Ser. Radiotekh. Radioaparatobuduv.*, 2017, No. 69, pp. 56–61. Retrieved from: http://nbuv.gov.ua/UJRN/VKPI_rr_2017_69_11

[35] A. Stanciu and M. Stanciu, "Optical fiber sensors in nuclear plants", *EEA J.*, 2005, Vol. 53, No. 4, pp. 15–20. Retrieved from: https://eea-journal.ro/ro/2005/eea-2005-53-4-015-en.pdf

[36] A. Morana *et al.*, "Radiation effects on fiber Bragg gratings: Vulnerability up to MGy doses", *Sensors*, 2022, Vol. 22, No. 21, pp. 8175. Retrieved from: https://doi.org/10.3390/s22218175

[37] M.A.S. Zaghloul *et al.*, "Radiation resistant fiber Bragg grating in random air-line fiber", *Opt. Express*, 2018, Vol. 26, No. 9, pp. 11775–11786. Retrieved from: https://doi.org/10.1364/OE.26.011775

Гліненко Л.К., Кость П.І.

МЕТОДИКА ВИБОРУ СТРУКТУРИ ПЕРЕДАВАЛЬНОГО ТРАКТУ ДЛЯ ТЕРМОЯДЕРНИХ УСТАНОВОК

Проблематика. У термоядерних установках передавання вимірювальних сигналів від сенсорів здійснюється в умовах інтенсивного іонізувального випромінювання, високих температур і значних електромагнітних завад, що призводить до деградації сенсорів і ліній передачі, зростання втрат сигналу і зниження відношення сигнал/шум. Особливо критичним є передавання слабких сигналів на великі відстані, що потребує обґрунтованого вибору структури передавального тракту на основі системного врахування характеристик сенсорів і ліній передачі, з урахуванням комплексу впливових факторів, зокрема радіаційного впливу, температурних режимів, електромагнітних завад, втрат сигналу і змін відношення сигнал/шум.

Мета дослідження. Метою роботи є обґрунтування формування методики вибору структури передавального тракту для довгих ліній передачі даних у термоядерних установках на основі системного та багатокритеріального аналізу характеристик сенсорів і каналів передачі з урахуванням умов їх експлуатації.

Методика реалізації. Використано системний аналіз сучасних сенсорних рішень і типів ліній передачі, а також багатокритеріальний підхід з урахуванням радіаційної стійкості, температурної стабільності, завадостійкості, відношення сигнал/шум і довготривалої стабільності параметрів. Передавальний тракт при цьому розглядається як сукупність взаємопов'язаних елементів: сенсора, локального перетворювача, лінії передачі та модуля збору даних, що визначають ефективність передавання сигналу. Для порівняння альтернатив застосовано нормування характеристик і їх візуалізацію за допомогою полярних діаграм.

Результати дослідження. Встановлено, що індуктивні сенсори характеризуються високою радіаційною стійкістю, але обмежені у вимірюванні постійних полів, тоді як Холл-сенсори забезпечують пряме вимірювання постійних і змінних магнітних полів, проте зазнають радіаційно-індукованого дрейфу. Показано, що вісмут і керамічні Холл-сенсори мають підвищену довготривалу стабільність. Визначено, що коаксіальні кабелі схильні до радіаційного старіння і втрат сигналу, тоді як оптоволоконні та мінерально ізольовані лінії забезпечують кращу завадостійкість і стабільність параметрів. Обґрунтовано доцільність локального оцифрування сигналів і використання оптичних каналів передачі. На основі проведеного аналізу сформовано модель структури передавального тракту, при цьому обґрунтовано доцільність локального оцифрування сигналів і використання оптоволоконних каналів передачі для підвищення достовірності та завадостійкості.

Висновки. Запропоновано методику вибору структури передавального тракту, який базується на комплексному врахуванні характеристик сенсорів і ліній передачі. Показано, що найбільш ефективними є комбіновані рішення побудови передавального тракту, які передбачають поєднання радіаційно стійких сенсорів, локальної обробки та оцифрування сигналів безпосередньо біля сенсора і використання оптоволоконних каналів передачі. Такий вибір структури забезпечує підвищення достовірності вимірювань і надійності передачі даних у довгих лініях передачі термоядерних установок в умовах дії іонізувального випромінювання, високих температур та електромагнітних завад.

Ключові слова: передавальний тракт; довгі лінії передачі даних; канали передачі інформації; завадостійкість; відношення сигнал/шум; електромагнітні завади; оптоволоконні канали зв'язку; цифрова обробка сигналів; телекомунікаційні системи; радіаційна стійкість.

Recommended by the Council
of the Faculty of Robotics
and Instrumentation Engineering
of Igor Sikorsky KPI

Received: 29 March 2026

Accepted: 08 June 2026

Published: 29 June 2026

АВТОМАТИЗАЦІЯ, КОМП'ЮТЕРНО-ІНТЕГРОВАНІ ТЕХНОЛОГІЇ ТА РОБОТОТЕХНІКА

DOI: https://doi.org/10.20535/kpisn.2026.2.357072
УДК 681.518

D.V. Petrenko[1*], https://orcid.org/0009-0003-7670-555X
A.G. Protasov[1], https://orcid.org/0009-0003-8770-7251
1National Technical University of Ukraine "Igor Sikorsky Kyiv Polytechnic Institute", Kyiv, Ukraine, https://ror.org/00syn5v21
*Відповідальний автор: petrenkod555@gmail.com

DEEP REINFORCEMENT LEARNING-BASED MAPLESS NAVIGATION ALGORITHM FOR HUSKY ROBOT WITH ADAPTIVE CURRICULUM LEARNING

Background. Mobile wheeled robots are widely used today in internal logistics environments of various industries, in particular in warehouses, production shops and sorting centers. However, in such environments, the robot operates under conditions of high variability, where the configuration of aisles, the placement of loads and the presence of people can change in real time. Therefore, the development of autonomous navigation of the robot in complex and dynamic environments is becoming one of the key tasks of robotics.
Objective. To improve navigation efficiency in dynamic mapless logistics environments, this work introduces an adaptive machine learning method based on curriculum Reinforcement Learning (RL) for four-wheeled autonomous robots. Methods. To achieve the set goal and solve the tasks of autonomous navigation in logistics environments, a comprehensive methodological approach was used, based on the following methods:
– Simulation Method: using the PyBullet physical engine to create a virtual logistics environment. This allowed for safe and high-repetition training, simulating the real-world kinematics of the Husky four-wheeled robot;
– Deep RL Methods: application and comparison of three state-of-the-art architectures: Soft Actor-Critic (SAC), Proximal Policy Optimisation (PPO), Twin Delayed DDPG (TD3);
– Adaptive Curriculum Learning (ACL): a step-by-step learning technique that automatically changes the complexity of the environment (number and speed of obstacles) depending on the current success of the agent. This avoids the degradation policy at early stages.
Results. The combination of ACL of the Husky mobile robot in complex dynamic environments and hybrid reward functions increased the navigation success rate by 35–40 % compared to direct learning in complex scenarios. The conducted comparative analysis of machine learning algorithms demonstrated the highest adaptability to non-stationary conditions and the best efficiency of using experience is the SAC algorithm, which achieves success in 89 % of cases of application with a minimum number of collisions.
Conclusions. This paper proposes an algorithm for mapless navigation of the autonomous mobile robot Husky in complex dynamic environments is proposed, based on a combination of adaptive learning and a physically interpreted hybrid reward function. Experiments conducted in the PyBullet simulator confirmed that a stepwise and adaptive increase in the complexity of the environment stabilises the learning process of modern deep RL algorithms (PPO, SAC, and TD3).
Keywords: machine learning with reinforcement; navigation without cartography; mobile robots; control systems; robot autonomy.

Introduction

Autonomous navigation is a crucial functional capability for mobile robots widely deployed in indoor logistics environments, such as warehouses, manufacturing plants, and sorting centres. In these settings, robots operate under highly dynamic conditions where the configuration of aisles, placement of cargo, and presence of humans can change in real time. This significantly complicates the use of classical navigation approaches based on accurate maps, prior localisation, and global path planning, which often require substantial computational resources or regular of map updates. In many prac-

Пропозиція для цитування цієї статті: Д.В. Петренко, А.Г. Протасов, «Алгоритм безкартографічної навігації робота Husky на основі моделей глибокого навчання з підкріпленням та адаптивного навчального плану», *Наукові вісті КПІ*, № 2, с. 36–43, 2026. doi: https://doi.org/10.20535/kpisn.2026.2.357072

How to cite this article: D.V. Petrenko, A.G. Protasov, "Deep reinforcement learning-based mapless navigation algorithm for Husky robot with adaptive curriculum learning", *KPI Science News*, No. 2, pp. 36–43, 2026. doi: https://doi.org/10.20535/kpisn.2026.2.357072

© The Autor(s).
The article is distributed under the terms of the license CC BY 4.0

tical scenarios, such approaches are either constrained or economically unfeasible. An alternative to traditional methods is mapless navigation, which involves reaching a goal based on local sensor observations without constructing a global map of the environment. This approach is particularly attractive for dynamic and unstructured logistics spaces where the environment is partially observable and non-stationary. Recent advancements in RL have enabled the implementation of end-to-end navigation policies that directly map sensory data to control actions, thereby reducing reliance on complex mapping and planning modules. Notably, mapless navigation based on Light Identification, Detection and Ranging (LiDAR) technology data combined with RL algorithms has gained popularity due to LiDAR's robustness to illumination changes and its ability to accurately capture the geometry of surrounding obstacles. Machine learning algorithms such as PPO, SAC, and TD3 demonstrate high effectiveness in relatively simple or static environments. However, their performance significantly deteriorates in complex dynamic logistics scenarios characterised by moving obstacles, dense traffic, and non-stationary dynamics.

A key challenge in such conditions is the instability of the learning process. As the complexity of the environment increases, standard RL algorithms often exhibit unstable policy evolution, slow convergence, or a complete failure to form a reliable navigation strategy. This indicates towards a problem related to the lack of effective mechanisms for managing task complexity during training for mapless navigation in dynamic and non-stationary environments. One promising approach to overcome this challenge is Curriculum Learning (CL), which involves gradually increasing task complexity during training. By extending this concept, ACL enables automatic adaptation of environment complexity according to the agent's current learning level, creating the necessary prerequisites for forming robust and generalisable navigation strategies in complex logistics environments.

Analysis of Previous Works and Publications

In contemporary research, Deep Reinforcement Learning (DRL) is actively applied for mapless navigation of mobile agents and local obstacle avoidance. Studies show that DRL agents can directly map local sensor data to continuous control actions, enabling robots to reach goals without constructing a global map or complex localisation. Notably, classical DRL approaches using the PPO algorithm demonstrate the ability to navigate in relatively simple or static environments by training an agent to avoid obstacles and move towards a target. However, these approaches are limited in cases of high complexity and dynamics, where statistical properties of observations may change during operation [1].

Current research continues to develop Adaptive Reinforcement Learning (ARL) methods for realistic navigation scenarios. For example, in the context of indoor logistics, a DRL scheme with an automatic learning curriculum (NavACL-Q) was proposed, combining SAC with automatic task complexity adaptation. This contributes to improving the quality of navigation policies compared to classical mapping approaches in complex warehouse environments [2].

The CL concept has been proposed as a strategy for gradually transitioning from simpler to more complex tasks, enhancing convergence speed and learning stability for RL agents [3]. In robotics, CL is often implemented through the manual adjustment of training environment parameters – for instance, sequentially increasing obstacle density or the complexity of dynamics. However, such manual strategies are ineffective for complex scenarios with high-dimensional observation spaces because they do not adapt to an agent's individual progress. Modern approaches to ACL propose the automatic assessment of an agent's progress with subsequent dynamic adjustment of environment complexity, leading to improved overall RL policy performance [4]. These methods have shown promise for navigation tasks in partially observable environments with varying complexity. However, their real-time application in non-stationary logistics remains a subject of ongoing research.

One of the key challenges in applying DRL to autonomous navigation is the gap between Simulation and Real-world conditions (Sim-to-Real gap) [5]. An agent trained in a simulator often exhibits a significant performance drop when transferred to a physical platform due to discrepancies in the environment model, sensor noise, dynamics, etc. To address this issue, domain randomisation is widely used. It involves varying physical parameters of the environment during training, enabling the agent to learn more generalised policies. Furthermore, combining Sim-to-Real approaches with adaptive methods like ACL or domain randomisation can significantly improve the stability of transferring a navigation policy from simulation to reality, contributing to more reliable operation of autonomous systems in practical logistics scenarios.

Despite significant progress in developing mapless navigation methods based on RL, most existing approaches remain limited to relatively simple or quasi-dynamic environments and do not ensure stable learning under conditions of high density of moving obstacles and non-stationary dynamics. ACL methods and Sim-to-Real approaches show considerable potential, but their integration into a unified framework for mapless navigation of four-wheeled mobile robots in complex logistics environments remains insufficiently explored. This justifies the need for further research aimed at developing adaptive learning strategies capable of ensuring stability, generalisation, and practical applicability of navigation policies in real-world dynamic conditions.

The purpose of this work is to improve the efficiency of mapless navigation for a four-wheeled autonomous mobile robot in dynamic logistics environments by applying ARL based on a curriculum.

Materials and Results of the Research

For the study of mapless navigation of an autonomous mobile robot, a virtual environment was developed in the PyBullet simulator, providing realistic modeling of contact dynamics, friction, and kinematics. The environment is designed to reproduce typical indoor logistics scenarios, particularly warehouse and manufacturing spaces with narrow aisles and various obstacles. As the robotic platform, a Husky robot model [6] was used, which is widely applied in autonomous navigation research and well replicates the dynamics of real-world ground mobile robots. The agent's state is defined by local sensor observations represented by LiDAR data, providing real-time information about the geometry of surrounding obstacles.

The simulated virtual environment (Fig. 1) represents a spacious enclosed space with rigid walls that limit the robot's working zone and prevent it from exiting the simulation. The floor surface is level and homogeneous. In the central part of the scene, a mobile robot is placed, and the target state is marked by a green spherical object whose position is randomly initialised for each episode. This task setup prevents memorising fixed trajectories and stimulates the formation of a generalised navigation policy. Obstacles in the environment differ in spatial arrangement, orientation, geometric dimensions, and dynamic properties. Some objects are static (marked red), while others are dynamic (marked blue) and move along stochastic trajectories.

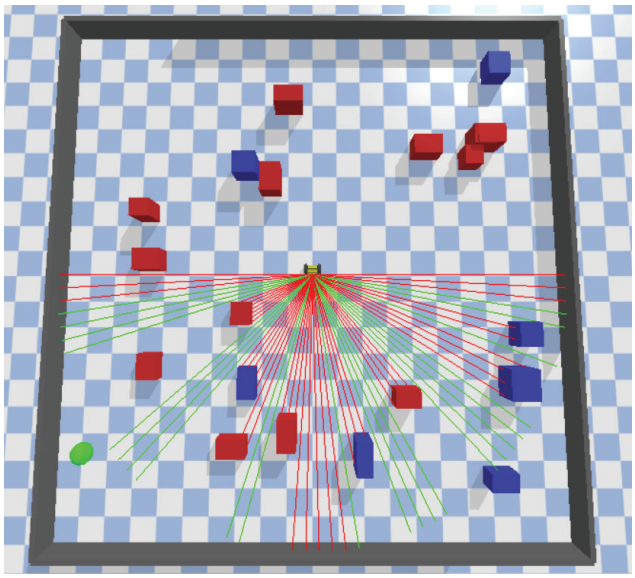


Fig. 1. Virtual environment featuring the agent, target, static red, and dynamic blue obstacles

At the beginning of each episode, all obstacles are initialised in random positions, ensuring a variety of scenarios and increasing learning complexity. The green and red rays on the visualisation correspond to LiDAR measurements. Green rays represent free directions of movement, while red ones signal the detection of obstacles or their dangerously close proximity. This sensory information is used by the agent to make real-time decisions.

Learning in a Static Environment. In the first stage of research, PPO, SAC, and TD3 algorithms were trained in a relatively simple static environment with fixed obstacles. Dynamic objects were absent at this stage, and the scene configuration remained unchanged within a single episode.

The stage aimed to:

– verify the correctness of the environment implementation and reward function;

– assess the basic ability of the algorithms to develop a navigation policy;

– establish benchmarks for further comparative analysis in more complex and dynamic environments.

Training of each algorithm was conducted over one million episodes, under identical simulation conditions and with comparable hyperparameters. The main performance indicator used was the success rate, defined as the proportion of episodes in which the robot successfully reached the target without collisions.

Fig. 2 shows the dynamics of changes in the navigation success rate depending on the number

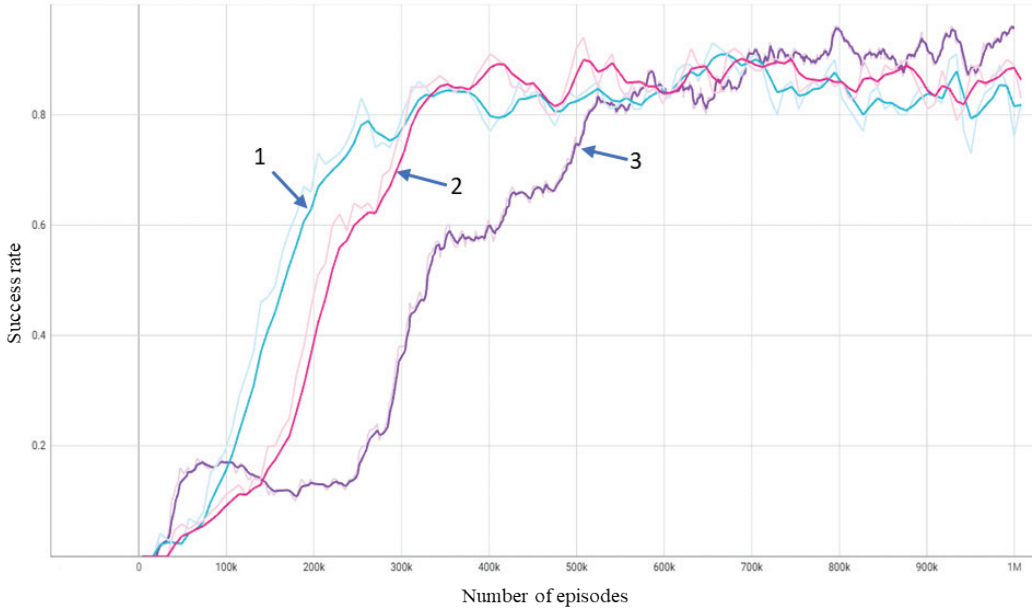


Fig. 2. Comparison of algorithms in a static environment over one million episodes:
1 – PPO, 2 – TD3, 3 – SAC

of training episodes. It is visible that all three algorithms demonstrate gradual growth in efficiency, confirming their ability to form a correct obstacle avoidance policy and reach the goal in a static environment.

The PPO algorithm is characterised by a smoother and more stable learning curve; however, it requires a larger number of episodes to achieve a high level of success. Conversely, SAC and TD3 demonstrate significantly faster initial convergence, achieving a success rate of over 0.8 in the early stages of training but are characterised by more pronounced fluctuations during further optimisation.

During the experiments, all three algorithms demonstrated the ability to learn correct obstacle avoidance behaviour and reach the goal in a static environment. However, differences were found in convergence speed and learning stability.

Specifically, PPO provided the most stable optimisation process, making it a reliable baseline method, but was characterised by slower convergence. The SAC and TD3 algorithms had higher sample efficiency, allowing them to achieve high success rates more quickly, but they were also more sensitive to hyperparameter choices and exhibited greater fluctuations during training. Table 1 demonstrates the results of algorithm training in a static environment under identical simulation conditions and matched hyperparameters.

Table 1. Algorithm Training Results

Indicators	PPO	SAC	TD3
Success rate	0.82	0.95	0.83
Collision rate	0.08	0.03	0.08
Average episode duration	160	230	210
Number of training episodes	one million	one million	one million

Learning in Complex Dynamic Environments. The next stage of the research involved complicating the simulation environment by adding dynamic obstacles that change their position during episodes. This environment is non-stationary, as the state distribution changes over time, and the behaviour of the surroundings cannot be considered fixed or completely predictable. In these conditions, the agent must not only avoid collisions with static objects but also adapt its control policy to moving obstacles, which significantly complicates the learning process. Training of PPO, SAC, and TD3 algorithms was conducted over one million episodes under similar hyperparameters as in the static environment to ensure proper result comparison.

The conducted experiments showed that under these conditions, standard RL algorithms face significant difficulties, namely:

– unstable policy parameter updates;

– slow convergence or its complete absence;
– increasing number of collisions with obstacles;
– significant fluctuations in cumulative reward between episodes.

Fig. 3 shows the dynamics of changes in the navigation success rate in a dynamic environment. Unlike the static case, none of the investigated algorithms demonstrates stable and monotonic convergence. The Success Rate values remain relatively low and are characterised by significant fluctuations throughout the entire learning process.

The PPO algorithm demonstrates the most stable but low-efficiency behaviour, failing to achieve high success rates even after prolonged training. The SAC and TD3 algorithms show slightly better results; however, their learning is accompanied by significant fluctuations and policy degradation at later stages, indicating high sensitivity to environment non-stationarity.

The results indicate that a classic approach to RL without explicit mechanisms for managing task complexity is insufficient for forming a reliable navigation policy in complex dynamic environments. Even algorithms with high data sampling efficiency prove incapable of consistently generalising experience in the presence of moving objects. Table 2 demonstrates the results of algorithm training in a complex dynamic environment.

Table 2. Algorithm Training Results

Indicators	PPO	SAC	TD3
Success rate	0.28	0.42	0.38
Collision rate	0.78	0.54	0.63
Average episode duration	530	410	480
Number of training episodes	one million	one million	one million

Applying ACL. To overcome the identified problems of instability and low convergence of algorithms in complex dynamic environments, this work proposes using the ACL approach. Its key idea lies in gradually and adaptively increasing the complexity of the learning environment based on the agent's current performance indicators. This allows for reducing task complexity in the early stages of training and avoids policy degradation.

Within the proposed approach, the following environment parameters were adaptively changed: the number of static and dynamic obstacles, the movement speed of dynamic objects, the initial distance to the goal, and the sensor noise level. Training each algorithm began in a simplified environment with a minimal number of obstacles and low dynamics, after which the complexity of the environment gradually increased under the condition that

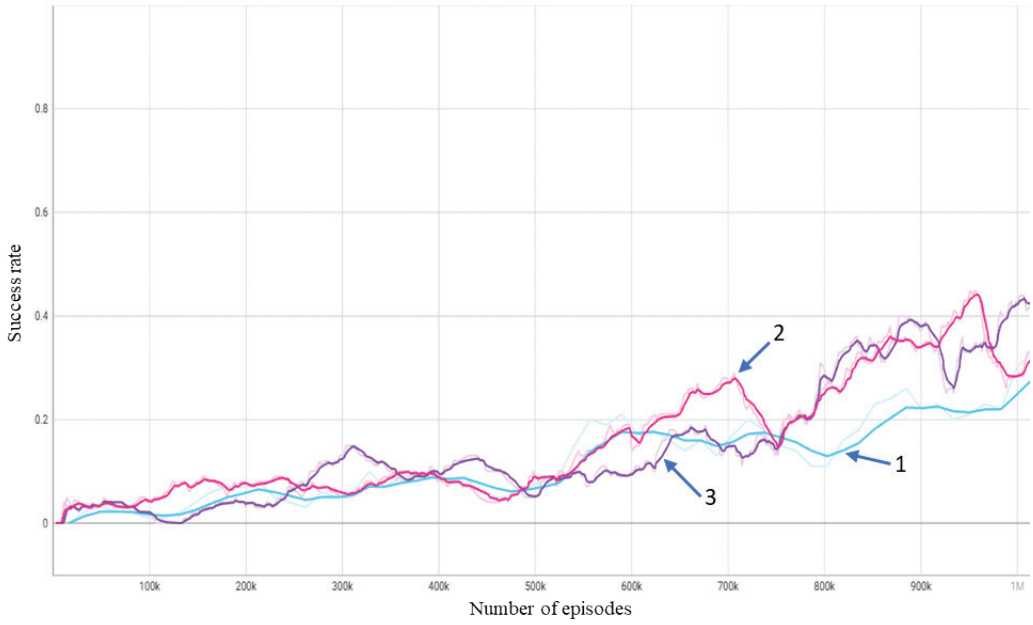


Fig. 3. Comparison of algorithms in a complex dynamic environment over one million episodes:
1 – PPO, 2 – TD3, 3 – SAC

the agent achieved predetermined efficiency criteria. These criteria included stable growth of cumulative reward and reduced collisions.

The proposed strategy enabled forming a more stable learning process and ensured smooth adaptation of the control policy to the increasing task complexity. Unlike direct training in a dynamic environment, using ACL reduced fluctuations in policy parameters and prevented sharp performance degradation between episodes (Fig. 4).

Experimental results showed that using ACL significantly improves learning stability, accelerates algorithm convergence, and reduces the number of collisions in complex dynamic environments compared to training without a curriculum strategy. The most noticeable effect was observed for the SAC and TD3 algorithms, which, under conditions of adaptive environment complexity increase, demonstrated more stable cumulative reward growth and superior generalisation capabilities. Table 3 shows the results of algorithm training following an adaptive learning program.

A comparative analysis of the learning results in static, dynamic, and curriculum-oriented environments confirmed the appropriateness of using an adaptive approach to forming training scenarios. Combining RL algorithms with ACL mechanisms allows overcoming the limitations of classical methods and increasing the efficiency of mapless navigation for autonomous mobile robots in complex and non-stationary environments. Table 4 shows the results of algorithm training.

Conclusions

The paper presents an algorithm for mapless navigation of a Husky autonomous mobile robot in complex dynamic environments, based on combining ACL and a physically interpretable hybrid reward function. Experiments conducted in the PyBullet simulator confirmed that stepwise and adaptive increase in environment complexity is a key factor in stabilising the training process of modern DRL algorithms, specifically PPO, SAC, and TD3.

Experimental results confirmed the effectiveness of the proposed approach based on ACL for mapless robot navigation in complex dynamic environments. It was shown that stepwise and adaptive complication of the environment eliminates policy degradation and ensures stable convergence of PPO, SAC, and TD3 algorithms, increasing the navigation success rate by 35–40 % compared to direct training in complex scenarios.

Comparative analysis showed that the SAC algorithm demonstrates the highest adaptability to non-stationary conditions and the best sample efficiency, achieving a success rate up to 89 % with a minimal number of collisions. Additionally, it was established that the proposed hybrid reward function with physical interpretation contributes to

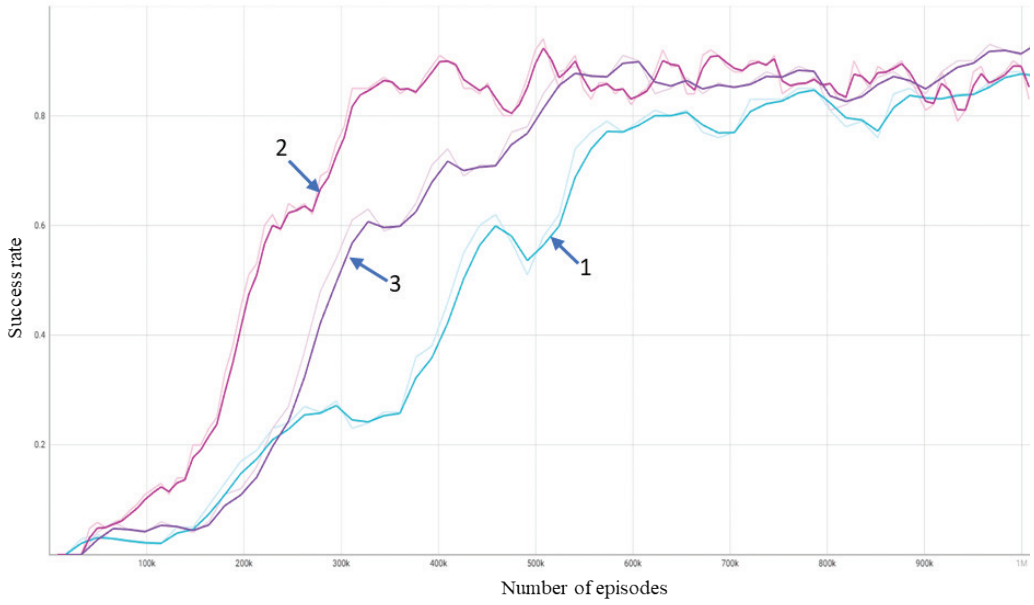


Fig. 4. Comparison of algorithms using ACL in a complex dynamic environment over one million episodes: 1 – PPO, 2 – TD3, 3 – SAC

Table 3. Algorithm Training Results

Indicators	PPO	SAC	TD3
Success rate	0.88	0.92	0.84
Collision rate	0.9	0.02	0.07
Average episode duration	305	360	340
Number of training episodes	one million	one million	one million

forming smoother and more stable movement trajectories, which increases the suitability of learned policies for further transfer to real robotics platforms.

However, this research has certain limitations. All experiments were conducted in the PyBullet simulator, leaving the challenge of the Sim-to-Real gap open for further investigation. Moreover, the used LiDAR sensor model with a limited number of beams may be insufficient for correctly identifying small or complex objects in real conditions. Further research will focus on implementing learned models on a real four-wheeled mobile robot and developing mechanisms for memory and motion prediction of dynamic obstacle using modern neural network architectures.

Table 4. Comparison of algorithm learning results by success rate in different simulation environments

Algorithms	Static environment	Dynamic environment	ACL and dynamic environment
PPO	82 %	28 %	88 %
SAC	95 %	42 %	92 %
TD3	83 %	38 %	84 %
Number of training episodes	one million	one million	one million

References

[1] D.V. Petrenko and A.H. Protasov, "Analysis of the effectiveness of Reinforcement Learning algorithms to increase the autonomy of mobile robots [Analiz efektyvnosti alhorytmiv Reinforcement Learning dlya pidvyshchennya avtonomnosti mobilnykh robotiv]", *Tekhnichna diahnostyka ta neruynivnyy kontrol*, No. 3, pp. 24–31, 2025. Retrieved from: https://doi.org/10.37434/tdnk2025.03.03

[2] C. Wei *et al.*, "Deep Reinforcement Learning with Heuristic Corrections for UGV Navigation", *J Intell Robot Syst*, Vol. 109, p. 18, 2023. Retrieved from: https://doi.org/10.1007/s10846-023-01950-y

[3] M. Anca *et al.*, "Achieving Goals Using Reward Shaping and Curriculum Learning", Lecture Notes in Networks and Systems. Cham: Springer Nat. Switz., pp. 316–331, 2023. Retrieved from: https://doi.org/10.1007/978-3-031-47454-5_24

[4] H. Xue *et al.*, "Using Deep Reinforcement Learning with Automatic Curriculum Learning for Mapless Navigation in Intralogistics", *Appl. Sci.*, Vol. 12, p. 3153, 2022. Retrieved from: https://doi.org/10.3390/app12063153

[5] N. Wang *et al.*, "Sim-to-Real: Mapless Navigation for USVs Using Deep Reinforcement Learning", *J. Mar. Sci. Eng.*, Vol. 10, No. 7, p. 895, 2022. Retrieved from: https://doi.org/10.3390/jmse10070895

[6] "Husky A300 unmanned ground vehicle". Clearpathrobotics. Accessed: 1 Feb. 2026. [Online]. Retrieved from: https://clearpathrobotics.com/husky-a300-unmanned-ground-vehicle-robot/

Д.В. Петренко, А.Г. Протасов

АЛГОРИТМ БЕЗКАРТОГРАФІЧНОЇ НАВІГАЦІЇ РОБОТА HUSKY НА ОСНОВІ МОДЕЛЕЙ ГЛИБОКОГО НАВЧАННЯ З ПІДКРІПЛЕННЯМ ТА АДАПТИВНОГО НАВЧАЛЬНОГО ПЛАНУ

Проблематика. Мобільні колісні роботи сьогодні широко застосовують у внутрішніх логістичних середовищах різноманітних виробництв, зокрема на складах, у виробничих цехах і сортувальних центрах. Втім, у таких середовищах роботи функціонують за умов високої мінливості, де конфігурація проходів, розміщення вантажів і присутність людей можуть змінюватися в режимі реального часу. Отже, розвиток автономної навігації роботів у складних і динамічних середовищах стає однією із ключових задач робототехніки.

Мета. Метою цієї роботи є підвищення ефективності навігації без картографії чотириколісного автономного мобільного робота в динамічних логістичних середовищах шляхом застосування адаптивного машинного навчання з підкріпленням на основі навчального плану.

Методика реалізації. Для реалізації поставленої мети було використано комплексний методологічний підхід, що ґрунтується на таких методах:

– метод імітаційного моделювання (симуляція) з використанням фізичного рушія PyBullet для створення віртуального логістичного середовища, що дозволило безпечно і з високою частотою ітерацій проводити навчання, моделюючи реальну кінематику чотириколісного робота Husky;

– методи глибокого навчання з підкріпленням для застосування й порівняння трьох сучасних архітектур: Soft Actor-Critic (SAC), Proximal Policy Optimization (PPO), Twin Delayed DDPG (TD3);

– метод адаптивного навчання за навчальним планом, що автоматично змінює складність середовища (кількість і швидкість перешкод) залежно від поточної успішності агента.

Результати дослідження. Запропоноване поєднання адаптивного навчання мобільного робота Husky у складних динамічних середовищах і гібридної функції винагороди підвищило показник успішності навігації на 35–40 % порівняно із прямим навчанням у складних сценаріях. Проведений порівняльний аналіз алгоритмів машинного навчання продемонстрував найвищу адаптивність до нестаціонарних умов і найкращу ефективність використання досвіду в алгоритма SAC, який досяг успішності у 89 % випадків застосування за мінімальної кількості зіткнень.

Висновки. Запропоновано алгоритм безкартографічної навігації автономного мобільного робота Husky в складних динамічних середовищах, оснований на поєднанні адаптивного навчання і фізично інтерпретованої гібридної функції винагороди. Проведені експерименти в симуляторі PyBullet підтвердили, що поетапне та адаптивне збільшення складності середовища стабілізує процес навчання сучасних алгоритмів глибокого навчання з підкріпленням (PPO, SAC та TD3).

Ключові слова: машинне навчання з підкріпленням; навігація без картографії; мобільні роботи; системи керування; автономність роботів.

Recommended by the Council
of the Faculty of Robotics
and Instrumentation Engineering
of Igor Sikorsky KPI

Received: 06 February 2026

Accepted: 08 June 2026

Published: 29 June 2026

DOI: https://doi.org/10.20535/kpisn.2026.2.352429
UDC 621.311.25:519.816

K.Yu. Brovko[1*], http://orcid.org/0000-0002-9669-9316
P.F. Budanov[1], http://orcid.org/0000-0002-1542-9390
O.V. Velykohorskyi[1], https://orcid.org/0009-0005-6102-0659
Yu.S. Oliinyk[1], https://orcid.org/0000-0002-5893-352X
N.D. Vynokurova[1], https://orcid.org/0009-0008-6210-838X
S.M. Voitenko[1], https://orcid.org/0009-0001-8829-2647
[1] V.N. Karazin Kharkiv National University, https://ror.org/03ftejk10
*Corresponding author: brovkokonstantin@gmail.com

SIMULATION MODEL OF A DIGITAL TWIN FOR AN NPP POWER UNIT TECHNOLOGICAL PROCESS

Background. Modern Nuclear Power Plant (NPP) units are characterised by high structural complexity, multi-level hierarchical Information and Control (I&C) systems, and a vast number of interconnected technological parameters. Existing digital twin models primarily focus on individual physical processes – such as neutron kinetics, thermal hydraulics, or protection logic – often overlooking the comprehensive structure of control systems. The lack of a formalised approach for real-time assessment of subsystems' hierarchical integrity limits the early detection of pre-accident states and proactive safety management.
Objective. The paper aims to develop a simulation model of a digital twin for the NPP technological process based on a system-cluster approach. This method enables the assessment of the hierarchical, self-similar scaled structure of subsystems using fractal dimension as a quantitative metric.
Methods. The study utilises a system-cluster approach, decomposing the power unit into functional sub-clusters: power control, protection system, coolant parameter regulation, and emergency shutdown. The mathematical framework integrates neutron kinetics equations, thermal-hydraulic relations, and logical-dynamic algorithms. To quantify structural complexity, the information space coverage method was employed to calculate fractal dimensions. The digital twin was implemented as a hardware-and-software complex integrated with the I&C systems, incorporating modules for data acquisition, structural identification, and predictive analytics.
Results. Fractal dimension values were obtained for key subclusters of the power unit, reflecting their hierarchical complexity (notably, the maximum of 1.83 for the coolant control system and the minimum of 1.0 for the protection system). Normalised ranges of fractal dimension were determined as indicators of normal operation. Furthermore, a monitoring algorithm was developed to detect the loss of structural levels or subsystem degradation before functional failures manifest. Practical implementation demonstrated the feasibility of real-time structural diagnostics and adaptive response.
Conclusions. The proposed fractal-cluster approach ensures comprehensive modelling of the NPP technological process by accounting for its hierarchical structure. Utilising fractal dimension as a structural diagnostic parameter expands the capabilities of traditional control methods and establishes the necessary framework for proactive safety management strategies based on digital twin technology.
Keywords: digital twin; power unit; fractal dimension; system-cluster approach; information and management system.

Introduction

The modern nuclear industry plays a crucial role as a key element of critical infrastructure, ensuring national strategic energy independence. In the context of global challenges – such as the need for guaranteed and uninterrupted power supply, adherence to high environmental standards, rational use of fuel and energy resources, and increasingly stringent safety requirements – scientific developments

Пропозиція для цитування цієї статті: К.Ю. Бровко, П.Ф. Буданов, О.В. Великогорський, Ю.С. Олійник, Н.Д. Винокурова, С.М. Войтенко, «Імітаційна модель цифрового двійника технологічного процесу енергоблока АЕС», *Наукові вісті КПІ*, № 2, с. 44–51, 2026. doi: https://doi.org/10.20535/kpisn.2026.2.352429

How to cite this article: K.Yu. Brovko, P.F. Budanov, O.V. Velykohorskyi, Yu.S. Oliinyk, N.D. Vynokurova, S.M. Voitenko, "Simulation model of the digital twin of the technological process of a NPP power unit", *KPI Science News*, No. 2, pp. 44–51, 2026. doi: https://doi.org/10.20535/kpisn.2026.2.352429

© The Autor(s).
The article is distributed under the terms of the license CC BY 4.0

aimed at improving NPP management technologies are becoming highly relevant. A priority vector for such research is the construction of high-fidelity digital twins of NPP power unit operating processes, which provide fundamentally new horizons for monitoring, technical diagnostics, and predicting the state of complex systems.

Operating processes on NPP power units are characterised by significant dynamics, a complex multi-layered hierarchy, and a massive array of interdependent parameters requiring constant supervision. Enhancing operational safety necessitates the application of intelligent analytical tools capable of detecting deviations and preconditions for accident situations in their incipient phases. In this regard, rapid progress in digital technologies is stimulating the realisation of the digital twin concept – a virtual prototype of a physical object that is constantly synchronised with real-time data and enables predictive modelling and optimisation of functionality.

However, the development of digital twins for NPP power units requires high-quality mathematical descriptions that reflect not only the physical nature of phenomena but also the structural complexity of the controlled system. Methods integrating a systemic approach, subdivision into subsystems (clustering), and the use of fractal indicators as quantitative markers of complexity level and hierarchical structure become crucial.

A review of the literature indicates that a significant number of studies are devoted to various aspects of modelling processes in Water-Water Power Reactor (WWER) with a nominal electric power of 1000 MW. For example, [1] examines the implementation of multi-zone models for controlling reactor power dynamics, but without applying control subsystem clustering or fractal indicators. Publication [2] presents a detailed thermal-hydraulic model of the reactor core in transient regimes, but does not consider the hierarchical structure of regulators and actuators. Research [3] focuses on visualising thermal processes in the reactor vessel, but without integrating neutron kinetics and analysing the control structure. Work [4] models the mechanics of control rod actuation based on a multi-body approach, allowing for the consideration of rod movement dynamics, but does not address the influence of structural complexity on system response time. Mathematical modelling of the nuclear fuel cycle presented in [5] encompasses energy balance and critical coefficients, but omits cluster decomposition of the reactor installation.

Several studies [6–8] explore fractal approaches and digital twin construction for complex technical systems. However, these methods are predominantly theoretical and not adapted to the specific structure of NPP power units. Studies [9, 10] analyse multi-level automation and the possibility of clustering control functions, but fractal dimension is not used as a quantitative measure of complexity.

Meanwhile, proceedings [11–14] demonstrate the potential of fractal metrics in technical monitoring tasks and neutron-physical modelling. However, these approaches are not combined with the hierarchical cluster structure of the power unit. Research [15] demonstrates the possibilities of modelling the consequences of control and protection system actuation in WWER-1000, but without systemic integration with other subsystems. Consequently, the existing literature reveals a gap: the absence of a comprehensive formalised model for controlling an NPP power unit based on a system-cluster approach using fractal characteristics.

Existing solutions typically focus on individual physical processes and do not consider the holistic multi-level structure of the control object. In this connection, an urgent scientific and applied problem is the development of a fractal-cluster mathematical model of a digital twin of the technological process of an NPP power unit, which would integrate neutron kinetics, thermofluidics, and control system dynamics into a single information platform.

Implementing such an approach will enable quantitative assessment of structural complexity, improve reliability of operation and predict emergency modes. This creates a foundation for implementing new generations of I&C systems.

Problem Statement

The research aims to develop a simulation model of a digital twin for the technological process of an NPP power unit using a system-cluster approach. This approach enables the analysis of the hierarchical self-similar scaled structure of subsystems based on fractal dimension evaluation.

To achieve this goal, the following tasks were defined:

– model the technological process of an NPP power unit using a system-cluster approach;

– investigate the hierarchical structure of the information-control system of an NPP power unit to facilitate the integration of digital twin algorithms;

– implement the system-cluster model based on the digital twin of the technological process of an NPP power unit.

Modelling the Technological Process of an NPP Power Unit Based on a System-Cluster Approach

Within the framework of the system-cluster approach for modelling complex technical objects, the technological process of an NPP power unit is treated as a multi-level structure with a cluster architecture. This enables formal representation of dependencies between its functional components [14].

In the proposed model, the primary cluster (cluster 1) represents the overall operation of the NPP power unit. It is structurally decomposed into four functional sub-clusters that encompass key aspects of dynamic control and safety of the reactor plant: power control sub-cluster ($C_{1,1}$); reactor protection sub-cluster ($C_{1,2}$); coolant parameter regulation sub-cluster ($C_{1,3}$); and reactor emergency shutdown sub-cluster ($C_{1,4}$).

Each of these sub-clusters characterises a distinct dynamic subsystem responsible for functionally critical tasks. These tasks ensure the safe and reliable operation of the reactor core during both normal operation and transient or accident conditions.

The power control sub-cluster $C_{1,1}$ manages the regulation of neutron flux and thermal power of the reactor core. Its model is based on point neutron equations modified to account for feedback on fuel and coolant temperatures. The dynamics of reactor power change and delayed neutron concentration are described by system of equations:

$$\begin{cases} \dfrac{dP(t)}{dt} = \dfrac{\rho(t)-\beta}{\Lambda} P(t) + \sum\limits_{i=1}^{n} \lambda_i C_i(t), \\ \dfrac{dC_i(t)}{dt} = \dfrac{\beta_i}{\Lambda} P(t) - \lambda_i C_i(t), \end{cases} \quad (1)$$

where dP is reactor power at time t, MW; ρ(t) is instantaneous reactivity, a dimensionless quantity representing the deviation from the critical state; β is total fraction of delayed neutrons; Λ is neutron generation period, s ($\Lambda \approx 10^{-3}$ s); λ_i is decay constant (attenuation) of the i-th group of delayed neutrons; $C_i(t)$ is concentration of delayed neutrons of the i-th group at time t; β_i is fraction of delayed neutrons for the i-th group.

The reactor protection sub-cluster ($C_{1,2}$) provides an automated response to critical deviations in the technological parameters of the NPP power unit. The protection system's operation is based on monitoring the threshold values for temperature, pressure, power, and neutron flux. The mathematical description of the sub-cluster is implemented via the following algorithm:

$$Z_k(t) = \begin{cases} 1, & x_k(t) \geq x_{thres}, \\ 0, & x_k(t) < x_{thres}, \end{cases} \quad (2)$$

where $Z_k(t)$ is the state of protection actuation for the k-th parameter; $x_k(t)$ is the current value of the technological parameter; x_{thres} is the threshold value of the technological parameter.

The coolant parameter regulation sub-cluster ($C_{1,3}$) is responsible for maintaining effective heat removal from the reactor core by controlling coolant temperature, pressure, and flow rate. The dynamics of the heat exchange processes are described by thermal-hydraulic equation:

$$\rho \frac{\partial h}{\partial t} + \rho \vec{\upsilon} \cdot \nabla h = Q - \nabla \cdot \vec{q}, \quad (3)$$

where ρ is coolant density, kg/m^3; h is specific enthalpy, J/kg; v is velocity vector, m/s; Q is internal heat sources, W/m^3; q is heat flux vector, W/m^2.

The reactor emergency shutdown sub-cluster ($C_{1,4}$) ensures the rapid termination of the nuclear chain reaction in the event of emergency. The mathematical model of the sub-cluster is based on introducing a step-wise negative reactivity, implemented by emergency insertion of absorber rods or boric acid injection:

$$\rho(t) = \rho_0 - \Delta\rho_{emer}, \quad (4)$$

where $\rho(t)$ is reactor reactivity after the emergency protection actuation; ρ_0 is the initial reactivity value; $\Delta\rho_{emer}$ is the magnitude of negative reactivity insertion due to the emergency drop of control rods or boric acid injection.

Within the system-cluster approach, the generalised state of the NPP power unit at the macro level is defined by an aggregated state variable $x_1(t)$. This variable integrates key process characteristics, including reactor thermal power, neutron density, and total reactivity. Its dynamics is governed by a differential equation that accounts for the interactions between sub-clusters, control inputs, and external disturbances, formulated as:

$$\frac{dx_1(t)}{dt} = a_0 x_1(t) + \sum_{j=1}^{n} a_j x_{1j}(t) + bu_1(t) + \omega_1(t), \quad (5)$$

where $x_1(t)$ is generalised state vector of the power unit (integral parameters: power, neutron flux, reactivity); $x_{1j}(t)$ is states of the functional sub-clusters (power control, reactor protection, coolant regulation, and emergency shutdown); a_j is structural influence coefficients reflecting sub-cluster inter-

actions ($a_j \in [0, 1]$); $a_0 x_1(t)$ is internal dynamics (intrinsic process evolution); $bu_1(t)$ is control inputs (control rods, I&C systems, pumping systems, to name a few); $\omega_1(t)$ is external disturbances (load changes, operational fluctuations, and uncertainties).

Each sub-cluster state variable $x_{1j}(t)$ represents a distinct physical or logical-dynamic subsystem, the summation of which defines the overall operational state of the NPP power unit. The structural influence coefficients a_j characterise the impact of the respective sub-clusters and can be determined via expert judgment, statistical analysis, or system identification procedures.

Control inputs $bu_1(t)$ are generated by the I&C system of the distributed control system. These include signals for power regulation, operational mode transitions, and the actuation of safety algorithms. External disturbances $\omega_1(t)$ account for uncontrolled factors, such as grid load fluctuations, coolant parameter variations, and power system transients.

Investigation of the Hierarchical Structure of the NPP Information and Control System for Digital Twin Implementation

According to fractal-cluster theory [7, 8, 11], an NPP power unit is viewed as a hierarchical, self-similar structure comprising interconnected clusters and lower-level sub-clusters. The hierarchical organisation of the NPP technological process control system, based on the proposed system-cluster approach, is illustrated in Fig. 1.

This approach enables the local modelling of subsystems with subsequent aggregation of results at the macro level. Each sub-cluster can be further decomposed into elementary functional components, including the reactor, turbine, generator, sensors, controllers, and actuators.

To evaluate the structural complexity of these sub-clusters, the fractal dimension is employed. This parameter is determined using the information space coverage method, which accounts for the system's inherent hierarchy and scale invariance.

For a discrete hierarchical structure, fractal dimension df is determined by formula [7, 14]:

$$d_f = \frac{\log_{10} N(\varepsilon)}{\log_{10}(1/\varepsilon)}, \qquad (6)$$

where $N(\varepsilon)$ is the number of elements (nodes, subsystems); ε is scaling factor (e.g., the fraction of the full structure into which the object is divided).

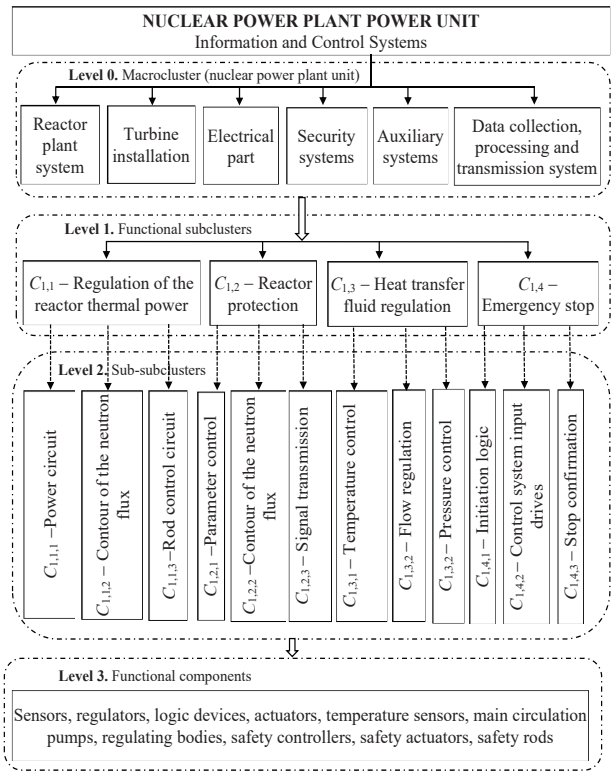


Fig. 1. Hierarchical structure of the control system of an NPP power unit based on a system-cluster approach

The power control sub-cluster $C_{1,1}$ provides regulation of the reactor thermal power and is described by equation:

$$\frac{dx_{11}(t)}{dt} = -k_p \cdot \left(x_{11}(t) - r(t)\right) + u_{11}(t), \qquad (7)$$

where $x_{11}(t)$ is the current thermal power; $r(t)$ is the power setpoint; k_p is the proportional gain; $u_{11}(t)$ is the control signal sent to the actuators, measured in real-time.

For sub-cluster $C_{1,1}$ a fractal dimension of $d_f = 1.584$ was obtained, corresponding to a scaled multi-level control structure. A decrease to $d_f < 1.5$ may indicate structural degradation, while exceeding $d_f > 1.7$ suggests excessive complexity.

The reactor protection sub-cluster $C_{1,2}$ implements emergency response logic:

$$x_{12}(t) = \begin{cases} 1, \text{ if } x_1(t) > x_{thres}, \\ 0, \text{ otherwise}, \end{cases} \qquad (8)$$

where $x_1(t)$ is the current reactor thermal power; x_{thres} is the safety threshold; $x_{1,2}(t)$ is the protection actuation signal (1 – active, 0 – inactive). A decrease in d_f below 0.9 may indicate reduced reliability or partial signal channel unavailability (a pre-accident state),

while exceeding d_f above 1.2 indicates a risk of response delays due to excessive structural complexity.

The coolant regulation sub-cluster $C_{1,3}$ is described by equation:

$$\frac{dx_{13}(t)}{dt} = -k_T \cdot \left(x_{13}(t) - T_{nom}\right) + u_{13}(t), \qquad (9)$$

where $x_{13}(t)$ is the coolant temperature; T_{nom} is the nominal temperature; $u_{13}(t)$ is the control signal for the Main Circulation Pump (MCP), measured in real-time; k_T is the thermal regulation coefficient determining the system's response speed.

For sub-cluster $C_{1,3}$, a value of $d_f = 1.83$, was determined, corresponding to a complex multi-level automation structure. A drop of d_f below 1.7 potentially indicates structural simplification, equipment decommissioning, or signal transmission failure. A value of d_f above 1.9 indicates a risk of over-complication, which may lead to synchronisation issues or reduced response speed.

The emergency shutdown sub-cluster $C_{1,4}$ implements the reactor scram function:

$$x_{14}(t) = \begin{cases} 1, \text{ if } x_{1,2}(t) = 1 \text{ or signal } MES, \\ 0, \text{ otherwise}, \end{cases} \qquad (10)$$

where $x_{14}(t)$ is the status of the emergency shutdown function; $x_{1,2}(t)$ is the actuation signal from the protection system sub-cluster $C_{1,2}$. For the emergency shutdown sub-cluster, a fractal dimension of $d_f = 1.585$ was obtained, corresponding to a redundant structure with high fault tolerance.

The summarised results indicate that the coolant regulation sub-cluster possesses the highest structural complexity, while the protection system is characterised by minimal hierarchical depth. Continuous updates of the sub-clusters' fractal dimensions enable dynamic monitoring of the NPP power unit's technological process.

The implementation algorithm for the digital twin model (Fig. 2) involves identifying the active elements of the sub-clusters, evaluating the hierarchical depth, and calculating the fractal dimension in real-time, followed by a comparison with predefined threshold values.

For each sub-cluster in normal operation, a reference fractal dimension df0, is determined and stored within the I&C system. During operation, the current value may fluctuate due to component degradation, communication channel failure, or control logic disruptions. The deviation is calculated using formula:

$$\Delta d_f(t) = \left| d_{f0} - d_f(t) \right|, \qquad (11)$$

where d_{f0} is the reference fractal dimension; $d_f(t)$ is the instantaneous value at time t. Under normal operating conditions, $d_f(t)$ remains close to d_{f0}.

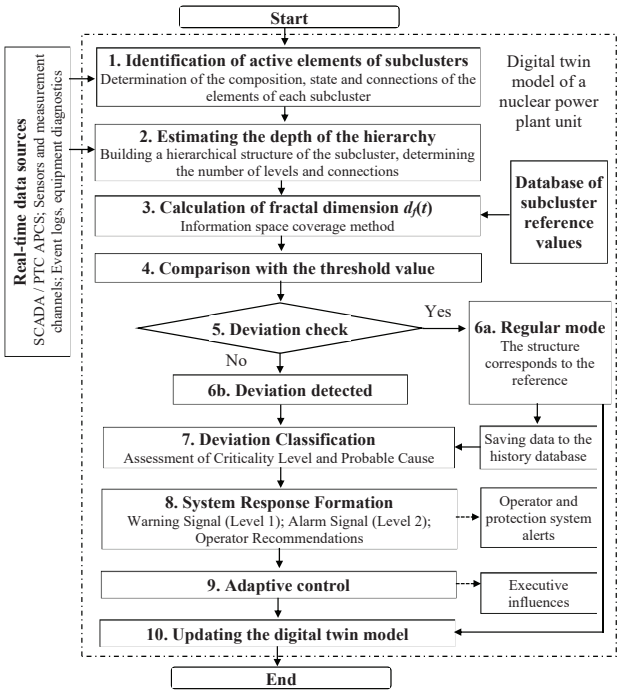


Fig. 2. Algorithm for implementing a digital twin model of the technological process of an NPP power unit

A decreasing fractal dimension indicates a simplification of the control structure due to the loss of active elements or hierarchical levels. If $\Delta d_f(t)$ exceeds the allowable tolerance, the system generates a warning signal or activates the emergency response mechanisms.

Thus, fractal dimension is used as a structural diagnostic parameter to detect hidden disruptions in the architecture of the NPP power unit control system.

Practical Implementation of the System-Cluster Model Within the NPP Power Unit Digital Twin Framework

The implementation of the NPP digital twin, based on the system-cluster approach, relies on modelling sub-cluster interactions, monitoring structural integrity, and evaluating fractal dimensions in real-time. This provides both a high-fidelity reflection of the current system state and the ability to predict potential deviations [14].

The digital twin is integrated with the I&C system and includes modules for data acquisition, structural identification, threshold comparison, visualisation, and predictive analytics.

An adaptive interface has been developed to monitor the power unit's status, displaying technological parameters, fractal analysis results, and the cluster states of subsystems in real-time. The interface panel includes tabs for core reactor parameters, dynamic fractal dimension graphs, and a radar chart (spider diagram) of the cluster structure (Fig. 3).

An interactive graphics library was utilised for data visualisation, enabling the construction of dynamic charts with automatic real-time updates. This facilitates the prompt display of parameter shifts, trend analysis, and the detection of potential anomalies within power unit subsystems.

The modular architecture ensures the flexibility and scalability of the software complex, allowing for future expansion through new analytical algorithms, diagnostic modules, and predictive tools. Furthermore, integration with Supervisory Control and Data Acquisition (SCADA) systems and NPP I&C systems platforms creates a foundation for deploying the digital twin in real-world nuclear power plant operating environments.

Conclusions

1. A system-cluster approach for modelling NPP technological processes has been developed and validated. The proposed simulation model provides a formal description of power unit behaviour across normal, transient, and emergency modes, establishing a robust framework for integrating digital twins into modern I&C systems. Unlike traditional localised models, this approach offers superior adaptability and scalability, accurately reflecting the complex structure of real-world NPP units.

2. The investigation of the I&C system's hierarchical structure established a clear correlation between sub-cluster structural complexity and functional characteristics. It was determined that the coolant regulation sub-cluster possesses the highest fractal dimension, indicating a significant degree of structural interdependence. Based on this, a structural diagnostic algorithm was developed, capable of detecting degradation and the loss of hierarchical levels before the onset of critical functional failures.

3. The practical implementation of the NPP digital twin with fractal monitoring confirmed the effectiveness of the proposed approach for early diagnostics and proactive control. Results show that structural shifts within sub-clusters are accompanied by corresponding changes in fractal dimension, enabling the automated identification of potential operational threats. The implemented adaptive response mechanism facilitates the activation of protective scenarios prior to emergency escalation, significantly enhancing the functional safety of the NPP power unit. Thus, this research creates the prerequisites for next-generation intelligent decision-support systems in the nuclear energy sector.

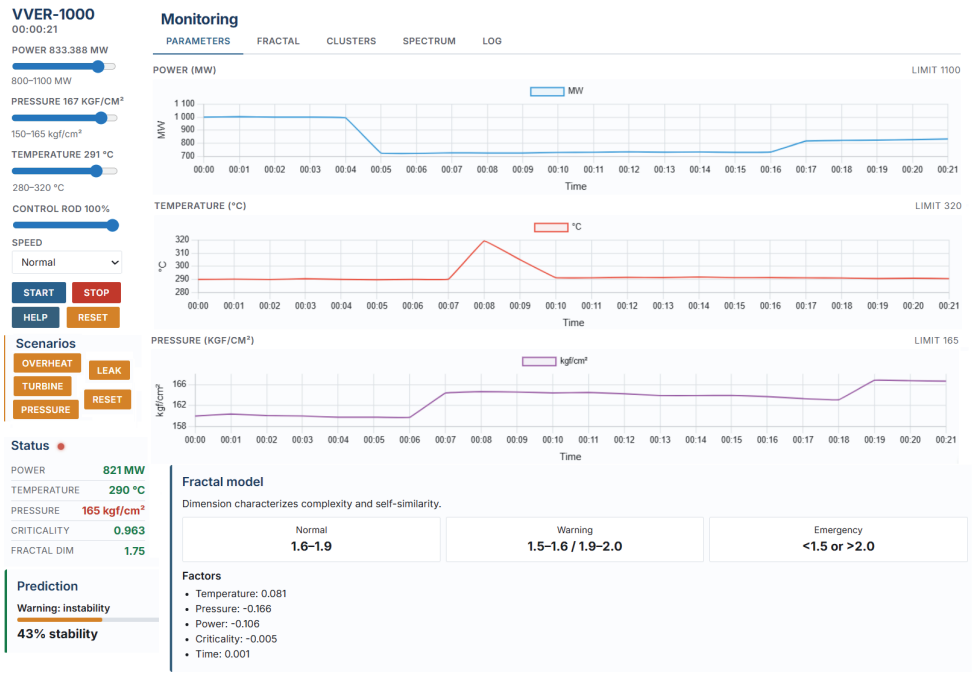


Fig. 3. Digital twin interface for the WWER-1000 technological process

References

[1] S.M. Bigonah Ghalehsari *et al.*, "A review of the evaluation, simulation, and control of the air conditioning system in a nuclear power plant", *Energies*, Vol. 18, No. 7, article 1719, 2025. Retrieved from: https://doi.org/10.36074/logos-01.03.2024.052

[2] M. Krecicki and D. Kotlyar, "Thermal hydraulic modeling of solid-fueled nuclear thermal propulsion reactors part II: Full-core coupled neutronic and thermal hydraulic analysis", *Annals of Nuclear Energy*, Vol. 179, article 109397, 2022. Retrieved from: https://doi.org/10.1016/j.anucene.2022.109397

[3] Y. Weng *et al.*, "The thermal-fluid-solid coupling effect in nuclear reactor vessel with direct vessel injection", *Progress in Nuclear Energy*, Vol. 152, article 104364, 2022. Retrieved from: https://doi.org/10.1016/j.pnucene.2022.104364

[4] K. Zhang *et al.*, "Towards safe, efficient long-reach manipulation in nuclear decommissioning: A case study on fuel debris retrieval at Fukushima Daiichi", *Journal of Nuclear Science and Technology*, Vol. 62, No. 1, pp. 1–16, 2025. Retrieved from: https://doi.org/10.1080/01691864.2023.2169588

[5] B.M.T. Costa Peluzo and E. Kraka, "Uranium: the nuclear fuel cycle and beyond", *International Journal of Molecular Sciences*, Vol. 23, No. 9, article 4655, 2022. Retrieved from: https://doi.org/10.3390/ijms23094655

[6] B. Dechenaux *et al.*, "Percolation properties of the neutron population in nuclear reactors", *Physical Review E*, Vol. 106, No. 6, article 064126, 2022. Retrieved from: https://asnr.hal.science/irsn-04122103/document

[7] P. Budanov *et al.*, "Fractal approach for researching information emergency features of technological parameters", *International Journal of Computing*, Vol. 24, No. 1, pp. 171–177, 2025. Retrieved from: https://doi.org/10.47839/ijc.24.1.3889

[8] P. Budanov *et al.*, "Dynamic fractal cluster model of informational space technological process of power station", *Lecture Notes on Data Engineering and Communications Technologies*, Vol. 221, pp. 141–155, 2024. Retrieved from: https://doi.org/10.1007/978-3-031-71801-4_11

[9] Y. Jiang *et al.*, "Eco-zoning management based on thresholds of NPP driving factors", *Frontiers in Forests and Global Change*, Vol. 8, article 1712019, 2025. Retrieved from: https://doi.org/10.3389/ffgc.2025.1712019

[10] A. Ramezani *et al.*, "A proposed improvement for the design of safety injection system in VVER-1000/V446 reactor", *Progress in Nuclear Energy*, Vol. 137, article 103767, 2021. Retrieved from: https://doi.org/10.1016/j.pnucene.2021.103767

[11] K. Brovko *et al.*, "Development of an integrated digital twin model for efficient operation of nuclear power plant units", *Tekhnichna Inzheneriya*, No. 2 (96), pp. 58–67, 2025. Retrieved from: https://doi.org/10.26642/ten-2025-2(96)-58-67

[12] K. Brovko *et al.*, "Providing quantitative assessment of quality of technological process control of a nuclear power unit using a digital twin", *Visnyk NTU "KhPI". Series: New Solutions in Modern Technologies*, No. 3 (25), pp. 3–12, 2025. Retrieved from: https://doi.org/10.20998/2413-4295.2025.03.01

[13] G. Espinosa-Paredes and C.A. Cruz-Lypez, "A new compartmental fractional neutron point kinetic equations with different fractional orders", *Nuclear Engineering and Design*, Vol. 423, article 113184, 2024. Retrieved from: https://doi.org/10.1016/j.nucengdes.2024.113184

[14] P. Budanov *et al.*, "Construction of an information model of the digital twin of the technological process in a power unit at a nuclear power plant", *Eastern-European Journal of Enterprise Technologies*, Vol. 4, No. 9 (136), pp. 39–49, 2025. Retrieved from: https://doi.org/10.15587/1729-4061.2025.335712

[15] S. Kordalivand *et al.*, "Quantifying the impact of risk mitigation measures using SPAR-H and RCM approaches: Case study based on VVER-1000 systems", *Nuclear Engineering and Design*, Vol. 423, article 113174, 2024. Retrieved from: https://doi.org/10.1016/j.nucengdes.2024.113174

К.Ю. Бровко, П.Ф. Буданов, О.В. Великогорський, Ю.С. Олійник, Н.Д. Винокурова, С.М. Войтенко

ІМІТАЦІЙНА МОДЕЛЬ ЦИФРОВОГО ДВІЙНИКА ТЕХНОЛОГІЧНОГО ПРОЦЕСУ ЕНЕРГОБЛОКА АЕС

Проблематика. Сучасні енергоблоки атомних електростанцій (АЕС) характеризуються високою структурною складністю, багаторівневою ієрархією інформаційно-керуючих систем і значною кількістю взаємопов'язаних технологічних параметрів. Відомі моделі цифрових двійників здебільшого орієнтовані на окремі фізичні процеси (нейтронну кінетику, теплогідравліку або логіку захисту) без комплексного врахування структурної організації систем управління. Відсутність формалізованого підходу до оцінювання ієрархічної цілісності підсистем у режимі реального часу обмежує можливості раннього виявлення передаварійних станів і проактивного керування безпекою.

Мета дослідження. Розроблення імітаційної моделі цифрового двійника технологічного процесу енергоблока АЕС на основі системно-кластерного підходу, що дозволяє оцінити ієрархічну самоподібну масштабовану структуру підсистем з використанням кількісної величини фрактальної розмірності.

Методика реалізації. Дослідження виконано на основі системно-кластерного підходу з декомпозицією енергоблока на функціональні підкластерні структури: керування потужністю, спрацювання системи захисту, регулювання параметрів теплоносія та контролювання аварійної зупинки. Математичний апарат моделі поєднує рівняння нейтронної кінетики, теплогідравлічні співвідношення та логіко-динамічні алгоритми. Для кількісної оцінки структурної складності застосовано метод покриття інформаційного простору з обчисленням фрактальної розмірності. Реалізацію цифрового двійника здійснено у вигляді

програмно-апаратного комплексу, інтегрованого з інформаційно-керуючою системою, з використанням модулів збирання даних, структурної ідентифікації та прогнозного аналізу.

Результати дослідження. Отримано значення фрактальної розмірності для ключових підкластерів енергоблока, що відображають їхню ієрархічну складність (зокрема, максимальне значення 1,83 для системи регулювання теплоносія й мінімальне значення 1 для системи захисту). Визначено нормовані діапазони фрактальної розмірності як індикатори штатного функціонування. Розроблено алгоритм моніторингу відхилень, який дозволяє виявляти втрату структурних рівнів або деградацію підсистем до появи функціональних збоїв. Практична реалізація цифрового двійника продемонструвала можливість оперативного структурного діагностування та адаптивного реагування.

Висновки. Запропонований фрактально-кластерний підхід забезпечує комплексне моделювання технологічного процесу енергоблока АЕС з урахуванням його ієрархічної структури. Використання фрактальної розмірності як структурного діагностичного параметра розширює можливості традиційних методів контролю і створює передумови для впровадження проактивних стратегій керування безпекою на основі цифрового двійника.

Ключові слова: цифровий двійник; енергоблок; фрактальна розмірність; системно-кластерний підхід; інформаційно-керуюча система.

Recommended by the Council
of the Faculty of Robotics
and Instrumentation Engineering
of Igor Sikorsky KPI

Received: 18 February 2026

Accepted: 08 June 2026

Published: 29 June 2026

DOI: https://doi.org/10.20535/kpisn.2026.2.351804
UDC 614.2+574/578+004.38

Ye.V. Pankratov[1*], https://orcid.org/0009-0004-1508-3053
G.S. Tymchik[1], https://orcid.org/0000-0003-1079-998X
[1] National Technical University of Ukraine "Igor Sikorsky Kyiv Polytechnic Institute", Kyiv, Ukraine, https://ror.org/00syn5v21
*Corresponding author: evegennomad@gmail.com

MICROSERVICE ARCHITECTURE AND ALGORITHMS OF A MODULAR AUTOMATION SYSTEM FOR SMALL BUSINESS TECHNOLOGICAL PROCESSES

Background. Small and medium-sized businesses in Ukraine operate under two simultaneous pressures: a prolonged martial law with strikes on energy infrastructure, and the need for digital transformation to remain competitive. Existing ERP and CRM systems assume stable infrastructure and large implementation budgets and are poorly suited to partial-availability operation, fast migration between on-premises and cloud environments, and phased deployment within tight budgets. This creates a need for architectural solutions for the class of small multi-channel retail-service businesses.
Objective. The paper aims to develop the architecture and algorithms of a modular digital automation system for the multi-channel retail-service small business class under martial law conditions, and to propose a verification and validation methodology for the microservice implementation of its components.
Methods. The architecture follows the principle of one microservice per business function and distributes responsibilities among nine services. Service interactions go through standardised APIs (REST, gRPC) and asynchronous messaging (RabbitMQ). The verification and validation methodology covers unit, contract, integration, end-to-end, and chaos testing. Validation was carried out on four enterprise types: retail with service support, e-commerce, food service with catering, and a full production-and-sales model.
Results. The architecture supports partial-availability operation when individual services fail, portability between on-premises and cloud infrastructure, phased deployment within tight budgets, and the absence of vendor lock-in due to the open-source stack. The proposed verification and validation methodology covers five testing levels and ties each architectural concern to a specific check type.
Conclusions. The modular microservice architecture is suitable for the class of multi-channel retail-service small businesses operating under unstable infrastructure conditions. Further work covers the collection of quantitative operational metrics and the integration of machine-learning-based forecasting modules.
Keywords: microservice architecture; small business; digital automation; multi-channel sales; verification and validation; martial law.

Introduction

Small and medium-sized businesses (SMBs) in Ukraine form the backbone of the country's economy: according to OECD estimates, these enterprises comprise 99.9 % of all business entities, provide 81.6 % of business employment, and generate 70.2 % of added value. Since 2022, this sector has been operating under systematic constraints: infrastructure destruction, electricity outage schedules, mobilisation of personnel, relocation from combat zones, and reduced consumer purchasing power. According to UNDP data, only about 57 % of SMBs were operational in March-April 2022; by 2023, this figure partially recovered to 84 %, and it has remained at approximately 85 % throughout 2024–2025. Alongside these crisis-related limitations, the demand for digital tools is rising: in 2024, Ukrainians spent UAH 239 billion on online goods and services, a 25 % increase from 2023, and the share of e-commerce in retail turnover reached 10 %. This creates a contradiction between limited enterprise resources and the simultaneous growth in requirements for digital support of operational processes.

Пропозиція для цитування цієї статті: Є.В. Панкратов, Г.С. Тимчик, «Мікросервісна архітектура та алгоритми модульної системи автоматизації технологічних процесів малого бізнесу», *Наукові вісті КПІ*, № 2, с. 52–58, 2026. doi: https://doi.org/10.20535/kpisn.2026.2.351804

How to cite this article: Ye.V. Pankratov, G.S. Tymchik, "Microservice architecture and algorithms of a modular automation system for small business technological processes", *KPI Science News*, No. 2, pp. 52–58, 2026. doi: https://doi.org/10.20535/kpisn.2026.2.351804

© The Autor(s).
The article is distributed under the terms of the license CC BY 4.0

Analysis of Previous Research and Publications

The issue of ensuring the functionality of a small business as a cyber-physical system supported by a digital twin is addressed in the authors' previous work [1]. Physical models for cyber-physical systems that combine software control levels with real production processes are discussed in [2]. The question of evaluating the reliability of information obtained from sensors in cyber-physical systems is investigated in [3]. A systemic strategy for guaranteed safety of complex engineering systems, where the software component ensures continuous operation, is formulated in [4]. The classic approach to software architecture design based on architectural characteristics and decision-making heuristics is summarised by L. Bass, P. Clements, and R. Kazman [5]. Principles of building microservice systems, service lifecycle, and observability issues are thoroughly elaborated by S. Newman [6]. The REST architectural style and its application in distributed systems are formulated in R. Fielding's dissertation [7]. A generalised definition of microservice architecture as a paradigm for building corporate systems is introduced by M. Fowler and J. Lewis [8]. Basic principles of building distributed systems (asynchronous communication, fault tolerance, state consistency) are systematically presented by A.S. Tanenbaum and M. van Steen [9]. Engineering aspects of software architecture design tied to specific classes of problems are considered by I. Horton [10].

While these proceedings address individual components of the problem, they do not encompass the specific class of enterprises in question: multi-channel retail and service SMBs operating during martial law conditions. The issue of formalising system automation requirements under unstable infrastructure conditions remains unresolved, as does the construction of an architecture with an explicit link between technical solutions and business requirements for this particular class of enterprise. Additionally, the organisation of verification and validation of microservice components within limited resources requires further investigation.

Problem Statement

The paper aims to develop an architecture and algorithms for a modular system for automating technological processes in multi-channel retail and service SMBs based on a microservice approach, as well as to establish a methodology for verifying and validating the microservice implementation of its components.

The Challenge of Automating Small Businesses During Martial Law Conditions

Since 2022, small businesses have been operating under conditions that systematically differ from the peaceful model of information system operation. Attacks on Ukraine's energy infrastructure, which began in October 2022, resulted in damage to approximately 50 % of the country's generating capacity as of early 2023. Available generating capacity fell by 51 % between the beginning of 2022 and April 2023. In November 2022 alone, up to 55 % of electricity supply was lost on some days, and the average Ukrainian household spent approximately five weeks without electricity during the period October-December 2022. In subsequent years, power outage schedules became a constant element in production planning.

Mobilisation, evacuation, and relocation of personnel reduce the available workforce and force a portion of employees to work remotely. Damage to warehouses and disruptions to supply chains require the inventory system to quickly readjust supply chain routing. Businesses remain in a state of cautious recovery with limited resources for infrastructure investments, rendering traditional models for implementing large ERP platforms unsuitable for SMBs. While e-commerce volume in Ukraine reached UAH 239 billion with a 25 % year-on-year growth, and the national digitalisation strategy for the economy [11] necessitates that businesses simultaneously support both physical and online sales. This significantly increases demands on the system's integration capabilities.

These constraints yield six architectural requirements for the small business automation system: operation in degraded mode upon failure of individual components; portability between on-premises and cloud infrastructure; phased deployment from critical modules to peripheral ones; low Total Cost of Ownership (TCO) through an open-source technology stack; multi-channel integration within a unified data model; remote access with audit trails. Traditional monolithic ERP and CRM systems only satisfy a subset of these requirements, necessitating a transition to a microservice architecture.

Business Profile of the Target Domain

The targeted class of activity is defined as multi-channel retail and service small businesses. These are enterprises with up to 50 employees that simultaneously sell products through a physical point of sale, an online store, and a service de-

partment or catering service. They require inventory management with warranty and after-sales support, operate on thin margins, and have limited IT budgets that preclude the implementation of large ERP platforms. This class includes retail stores with repair services, small food establishments with catering, online stores with their own warehouse, and small manufacturing enterprises with their own retail network. Information flows in such businesses cover procurement and replenishment of inventory, warehouse accounting, sales through physical and online channels, after-sales service, financial settlements, and personnel accounting.

Automation System Architecture

The architectural solution is tailored to the six requirements outlined in the previous section. Decomposition into independent microservices based on business functions, aligned with typical deployment patterns for microservice architectures [12], implements the requirements for partial availability and phased implementation: each service has its own database and deployment lifecycle, preventing cascading failures. Containerisation of services and declarative infrastructure description ensure portability between on-premises servers and the cloud. An open-source technology stack (ASP.NET Core, PostgreSQL, MongoDB, RabbitMQ, gRPC) reduces ownership costs and eliminates vendor lock-in. A single Product catalogue and Webretail/Shop adapters with support for REST, WebSocket, MQTT for external integrations facilitate multi-channel functionality. Web access and auditing are implemented through a Gateway with JWT authentication and Identity with role-based access control.

The overall system architecture is depicted in Fig. 1. The architecture consists of three horizontal layers: the client channel level (physical point of sale, web storefront, mobile application, IoT devices), the API gateway and security level (Gateway, Identity), and the business services and data level (Act, Service, Product, Financial, Shop, Webretail, Fileservice each with its own persistent storage). Asynchronous events and commands are transmitted through a message broker.

Five architectural characteristics have been defined for the system: resilience through the isolation of failures in individual services, portability through containerisation, scalability through independent horizontal scaling of critical services, evolvability through clear contracts between services, and low TCO due to the use of an open-source technology stack. These characteristics serve as criteria for verification and validation.

Microservice Implementation of Components

Each service implements a defined area of responsibility, has its own data store, and its own set of algorithms. A list of components is summarised in Table 1.

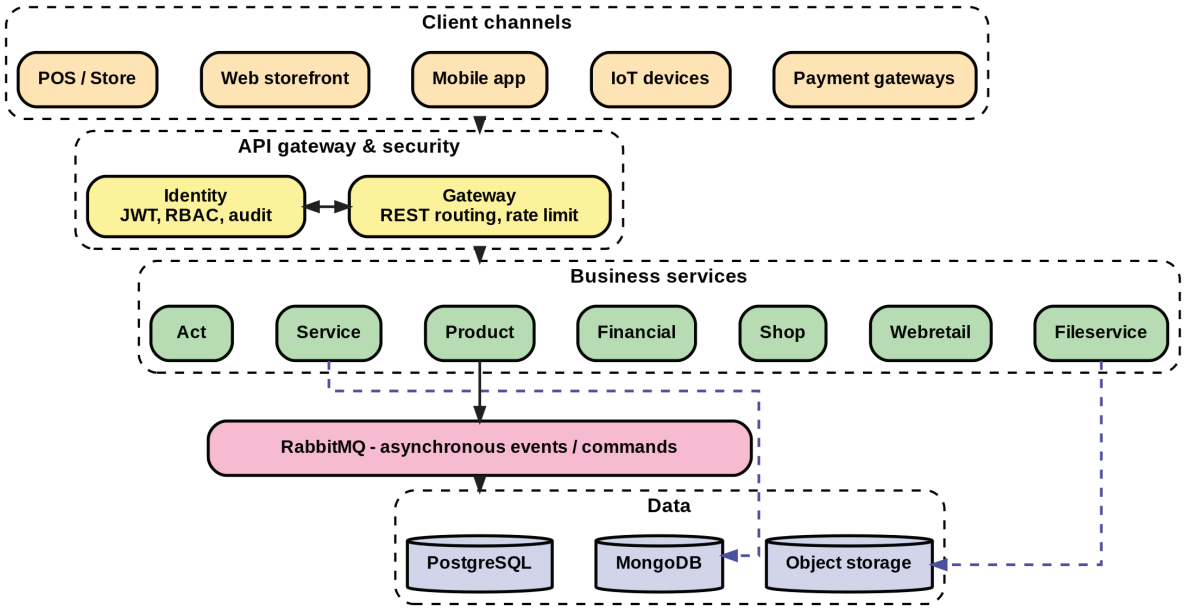


Fig. 1. System architecture: components and interactions

Table 1. List of system microservices

Service	Area of Responsibility	Key Algorithms
Gateway	Single point of entry, routing, rate limiting	URL template routing, rate limiting, JWT pre-verification
Identity	Authentication, authorisation, roles, audit	JWT issuance and verification, RBAC, action logging
Act	Documents, Statements, invoices, receipts, inventory	Verification of related data, number generation, cancellation processing
Service	After-sales service, catering events	Resource planning, stage completion tracking
Product	Product catalogue, inventory balances, product operations	Data normalisation, balance recalculation, RabbitMQ notifications
Financial	Financial transactions, payments, currencies, receipts	Transaction confirmation, currency conversion, logging
Shop	Business units, statistics, personnel accounting	Salary calculation, indicator aggregation
Webretail	Frontend solutions for retail and online store	Storefront synchronisation, cart processing
Fileservice	File storage, media, documents	Type checking, size optimisation, access control

The technological stack is unified: ASP.NET Core for service implementation and REST APIs, PostgreSQL for critical data, MongoDB for dynamic structures (Service uses both). Interaction between services is organised in two types: synchronous requests via REST and gRPC (gRPC for inter-service communication with strict typing) and asynchronous events through RabbitMQ. The sequence of processing a typical order placement scenario is shown in Fig. 2.

The order processing algorithm consists of the following steps. A user submits a request via Webretail. The request passes through Gateway, where JWT verification is performed in the Identity service. Upon success, the request is forwarded to Product for stock reservation. Product publishes a reservation event in RabbitMQ, which Financial (amount calculation) and Webretail (storefront update) are subscribed. After payment confirmation, Financial publishes a transaction completion event, subscribed to

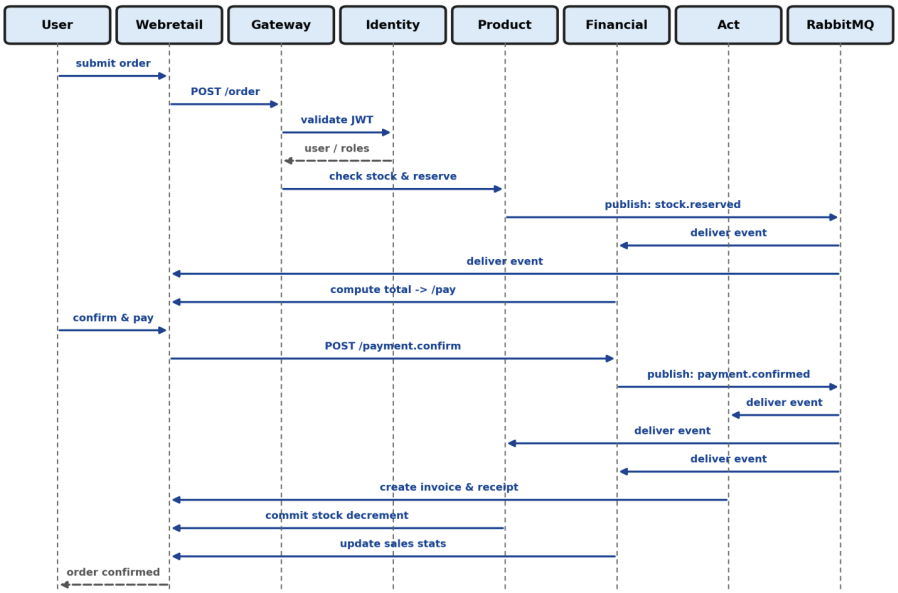


Fig. 2. Order processing sequence between services

by Act (document generation), Product (inventory deduction), and Shop (statistics). In case of failure at any stage, a compensating transaction is triggered to roll back the system state.

Examples, Verification, and Validation

The system has been tested on four types of enterprises belonging to the targeted class. In a bicycle shop with a repair workshop, active services Product, Shop, Service, Financial, Act supported a catalogue of bicycles and spare parts, a cash register zone, service requests for repairs, fiscal receipts, and work completion certificates. In an online store, services Webretail, Product, Financial, Fileservice, Act, Identity provided a web storefront, shopping cart, integration with a payment gateway, and order processing with logic for returning to the visitor database in case of failure. In a restaurant with catering, services Product, Act, Financial, Service, Shop maintained a menu catalogue, inventory write-off records, expense accounting by shift, catering event planning, and personnel management. In a full production-to-sales cycle model, all nine services were active, covering raw material procurement, production stages, warehouse accounting, sales, and financial analysis.

Verification of the microservice implementation is performed according to modern practices at five levels. Unit testing checks the correctness of the business logic of each service in isolation from external dependencies. Integration testing verifies the interaction of a service with its own database, message broker, and adjacent services. Contract testing creates tests from the provider and consumer side for each gRPC and REST contract, allowing updates to individual services without a full system regression. End-to-end testing* reproduces typical business scenarios (order placement, service request, salary calculation) that pass through all involved services. Resilience testing (chaos tests) intentionally disables services and damages connections between them to test the system's transition into degraded mode.

Validation links each architectural characteristic to a target verification type (Table 2).

Quantitative indicators from pilot launches (response time, throughput, error rate, recovery time after failure) are not provided in this publication, as accumulating such data requires long-term observation. This is a subject of separate research.

Conclusions

1. Existing business automation solutions (SAP ERP, Microsoft Dynamics 365, Oracle NetSuite, BAS ERP, Parus) are primarily designed for stable infrastructure and significant implementation budgets, fail to sufficiently address the specificities of operating in conditions of unstable infrastructure and limited resources. This work formulated six specific requirements for a multi-channel retail and service automation system for small businesses in martial law conditions and identified five architectural characteristics: resilience, portability, scalability, evolvability, and low TCO.

2. A modular microservice architecture is proposed, where each architectural solution is tied to a specific requirement of the targeted class of activity and algorithms for the interaction of nine services through standardised APIs and a message broker. Unlike existing monolithic solutions, the proposed architecture ensures operation in degraded mode upon failure of individual components, portability between local and cloud infrastructure, phased deployment, and the avoidance of vendor lock-in thanks to an open-source technology stack.

Table 2. Linking architectural characteristics to verification types

Characteristic	Type of Verification	Example Scenario
Resilience	Chaos testing	Disabling Financial: Webretail keeps orders in "awaiting payment" state; after Financial recovery, it processes the queue
Portability	Migration run	Deploying the entire stack from local hosting to the cloud based on a manifest, verifying data integrity
Scalability	Load testing	Increasing requests to Product by 10 times: horizontal scaling of instances without affecting other services
Evolvability	Contract testing	Updating Identity with the addition of a role: backward compatibility with consumers is maintained
Low TCO	Calculated validation	Comparing required resources and licenses with market prices for the SME segment

3. Based on the proposed architecture, the problem of building an enterprise information system is solved, which maintains functionality during power outages and internet connectivity issues and integrates all sales channels in a single environment. A verification and validation methodology is proposed that covers five levels of testing and links each architectural characteristic to the appropriate verification type. The practical implementation has been tested on four types of enterprises: a bicycle shop with a repair workshop, an online store, a restaurant with catering, and a full production-to-sales cycle model.

4. Further work involves accumulating quantitative performance indicators of the system (average response time, throughput, error rate, recovery time after failure) over an extended monitoring period, expanding the system with modules for demand forecasting and inventory optimisation based on machine learning, as well as integrating with industrial IoT devices for managing small-scale manufacturing processes.

References

[1] N.D. Pankratova *et al.*, "Strategy of the cyber-physical system for a small business enterprise guaranteed functioning with the digital twin support", *System Research And Information Technologies*, No. 2, pp. 7–20, 2024. Scopus. Retrieved from: https://doi.org/10.20535/SRIT.2308-8893.2024.2.01

[2] N.D. Pankratova, "Creation of Physical Models for Cyber-Physical Systems. Lecture Notes in Networks and Systems", 2020, pp. 68–77. Retrieved from: https://doi.org/10.1007/978-3-030-34983-7

[3] N.D. Pankratova, V.A. Pankratov, "Evaluation of information reliability sensors of cyber-physical system", *15th International Scientific and Practical Conference "Mathematical and Simulation Modelling of Systems. MODS'2020"*, June 29–July 01, Chernihiv, Ukraine, 2020, pp. 256–260.

[4] N.D. Pankratova, "System strategy for guaranteed safety of complex engineering systems", *Cybernetics and System Analysis*, 2010, No. 2 (46), pp. 243–251.

[5] L. Bass *et al.*, "Software Architecture in Practice", 4th ed., Boston: Addison-Wesley, 2021, 624 p.

[6] S. Newman, "Building Microservices: Designing Fine-Grained Systems", 2nd ed., O'Reilly Media, 2021, 428 p.

[7] R.T. Fielding, "Architectural Styles and the Design of Network-based Software Architectures", Doctoral dissertation, University of California, Irvine, 2000, 180 p.

[8] M. Fowler and J. Lewis, "Microservices: a definition of this new architectural term", MartinFowler.com, 2014. [Online]. Retrieved from: https://martinfowler.com/articles/microservices.html. Accessed: Aug. 10, 2025.

[9] A.S. Tanenbaum and M. van Steen, "Distributed Systems: Principles and Paradigms", 2nd ed., Prentice Hall, 2007, 704 p.

[10] I. Gorton, "Essential Software Architecture", 2nd ed., Springer, 2011, 242 p.

[11] Ministry of Digital Transformation of Ukraine [Ministerstvo tsyfrovoi transformatsii Ukrainy], Open data sources for digital transformation of enterprises [Dzherela vidkrytykh danykh dlia tsyfrovoi transformatsii pidpryiemstv], TheDigital.gov.ua, 2025. [Online]. Retrieved from: https://thedigital.gov.ua. Accessed: Aug. 10, 2025.

[12] Microsoft Docs, "Microservices architecture: Principles, advantages, challenges", 2025. [Online]. Retrieved from: https://learn.microsoft.com/microservices-architecture. Accessed: Aug. 10, 2025.

Є.В. Панкратов, Г.С. Тимчик

МІКРОСЕРВІСНА АРХІТЕКТУРА ТА АЛГОРИТМИ МОДУЛЬНОЇ СИСТЕМИ АВТОМАТИЗАЦІЇ ТЕХНОЛОГІЧНИХ ПРОЦЕСІВ МАЛОГО БІЗНЕСУ

Проблематика. Малий і середній бізнес в Україні працює в умовах одночасної дії двох викликів: довготривалий воєнний стан з ударами по енергетичній інфраструктурі й необхідність цифрової трансформації для збереження конкурентоспроможності. Наявні ERP- і CRM-системи розраховані на стабільну інфраструктуру і великі бюджети впровадження і слабо пристосовані до режиму часткової роботи, швидкої міграції між власним і хмарним середовищем, поетапного розгортання за обмеженого бюджету. Це створює потребу в архітектурних рішеннях для класу малого торгово-сервісного бізнесу з багатоканальною реалізацією.

Мета. Розробити архітектуру й алгоритми модульної системи цифрової автоматизації для багатоканального торгово-сервісного малого бізнесу в умовах воєнного стану та запропонувати методологію верифікації і валідації мікросервісної реалізації її компонентів.

Методика реалізації. Архітектура побудована за принципом «мікросервіс на бізнес-функцію» з розподілом між дев'ятьма сервісами. Взаємодія проходить через стандартизовані API (REST, gRPC) та асинхронний обмін повідомленнями (RabbitMQ). Методологія верифікації і валідації спирається на сучасні практики тестування мікросервісних систем: модульне, контрактне, інтеграційне, наскрізне та хаос-тестування. Апробацію проведено на чотирьох типах підприємств.

Результати дослідження. Архітектура забезпечує роботу системи в режимі часткової доступності у разі відмови окремих сервісів, переносимість між локальною і хмарною інфраструктурою, поетапне розгортання за обмеженого бюджету й відсутність

вендор-локу завдяки відкритому стеку. Методологія верифікації і валідації покриває п'ять рівнів тестування і прив'язує кожну архітектурну вимогу до конкретного типу перевірки.

Висновки. Модульна мікросервісна архітектура придатна для класу багатоканального торгово-сервісного малого бізнесу в умовах нестабільної інфраструктури. Подальша робота передбачає накопичення кількісних показників експлуатації та інтеграцію із прогнозними модулями на основі машинного навчання.

Ключові слова: мікросервісна архітектура; малий бізнес; цифрова автоматизація; багатоканальна реалізація; верифікація і валідація; воєнний стан.

Recommended by the Council
of the Faculty of Robotics
and Instrumentation Engineering
of Igor Sikorsky KPI

Received: 07 February 2026

Accepted: 08 June 2026

Published: 29 June 2026

АВТОРИ НОМЕРА

Бровко Костянтин Юрійович
http://orcid.org/0000-0002-9669-9316

Буданов Павло Феофанович
https://orcid.org/0000-0002-1542-9390

Великогорський Олег Володимирович
https://orcid.org/0009-0005-6102-0659

Винокурова Наталія Дмитрівна
https://orcid.org/0009-0008-6210-838X

Войтенко Сергій Миколайович
https://orcid.org/0009-0001-8829-2647

Гліненко Лариса Костянтинівна
https://orcid.org/0000-0002-3105-4568

Голубінка Віталій Петрович
https://orcid.org/0009-0001-3676-3566

Грішин Костянтин Дмитрович
https://orcid.org/0009-0006-5950-3739

Кость Павло Ігорович
https://orcid.org/0009-0002-9863-6172

Недашківська Надія Іванівна
https://orcid.org/0000-0002-8277-3095

Олійник Юлія Сергіївна
https://orcid.org/0000-0002-5893-352X

Петренко Дмитро Володимирович
https://orcid.org/0009-0003-7670-555X

Протасов Анатолій Георгійович
https://orcid.org/0000-0002-2965-3334